

AD-A043 069

ARMY ENGINEER WATERWAYS EXPERIMENT STATION VICKSBURG MISS F/G 8/13
FINITE ELEMENT ANALYSIS OF A REINFORCED EARTH WALL.(U)
JUL 77 M M AL-HUSSAINI, L D JOHNSON

UNCLASSIFIED

WES-TR-S-77-6

NL

1 OF 2

AD
A043069



Code 23
0-13



12
B.S.



TECHNICAL REPORT S-77-6

FINITE ELEMENT ANALYSIS OF A REINFORCED EARTH WALL

by

Mosaid M. Al-Hussaini, Lawrence D. Johnson

Soils and Pavements Laboratory
U. S. Army Engineer Waterways Experiment Station
P. O. Box 631, Vicksburg, Miss. 39180

AD A 043069

FINITE ELEMENT ANALYSIS OF A REINFORCED EARTH WALL

July 1977
Final Report

Approved For Public Release; Distribution Unlimited

DDC
RECEIVED
AUG 18 1977
A



Prepared for Office, Chief of Engineers, U. S. Army
Washington, D. C. 20314

Under Project 4A161102AT22, Task A2
Work Unit 004

COPY AVAILABLE TO DDC DOES NOT
PERMIT FULLY LEGIBLE PRODUCTION

AD WJ.
DDC FILE COPY

JULY 1977

Destroy this report when no longer needed. Do not return
it to the originator.

Unclassified

SECURITY CLASSIFICATION OF THIS PAGE (When Data Entered)

REPORT DOCUMENTATION PAGE		READ INSTRUCTIONS BEFORE COMPLETING FORM
1. REPORT NUMBER Technical Report S-77-6	2. GOVT ACCESSION NO.	3. RECIPIENT'S CATALOG NUMBER
4. TITLE (and Subtitle) FINITE ELEMENT ANALYSIS OF A REINFORCED EARTH WALL.	5. TYPE OF REPORT & PERIOD COVERED Final report.	6. PERFORMING-ORG. REPORT NUMBER Jul 75 - Feb 77
7. AUTHOR(s) Mosaid M. Al-Hussaini Lawrence D. Johnson	8. CONTRACT OR GRANT NUMBER(s)	
9. PERFORMING ORGANIZATION NAME AND ADDRESS U. S. Army Engineer Waterways Experiment Station Soils and Pavements Laboratory P. O. Box 631, Vicksburg, Miss. 39180	10. PROGRAM ELEMENT, PROJECT, TASK AREA & WORK UNIT NUMBERS Project 4A161102AT22 Task A2 Work Unit 004	
11. CONTROLLING OFFICE NAME AND ADDRESS Office, Chief of Engineers, U. S. Army Washington, D. C. 20314	12. REPORT DATE July 1977	13. NUMBER OF PAGES 127
14. MONITORING AGENCY NAME & ADDRESS (if different from Controlling Office) 12131p.	15. SECURITY CLASS. (of this report) Unclassified	15a. DECLASSIFICATION/DOWNGRADING SCHEDULE
16. DISTRIBUTION STATEMENT (of this Report) Approved for public release; distribution unlimited.		
17. DISTRIBUTION STATEMENT (of the abstract entered in Block 20, if different from Report) 14 WES-TR-S-77-6		
18. SUPPLEMENTARY NOTES		
19. KEY WORDS (Continue on reverse side if necessary and identify by block number) Finite element method Reinforced earth Walls		
20. ABSTRACT (Continue on reverse side if necessary and identify by block number) Reinforced earth consists of a soil mass whose engineering characteristics and performance have been improved by the introduction of small quantities of frictional material that possesses a relatively high tensile strength. The analysis of a reinforced earth system which incorporates metal strips placed at known intervals in the vertical and transverse directions within the soil mass is a complex problem. The complexity arises from the fact that reinforced earth is a three-dimensional problem and cannot be solved without imposing (Continued)		

DD FORM 1 JAN 73 1473 EDITION OF 1 NOV 65 IS OBSOLETE

Unclassified

SECURITY CLASSIFICATION OF THIS PAGE (When Data Entered)

038100

JP

Unclassified

SECURITY CLASSIFICATION OF THIS PAGE(When Data Entered)

20. ABSTRACT (Continued).

simplification with regard to the mechanical behavior of the system as well as the constitutive relationship governing the interaction between various components of the reinforced earth mass.

The investigation reported herein describes a simplified approach for analyzing the instrumented reinforced earth wall which was previously constructed and loaded to failure at the U. S. Army Engineer Waterways Experiment Station. The three-dimensional problem was approximated by a structurally equivalent two-dimensional system and a two-dimensional finite element method was used in the analysis. The nonlinear behavior of the earth fill of the reinforced earth wall was simulated by hyperbolic formulation. The behavior of the metal skin element and reinforcing strips was assumed linear elastic until the yield stress was reached; thereafter, these metal components were assumed to fail plastically. Interface elements, to accommodate slippage between components of the reinforced earth wall, were also employed in the analysis.

Unclassified

SECURITY CLASSIFICATION OF THIS PAGE(When Data Entered)

THE CONTENTS OF THIS REPORT ARE NOT TO BE
USED FOR ADVERTISING, PUBLICATION, OR
PROMOTIONAL PURPOSES. CITATION OF TRADE
NAMES DOES NOT CONSTITUTE AN OFFICIAL EN-
DORSEMENT OR APPROVAL OF THE USE OF SUCH
COMMERCIAL PRODUCTS.

ACCESSION No.	
RTIS	White Section <input checked="" type="checkbox"/>
DDC	Black Section <input type="checkbox"/>
UNANNOUNCED	<input type="checkbox"/>
JUSTIFICATION:	
BY	
DISTRIBUTION/AVAILABILITY CODES	
Dist.	AVAIL. NO. OF SPECIAL
A-23	

OS.

PREFACE

The study reported herein was conducted at the U. S. Army Engineer Waterways Experiment Station (WES) under the sponsorship of the Office, Chief of Engineers, Project 4A161102AT22, "Theory and Principles of Reinforced Earth," Task A2, Work Unit 004.

The finite element and parametric studies described were performed during the period July 1975 through February 1977 by Drs. M. M. Al-Hussaini and L. D. Johnson, assisted by Mr. Y. S. Jeng, all of the Soil Mechanics Division (SMD), Soils and Pavements Laboratory (S&PL). This report was written by Dr. Al-Hussaini, assisted by Dr. Johnson, under the general direction of Mr. C. L. McAnear, Chief, SMD, and Mr. J. P. Sale, Chief, S&PL.

Directors of WES during the investigation and the preparation of this report were COL G. H. Hilt, CE, and COL J. L. Cannon, CE. Technical Director was Mr. F. R. Brown.

CONTENTS

	<u>Page</u>
PREFACE	2
CONVERSION FACTORS, U. S. CUSTOMARY TO METRIC (SI) UNITS OF MEASUREMENT	4
PART I: INTRODUCTION	5
Background	5
Purpose and Scope	8
PART II: MODELING THE MATERIAL BEHAVIOR OF THE REINFORCED EARTH WALL	10
Stress-Strain Behavior of Foundation Material	10
Stress-Strain Behavior of Sand Fill	15
Stress-Strain Behavior of Reinforcing Strips	16
Elastic Behavior of Skin Element	17
Behavior of Interface Elements	17
PART III: IDEALIZATION OF THE REINFORCED EARTH WALL	30
Idealization as 2D Problem	30
FE Mesh Design	35
Examination of the FE Mesh	37
PART IV: FE ANALYSIS OF THE REINFORCED EARTH WALL	43
FE Analysis	44
Concluding Remarks on the FE Analysis	53
PART V: PARAMETRIC STUDY	55
General Objectives	55
Concluding Remarks on the Parametric Study	60
PART VI: CONCLUSIONS AND RECOMMENDATIONS	63
Conclusions	63
Recommendations	64
REFERENCES	65
APPENDIX A: COMPUTER CODE	A1
APPENDIX B: NONLINEAR STRESS-STRAIN BEHAVIOR FOR SOIL	B1
Homogeneous Soil Element	B2
Interface Soil Elements	B4
APPENDIX C: NOTATION	C1

CONVERSION FACTORS, U. S. CUSTOMARY TO METRIC (SI)
UNITS OF MEASUREMENT

U. S. customary units of measurement used in this report can be converted to metric (SI) units as follows:

<u>Multiply</u>	<u>By</u>	<u>To Obtain</u>
inches	25.4	millimetres
feet	0.3048	metres
square inches	6.4516	square centimetres
square feet	0.09290304	square metres
pounds (mass)	0.4535924	kilograms
pounds (force) per square inch	6894.757	pascals
pounds (force) per square foot	47.88026	pascals
kips (force) per square inch	6894.757	kilopascals
pounds (mass) per cubic foot	16.01846	kilograms per cubic metre
inches per minute	25.4	millimetres per minute
degrees (angle)	0.01745329	radians

FINITE ELEMENT ANALYSIS OF A REINFORCED EARTH WALL

PART I: INTRODUCTION

Background

1. Reinforced earth consists of a soil mass whose engineering characteristics and performance have been improved by the introduction of small quantities of frictional material that possess a relatively high tensile strength. Many reinforced earth walls are designed as gravity structures, the stability of which depends on the frictional stresses between the reinforcing elements and the surrounding soil and the strength and elastic properties of the reinforcing material. The basic design concept of a reinforced earth wall assumes that the soil mass is in active failure governed by Rankine earth pressure theory. The developed lateral pressure is assumed to be counterbalanced by the friction force that develops between the reinforcement and the surrounding soil.

2. An instrumented reinforced earth wall was constructed at the U. S. Army Engineer Waterways Experiment Station (WES) to determine the performance of such a wall during construction and surcharge loading.¹ The wall, shown in Figure 1, was reinforced with galvanized steel strips, 4 in.* wide, 0.024 in. thick, and 10 ft long, spaced at intervals of 2 and 2.5 ft in the vertical and horizontal directions, respectively. Three galvanized strips along the center line of the wall, located at elevations 1, 5, and 9 ft above the bottom of the wall (Figure 2), were instrumented with full SR-4 strain gage bridges at points 1, 2.5, 5, and 7.5 ft from the face of the wall. At the elevation of each instrumented tie and 1 ft away from the face of the wall (i.e., skin element), two pressure cells were placed to measure the induced vertical and horizontal pressures within the fill material.

* A table of factors for converting U. S. customary units of measurement to metric (SI) units is shown on page 4.

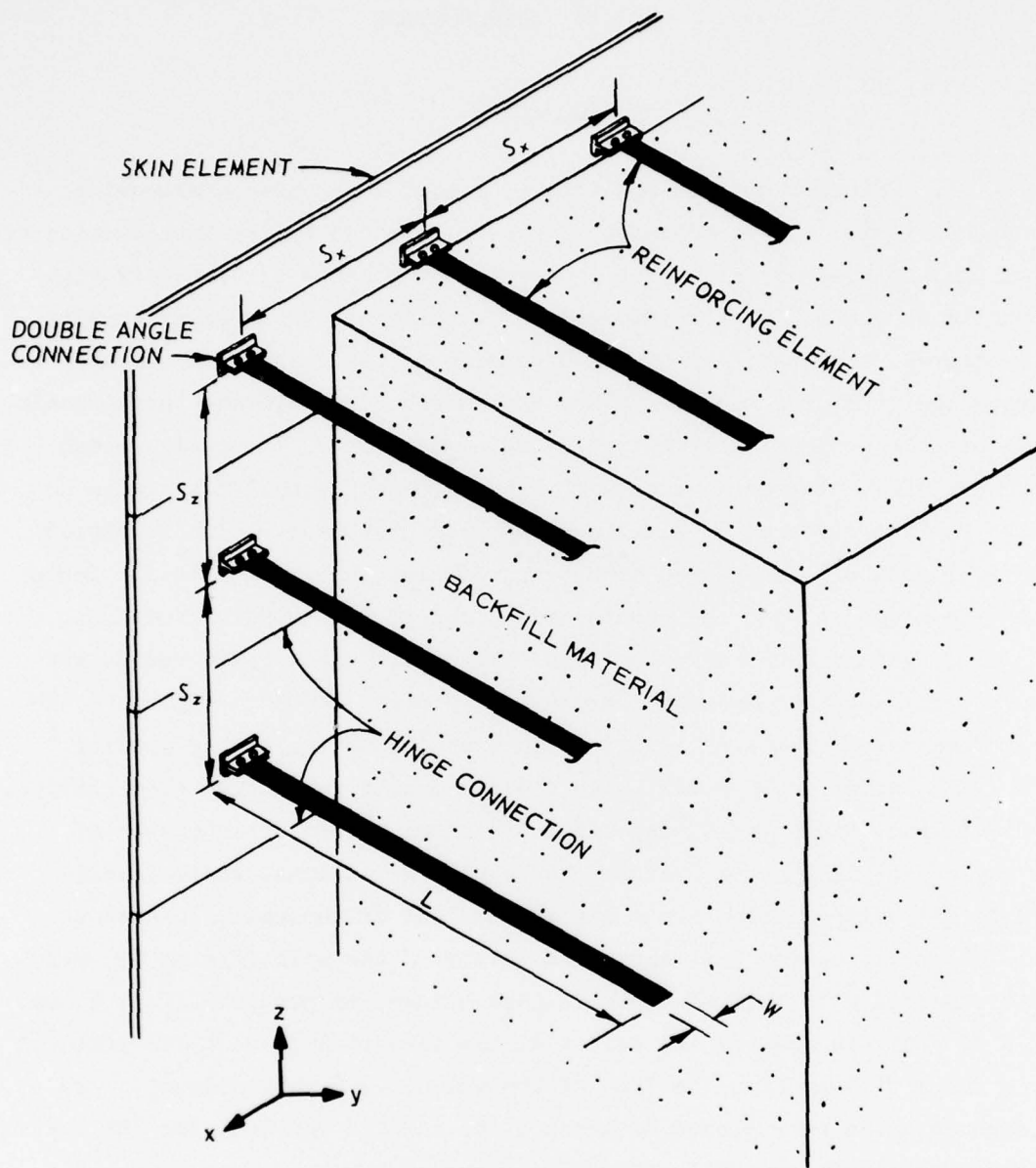


Figure 1. Schematic of major elements of reinforced earth wall

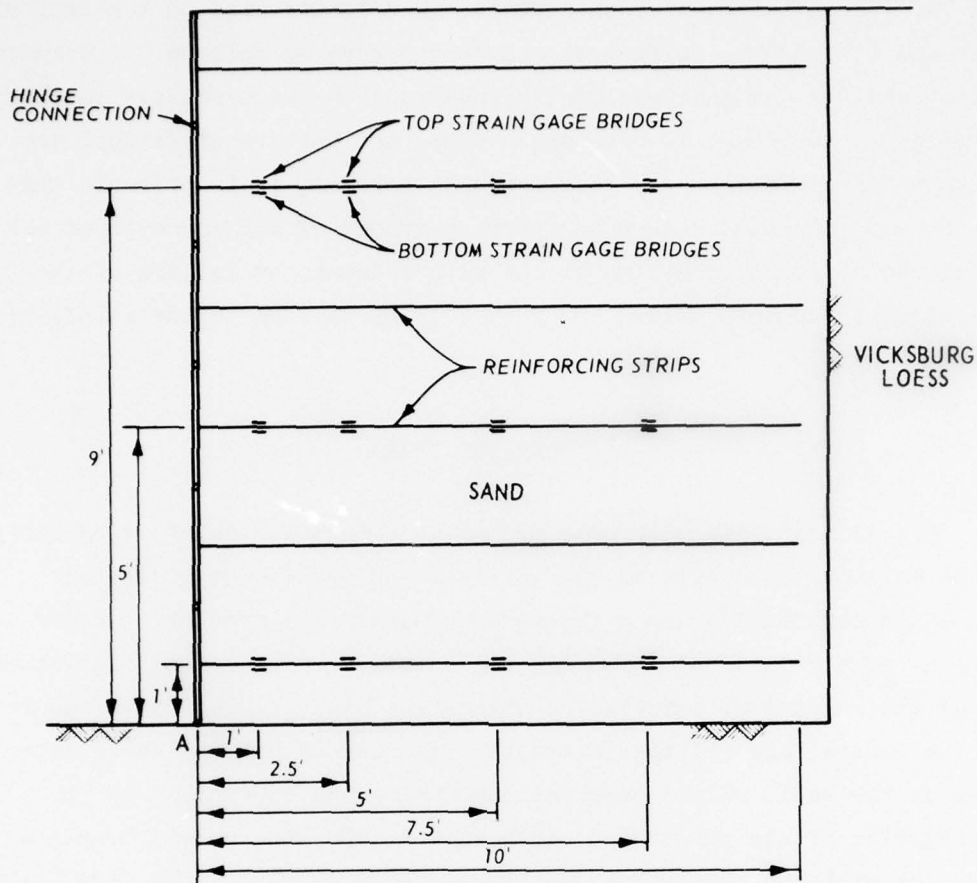


Figure 2. Schematic showing the location of the electric strain gage bridges along the center line of the retaining wall

3. The skin element, which comprised the exposed surface of the wall, was made of Alcoa T11 high-strength aluminum panels normally used in the expedient construction of airfields. Each panel was 2 ft wide, 12 ft long, and 1.6 in. thick and can be connected lengthwise to other panels by integral hinge-type connections, Figures 1 and 2. The reinforcing elements were fixed to the skin element by double angle connectors, Figure 1. Further details of these components are discussed later. A full description of the reinforced earth wall is presented by Al-Hussaini and Perry.¹

4. The reinforced earth structure was constructed to a height of 12 ft and loaded by a uniform surcharge pressure to failure. Instrumentation readings and analyses during construction and surcharge loading are given in Reference 1. The exact cause and pattern of failure are not known since failure was catastrophic; however, it is probable that failure was initiated either by fracture of one of the connections which joined the reinforcing strips to the skin element, by failure of the skin element due to buckling and shear, or by failure of the reinforcing strips.

Purpose and Scope

5. Accurate analysis of a system incorporating reinforcing strips placed at known intervals in the vertical and transverse directions within the soil mass poses a three-dimensional (3D) problem. Proper modeling of a reinforced earth wall also involves reasonable simulation of (a) the mechanical behavior of the earth fill, skin element, and reinforcing strips, and (b) the interaction mechanisms between these components of the wall. Field observations during and subsequent to the construction of the reinforced earth wall at WES were not in complete agreement with the theoretical method proposed originally by Vidal² and later by Lee.³

6. The finite element (FE) method was consequently proposed to simulate as closely as possible various sequences of construction of the reinforced earth wall constructed at WES and to predict the distribution of stresses and deformations within the reinforced earth mass. Although 3D formulations and codes based on the FE method are possible, their use for reinforced earth walls would involve great amounts of human and computer effort. The 3D problem is therefore approximated by a structurally equivalent two-dimensional (2D) system.

7. The soil-structure plane strain 2D FE code originally developed by Clough and Duncan⁴ for analyses of Port Allen and Old River Locks and subsequently modified by Radhakrishnan and Jones⁵ was adopted for use in this study. This code (see Appendix A), which uses the

5-node isoparametric quadrilateral element, is capable of simulation of the incremental buildup of the wall and the concentrated loading construction sequences needed for this study. The nonlinear behavior of the earth fill of the reinforced wall is simulated by a hyperbolic formulation developed by Duncan and Chang.⁶ The behavior of the metal skin element and reinforcing strips is assumed linear elastic until the yield stress is reached; thereafter, these metal components are assumed to fail plastically.

8. Interface elements available in the FE code were also used to accommodate slippage between and separation of the components of the reinforced wall. The interface elements are especially important in separating the ends of the reinforcing strips from the original in situ earth face which supports the back of the reinforced earth mass, thereby permitting the stresses in the reinforcing strips to approach zero at the ends.

9. FE analyses of the reinforced wall were performed for the construction of the wall and surcharge loading to failure. The numerical predictions of the FE analyses are compared with field observations, and conclusions regarding design analyses are presented.

PART II: MODELING THE MATERIAL BEHAVIOR OF
THE REINFORCED EARTH WALL

10. Because of the composite nature of the reinforced earth wall, it is essential that the stress-strain relationships for the foundation soil, fill material, reinforcing strips, and skin element are accurately defined. It is also essential that the interaction between these composite materials within the reinforced mass be considered.

Stress-Strain Behavior of Foundation Material

11. The stress-strain relationship for the foundation material was approximated by the hyperbolic formulation, summarized in Appendix B, and stated by the following expressions:*

$$E_t = (1 - \lambda_1)^2 E_i \quad (1a)$$

$$E_i = K P_a \left(\frac{\sigma_3}{P_a} \right)^n \quad (1b)$$

$$\lambda_1 = \frac{R_f (\sigma_1 - \sigma_3) (1 - \sin \phi)}{2c \cos \phi + 2\sigma_3 \sin \phi} \quad (1c)$$

where

- E_t = tangent modulus
- E_i = initial modulus
- K = hyperbolic loading parameter
- P_a = atmospheric pressure
- σ_3 = minor principal stress
- n = pure number
- R_f = failure ratio

* For convenience, symbols and abbreviations used herein are listed and defined in the Notation (Appendix C).

σ_1 = major principal stress
 ϕ = angle of internal friction
 c = cohesion

12. Laboratory tests were not conducted on the foundation material because these tests were not required in the conventional design analysis of the wall. However, several triaxial Q tests previously conducted on soil specimens with similar characteristics were used in the FE analysis. The stress-strain curves and Mohr-Coulomb criteria of the ML soil used in the FE analysis are presented in Figures 3 and 4, respectively. The stress-strain data were replotted in the linear form, Figure 5, which shows that most of the data points of each test fell on a straight line, indicating that the shape of the stress-strain curve of the ML material conforms with the hyperbolic representation. From Figure 5, the value of the initial modulus E_i , represented by the inverse of the intercept on the ordinate, and the value of $(\sigma_1 - \sigma_3)_{ult}$, represented by the inverse of the slope of the line, were obtained. The failure ratio R_f is equal to $(\sigma_1 - \sigma_3)_f / (\sigma_1 - \sigma_3)_{ult}$ where $(\sigma_1 - \sigma_3)_f$ is the principal stress difference at failure, as illustrated in Figure 3. A summary of the ML soil parameters needed for the hyperbolic stress-strain representation is tabulated below.

σ_3 psi	E_i psi	$(\sigma_1 - \sigma_3)_f$ psi	$(\sigma_1 - \sigma_3)_{ult}$ psi	R_f	$(\frac{\sigma_3}{P_a})$
6.95	3,700	27.78	29.85	0.93	0.473
20.84	5,550	62.51	70.42	0.89	1.418
41.67	8,000	111.12	125.00	0.89	2.835
69.45	12,500	168.75	188.70	0.89	4.790
				Average	0.90

13. The values of the loading stiffness K and the exponential constant n needed to incorporate the effect of the confining pressure σ_3 in the hyperbolic constitutive model are obtained by plotting E_i versus (σ_3/P_a) as shown in Figure 6. The best fit line was used for the

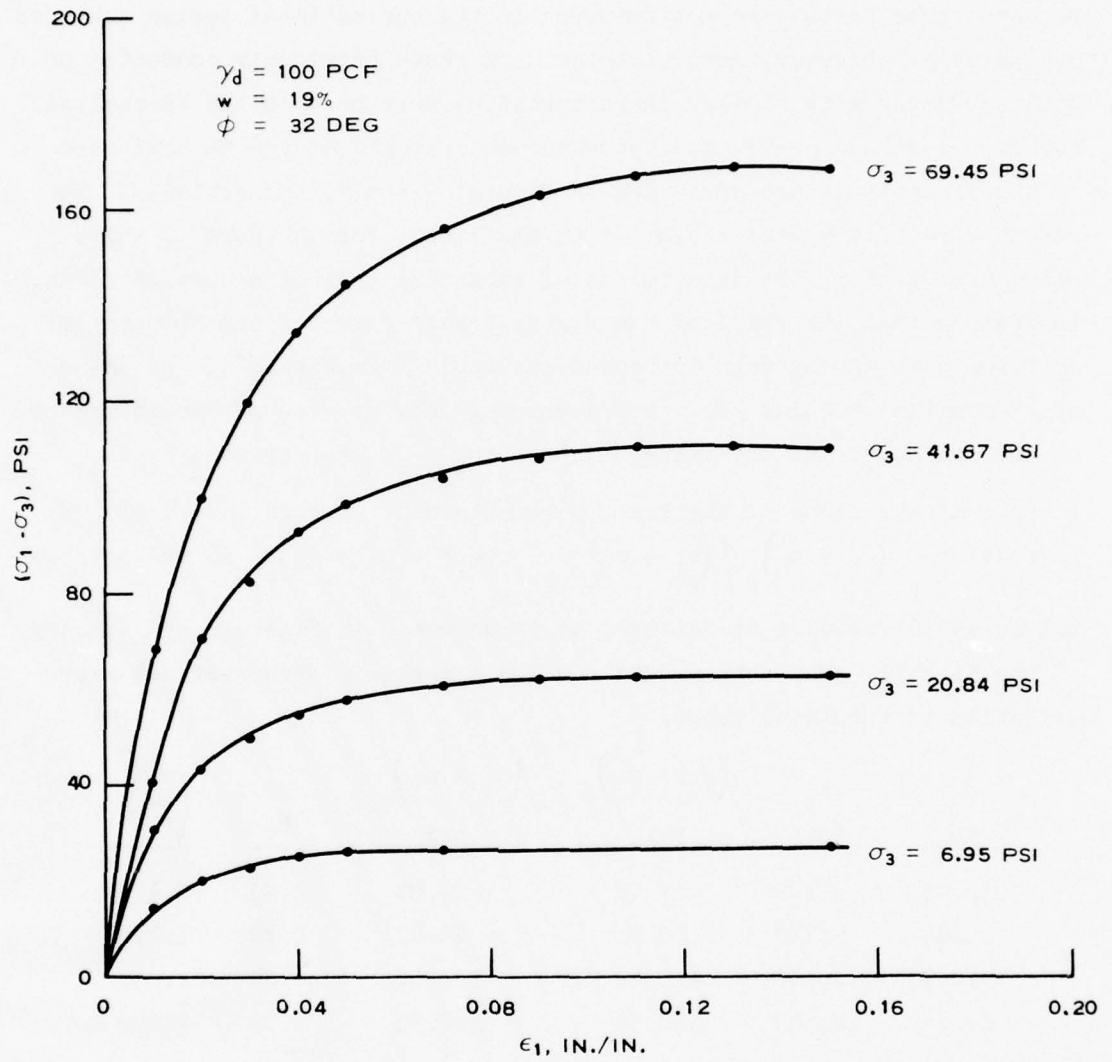


Figure 3. Stress-strain curves for the ML soil

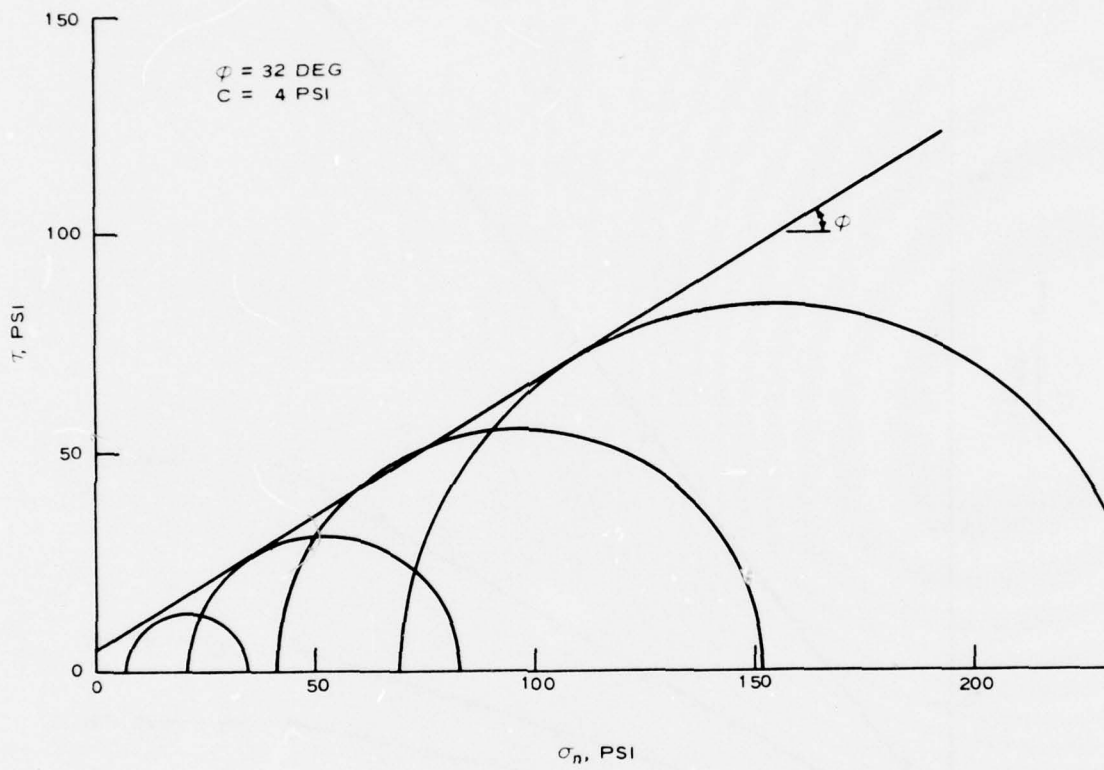


Figure 4. Mohr's failure envelope for the ML soil

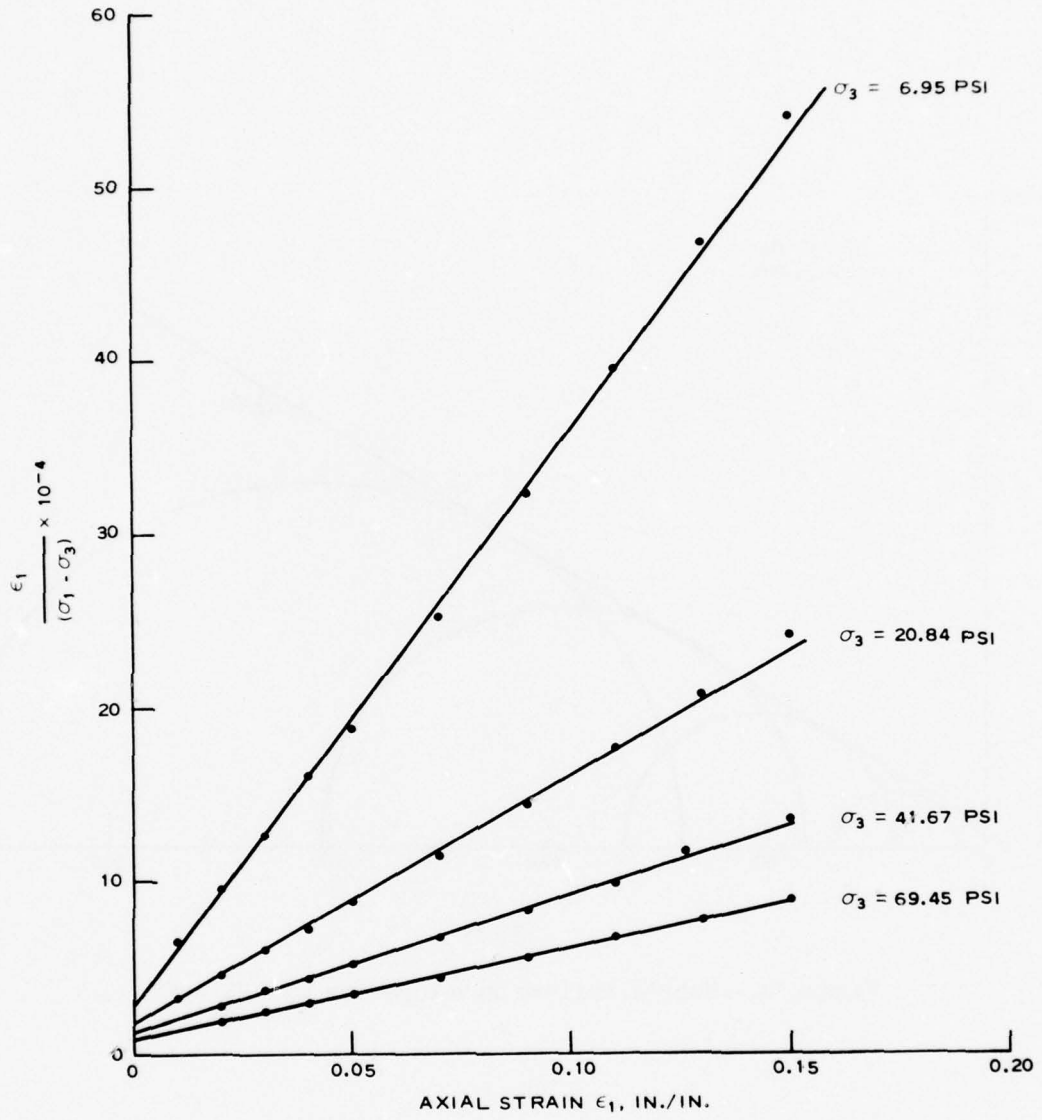


Figure 5. Linearized stress-strain curves for the ML soil

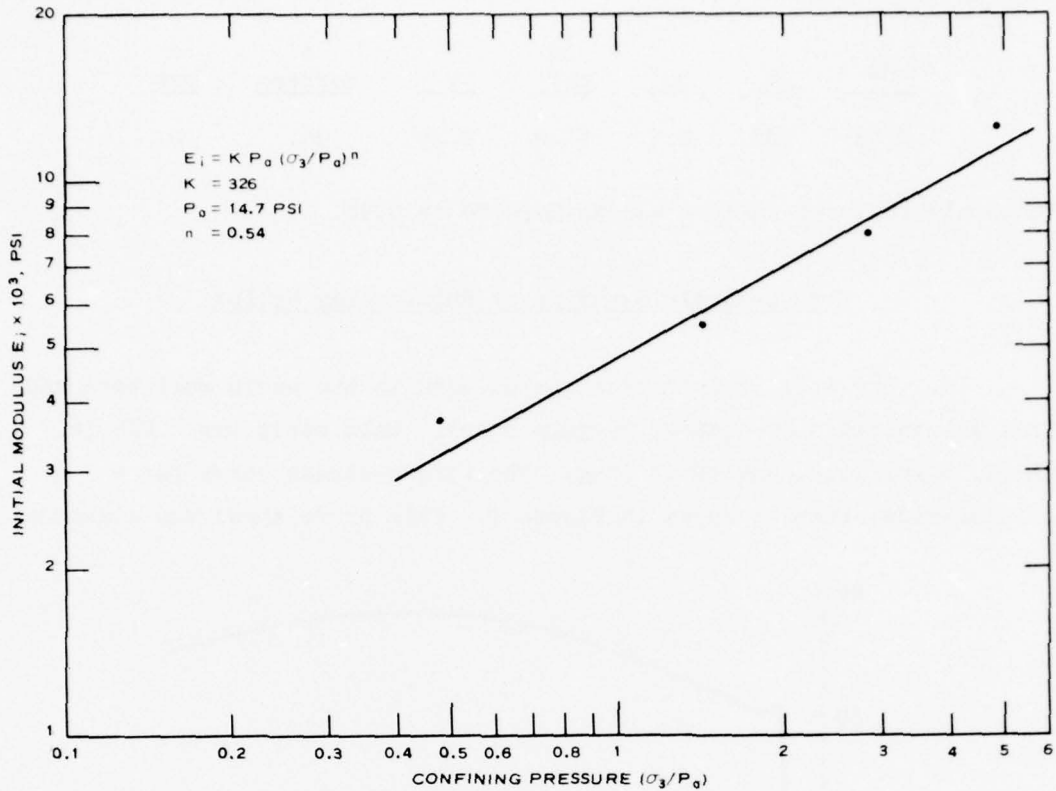


Figure 6. Variation of the initial modulus E_i versus (σ_3/P_a) for the ML soil

analysis. Since adequate information on the volumetric behavior of the ML soil was not available, Poisson's ratio ν was assumed constant at 0.33. Poisson's ratio at failure was assumed to be 0.48.

Stress-Strain Behavior of Sand Fill

14. The fill material used in the construction of the reinforced earth wall was clean concrete sand with particles ranging from subangular to angular. More detailed physical properties of the sand fill used are presented in an earlier report.¹ The same procedure of hyperbolic stress-strain analysis, presented previously in describing the behavior of the foundation soil, was used to obtain the constitutive equations for the sand fill. The hyperbolic parameters and other properties adopted for the FE analysis were as follows:

R_f	K	n	γ_d pcf	ν	ϕ degrees	c psf
0.85	580	0.5	97.2	0.30	36	0

Poisson's ratio at failure was assumed to be 0.48.

Stress-Strain Behavior of Reinforcing Strips

15. The steel reinforcing strips used in the earth wall were made from galvanized zinc-coated, 24-gage steel. Each strip was 0.025 in. thick, 4 in. wide, and 10 ft long. The stress-strain curve for a 1/2-in.-wide strip is shown in Figure 7. This curve shows the classical

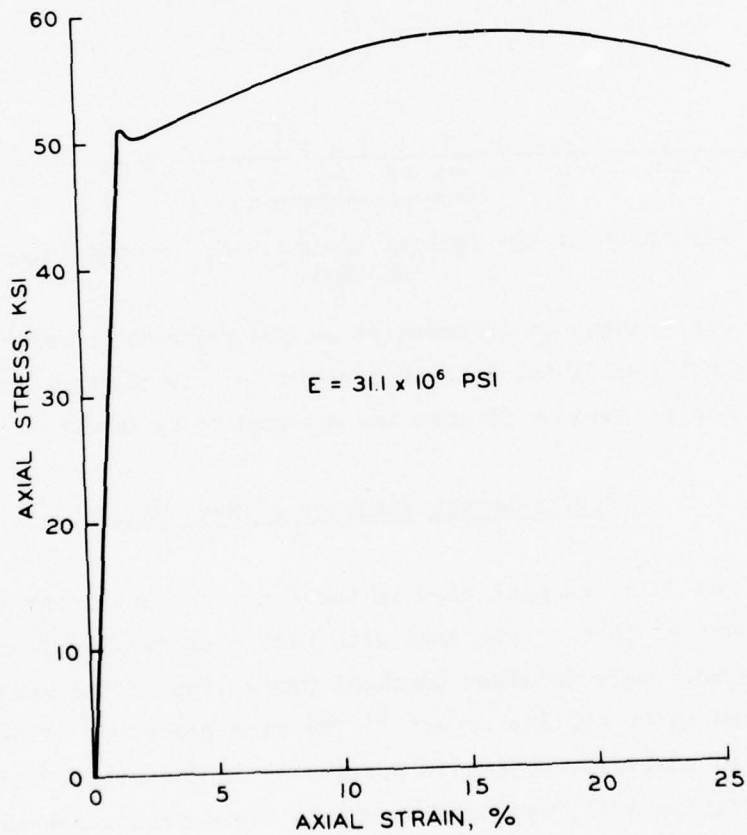


Figure 7. Average stress-strain relationship for the galvanized steel strips

stress-strain curve with modulus of elasticity $E = 31.1 \times 10^6$ psi and yield stress $\sigma_y = 51$ ksi. The Poisson's ratio ν needed for the FE analysis was assumed equal to 0.28.

Elastic Behavior of Skin Element

16. The skin element was made of Alcoa T11 high-strength aluminum panels, 2 ft wide, 12 ft long, and 1.6 in. thick, connected lengthwise to each other by a hinge connector. The physical and elastic properties of the panels are shown below.

Moment of inertia per foot of panel width	= 1.368 in. ³
Section modulus per foot of panel width	= 1.396 in. ³
Modulus of elasticity	= 10×10^6 psi
Weight per square foot	= 4.61 lb
Poisson's ratio	= 0.33
Thickness of the panel	= 1.6 in.
Thickness of the sheet	= 0.1 in.
Yield stress	= 35,000 psi

17. The reinforcing elements were fixed to the skin element through a connector as shown in Figure 8. The connector consisted of double angles, each of which was 1-1/2 by 3 by 1/4 in. and 12 in. long, used to grip the reinforcing strip and tie it to the skin element by two 1/4-in. bolts. This type of connection was simple and adequate as long as the skin element exhibited very small or no bending deformations.

Behavior of Interface Elements

18. The interface element formulation introduced by Goodman and his coworkers⁷ was incorporated in the FE program used in this study. The constitutive behavior of the interface elements was based on the hyperbolic shear stress-displacement model originally formulated by Duncan and Chang⁶ (Appendix A) and summarized by the following equations:

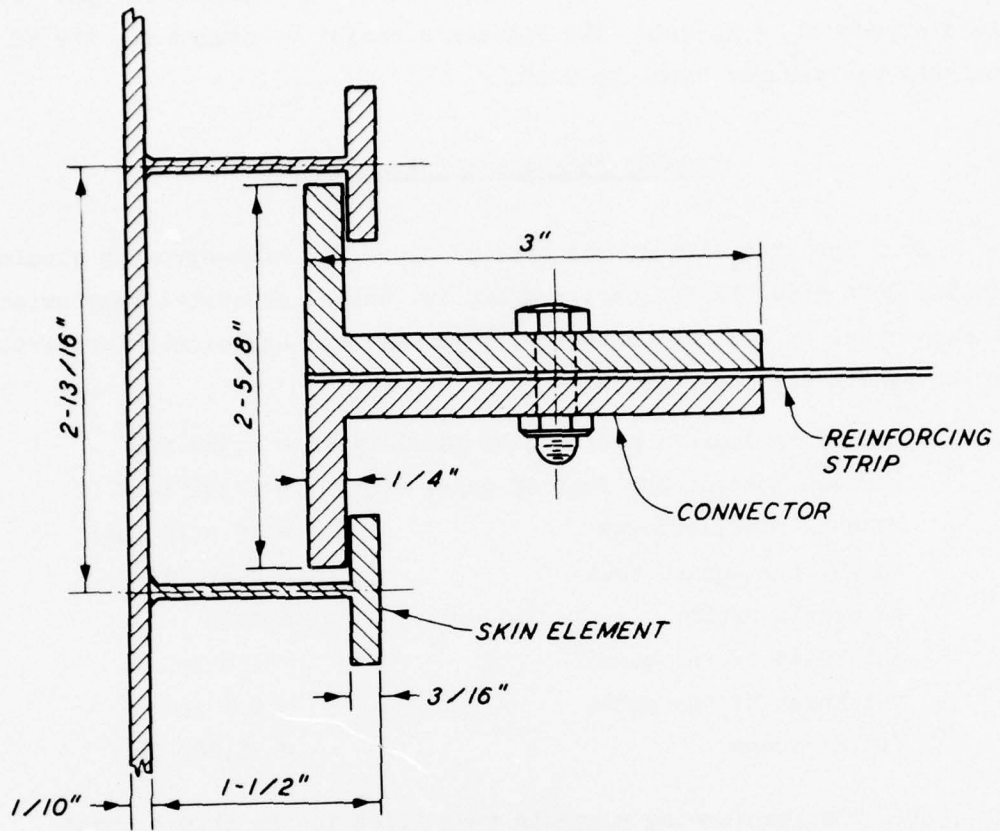


Figure 8. Details of the connector tying the reinforcing strip to the skin element

$$K_{st} = (1 - \lambda_2)^2 K_i \quad (2a)$$

$$K_i = K_j \gamma_w \left(\frac{\sigma_n}{P_a} \right)^m \quad (2b)$$

$$\lambda_2 = \frac{R_f \tau}{C_a + \sigma_n \tan \delta} \quad (2c)$$

where

K_{st} = tangent shear stiffness

K_i = initial shear stiffness

K_j = dimensionless number
 γ_w = unit weight of water
 σ_n = normal stress
 m = exponential number
 τ = shear stress
 C_a = adhesion
 δ = angle of friction

The normal stiffness of the interface element is assumed to behave elastically and, given a high value of 10^8 psf, to inhibit mutual penetration of the materials adjacent to the interface element. The tangent shear and normal stiffnesses were each set to a small residual value K_r of 10 psf if the normal stress of the interface element became tensile, permitting voids to develop in the interface. The shear stiffness is also reduced to the residual shear stiffness K_r if the shear stress at the interface equals or exceeds the Mohr-Coulomb strength.

Interface behavior
between reinforcing strip and sand

19. The nonlinear shear stress-displacement relationship between the sand and the reinforcing was determined, prior to the field test, using a specially designed shear box. The testing device, shown in Figure 9, is similar to the direct shear box except that the lower frame was replaced by a sheet of the galvanized steel glued to a wooden block.

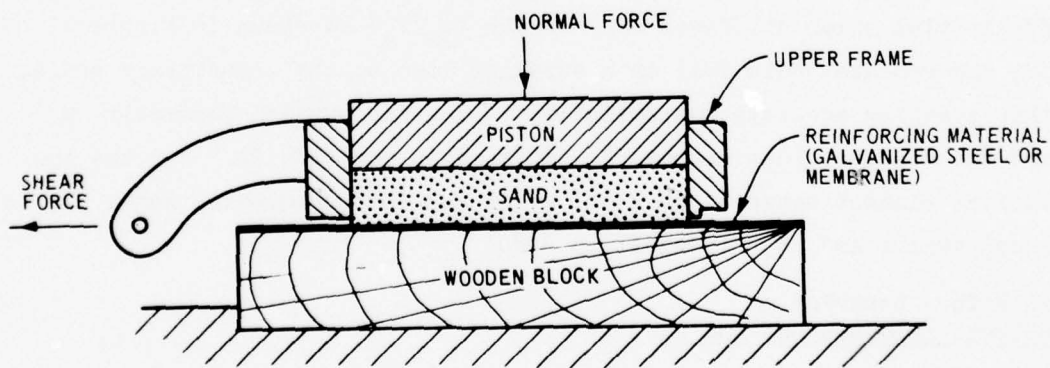


Figure 9. Modified shear box for determining skin friction angle between the sand and the reinforcing material

The sand was compacted to a dry density of 101.7 pcf. Three direct shear tests were conducted with normal stresses of 10, 50, and 100 psi, respectively, at a shear deformation rate of 0.5 in. per min.

20. The shear stress-deformation relationship between the sand and the galvanized steel is shown in Figure 10; these curves provide a reasonably accurate determination of the initial shear stiffness K_i . The ultimate shear stress τ_{ult} was obtained from the inverse of the slope of the linearized shear stress-deformation relationship as shown in Figure 11. The failure ratio R_f was obtained by dividing the peak shear stress τ_{max} , as measured from Figure 10, by the ultimate shear stress τ_{ult} ; for these tests the value R_f was approximately equal to unity. The angle of friction δ and the adhesion C_a were obtained by plotting the shear stress at failure τ_{max} versus σ_n as shown in Figure 12. A summary of the parameters needed for the hyperbolic shear stress-displacement behavior of the interface elements between the sand fill and the galvanized steel is presented below.

σ_n psi	τ_{max} psi	K_i psi	C_a psi	δ degrees	R_f
10	3.06	81	0	18	1.0
50	11.95	444	0	18	1.0
100	32.09	1020	0	18	1.0

21. The influence of stress level was accounted for by plotting the initial shear stiffness K_i versus (σ_n/P_a) as shown in Figure 13. The experimental data fell on a straight line on the logarithmic scale, thus enabling accurate determination of the exponential parameter m and the dimensionless number K_j defined in Equation 2b. For the interface element between the steel strip and the surrounding sand, m is equal to 1.1 and K_j is equal to 3280.

Interface behavior
between skin element and sand

22. No direct shear test was conducted to examine the interface behavior between the skin element and the sand fill. However, the non-linear parameter obtained previously for the sand on galvanized steel

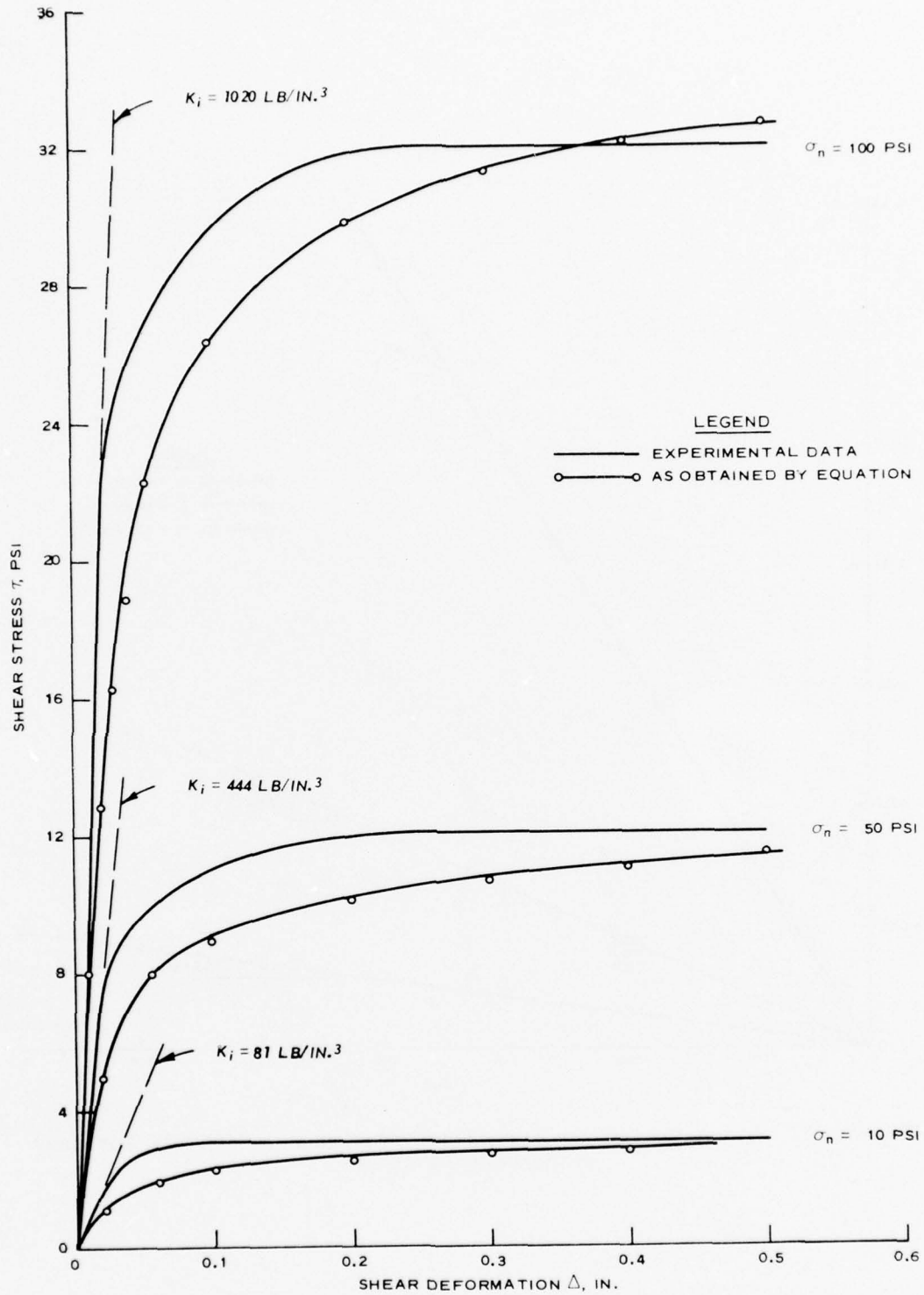


Figure 10. Shear stress-deformation relationship between the sand and the galvanized steel strips

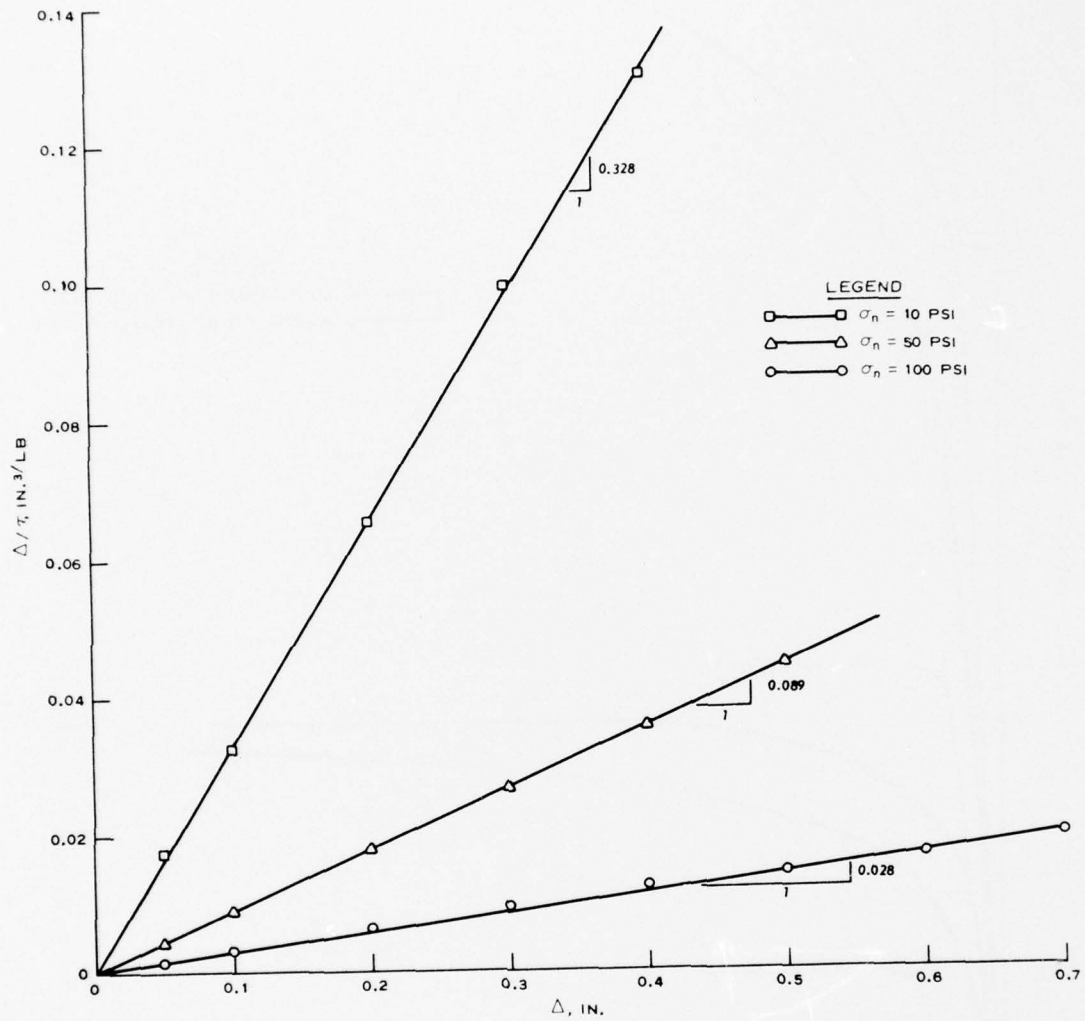


Figure 11. Linearized shear stress-deformation relationship for sand on galvanized steel

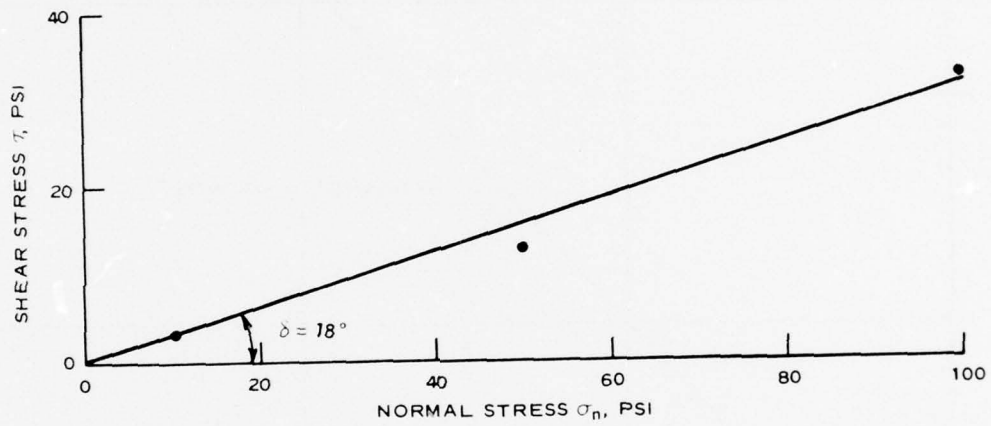


Figure 12. Mohr-Coulomb envelope for sand on galvanized steel

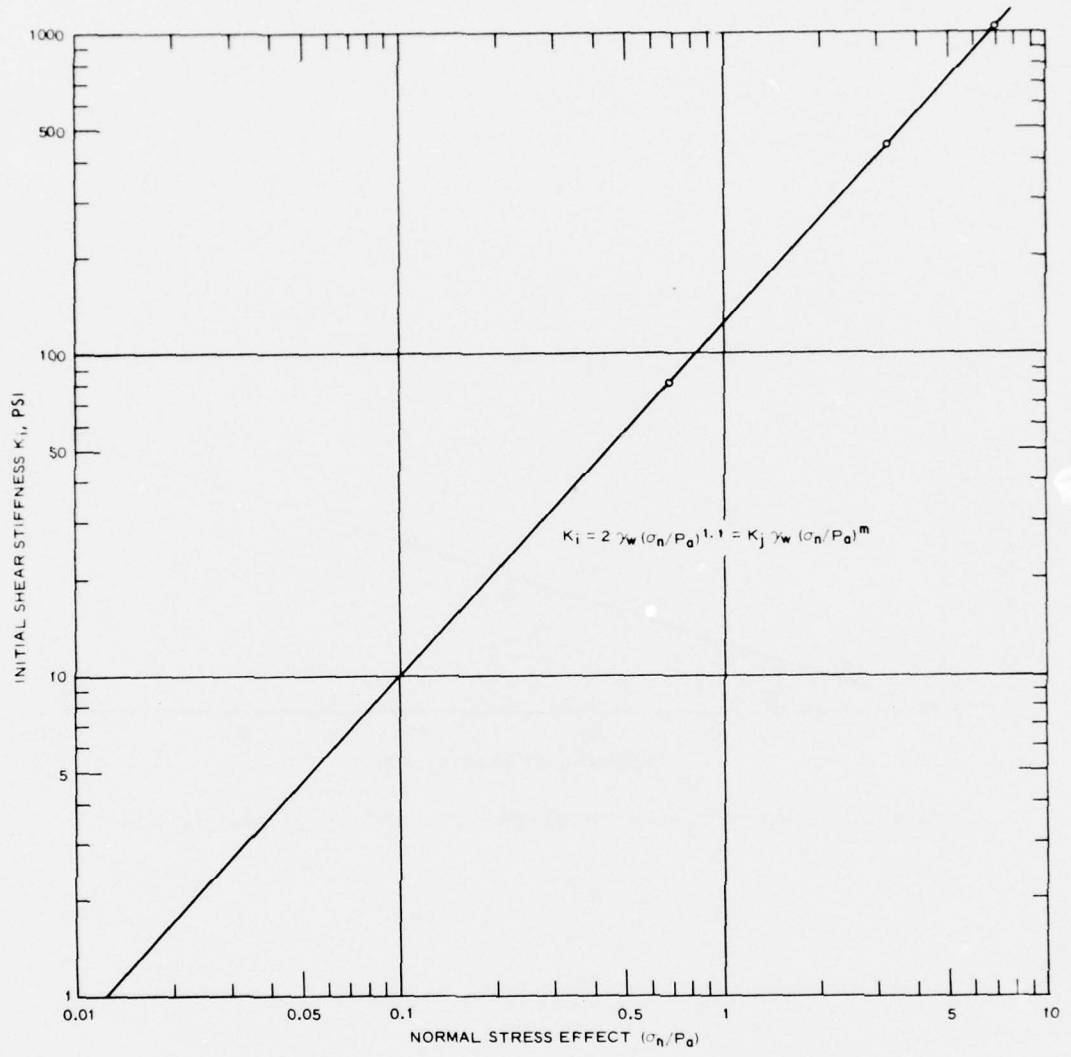


Figure 13. Variation of K_i versus (σ_n/P_a) for sand on galvanized steel

was used to describe the interface behavior between the skin element and the sand.

Interface behavior
between sand and natural soil

23. The nonlinear constitutive equation presented in Equation 2 was used to describe the interface behavior between the sand fill and the surrounding natural ground. Three direct shear tests in which the lower part of the shear box was filled with the ML soil and the upper part was filled with compacted sand were conducted, and the linearized shear stress-displacement relationship is presented in Figure 14. The figure shows that the experimental points deviate slightly from the straight line, which indicates that the hyperbolic representation is only an approximation for the behavior of this material. The Mohr-Coulomb failure envelope for sand on silt, presented in Figure 15, showed an angle of friction of 34 deg and a small adhesion of 0.05 psi.

24. The influence of the stress level on the behavior of the interface elements between the sand and the natural ML soil was accounted for by plotting the initial shear stiffness K_i versus (σ_n/P_a) as shown in Figure 16. The figure shows that the experimental points deviate significantly from the ideal straight line; however, the best fit line was used for evaluating m and K_j . A summary of the parameters needed for the nonlinear constitutive equation for the interface element between the sand and the natural ML soil is presented below.

<u>C_a</u> psi	<u>δ</u> degrees	<u>R_f</u>	<u>K_j</u>	<u>m</u>
0.05	34	0.86	14,523	0.68

25. Comparison between the shear stress-deformation curves obtained by experimental tests and those generated by the hyperbolic formulation, shown in Figure 17, indicates a reasonable agreement between the two respective curves.

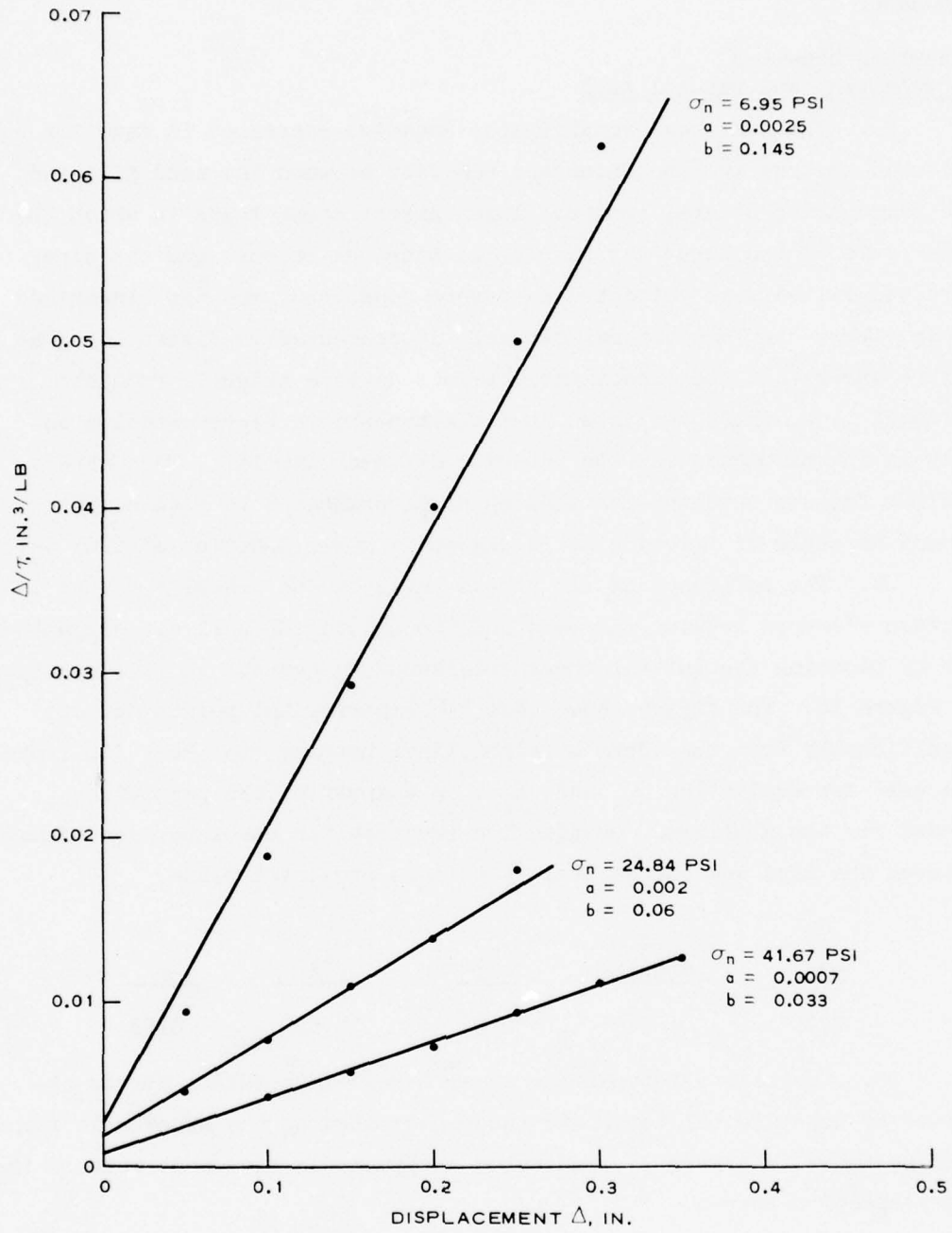


Figure 14. Linearized shear stress-displacement relationship for sand on silt

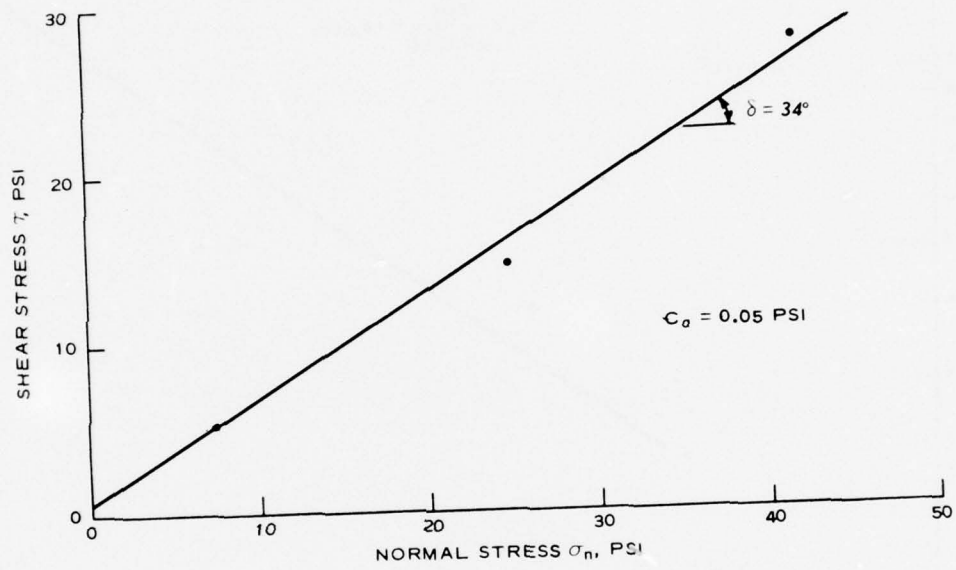


Figure 15. Shear stress versus normal stress at failure for sand on silt

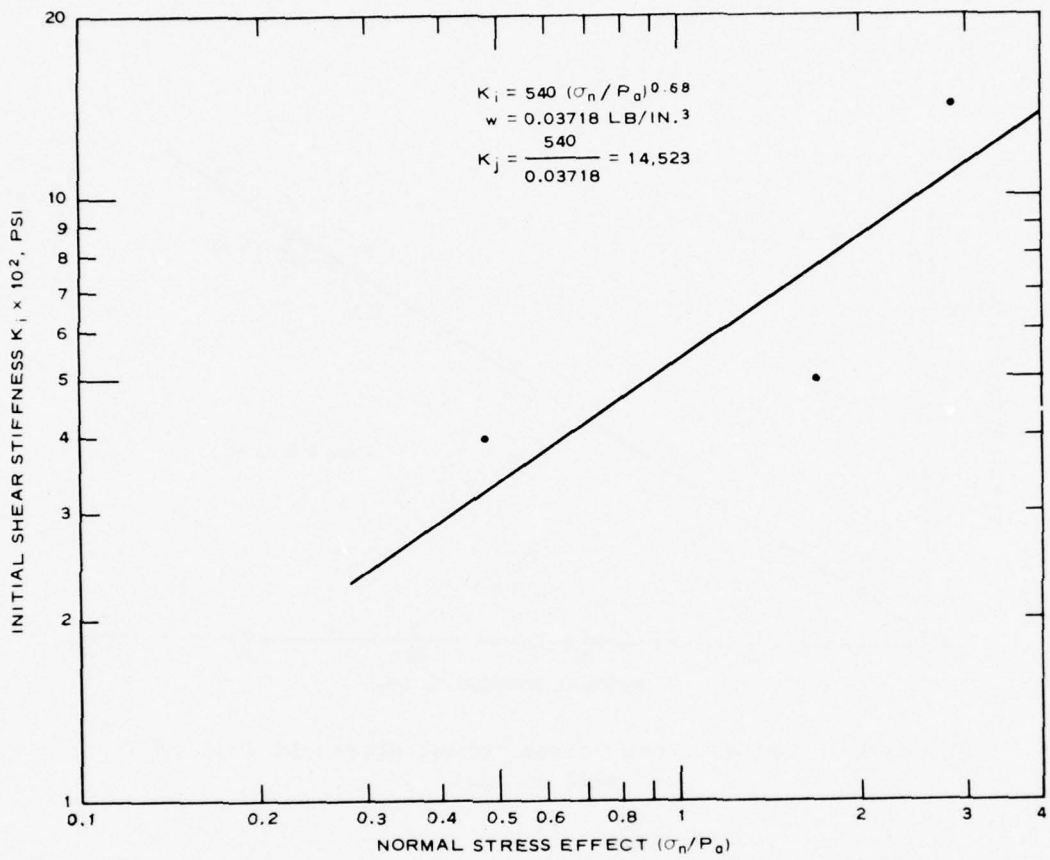


Figure 16. Variation of initial shear stiffness with respect to (σ_n/P_a) for interface element between the sand fill and the natural ML soil

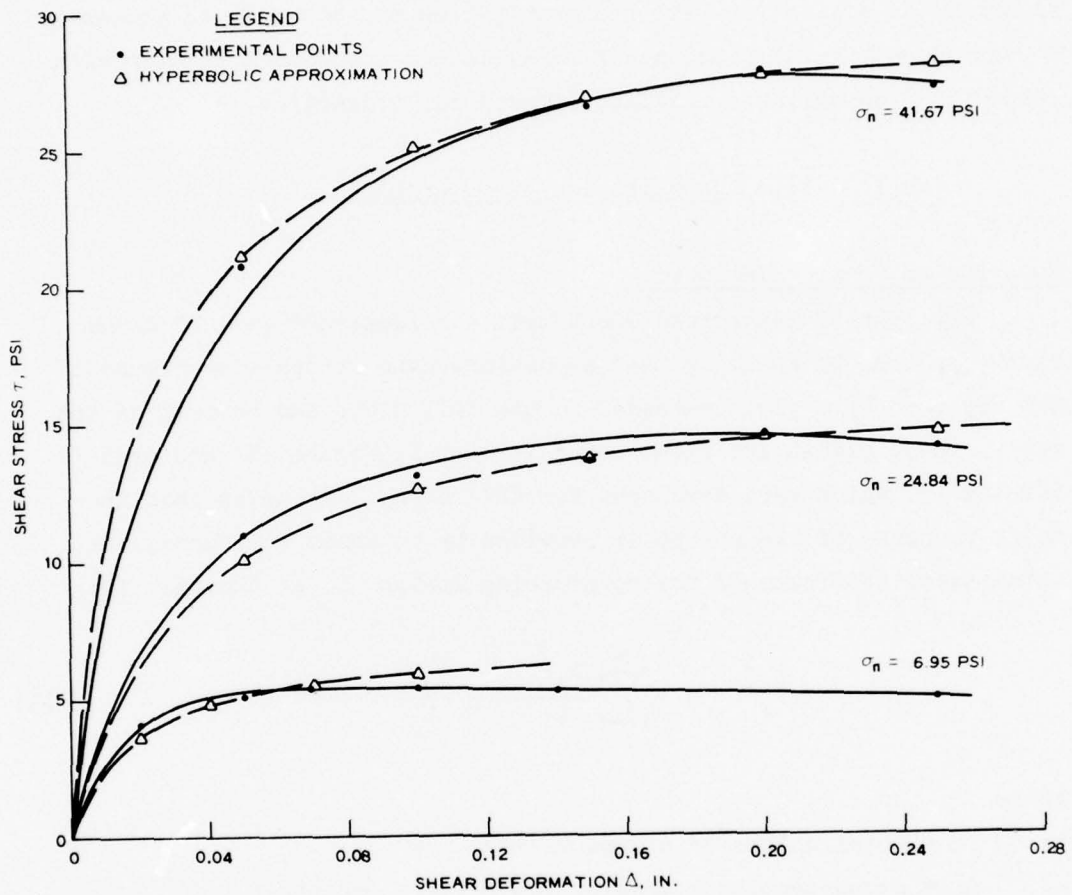


Figure 17. Shear stress-deformation relationship along plane between the sand fill and the ML soil

PART III: IDEALIZATION OF THE REINFORCED EARTH WALL

26. The reinforced earth wall is a complicated 3D problem, the complexity of which is compounded by the introduction of the steel strips as a reinforcing element. The solution of such a problem requires a substantial amount of human effort and computer time. In order to arrive at a solution with reasonable time and cost, it is necessary to introduce a certain amount of idealization and simplification with respect to geometry and modeling of material properties.

Idealization as 2D Problem

Modeling of reinforcing strip

27. The 3D reinforced earth wall was idealized as a 2D plane strain problem by assuming that the reinforcing strips (see Figure 1) are replaced by a plate extended to the full width and breadth of the wall. These plates are illustrated in mesh I (Figure 18) and mesh II (Figure 19) which were developed for this study. Assuming that the major response of the strips is provided by an axial stiffness, the total axial stiffness of the reinforcing strips S of the wall is:

$$S = \sum_{j=1}^n \frac{A_j E_j}{L_j} = n \frac{A_s E_s}{L_s} \quad (3)$$

where

n = total number of strips in each row

A_s = cross-sectional area of the reinforcing strip

E_s = modulus of elasticity of the galvanized steel

L_s = length of the reinforcing strip

28. The equivalent stiffness of the plate that substitutes for each row of steel strips S_e may be defined as

$$S_e = \frac{A_e E_e}{L_e} \quad (4)$$

BEST AVAILABLE COPY

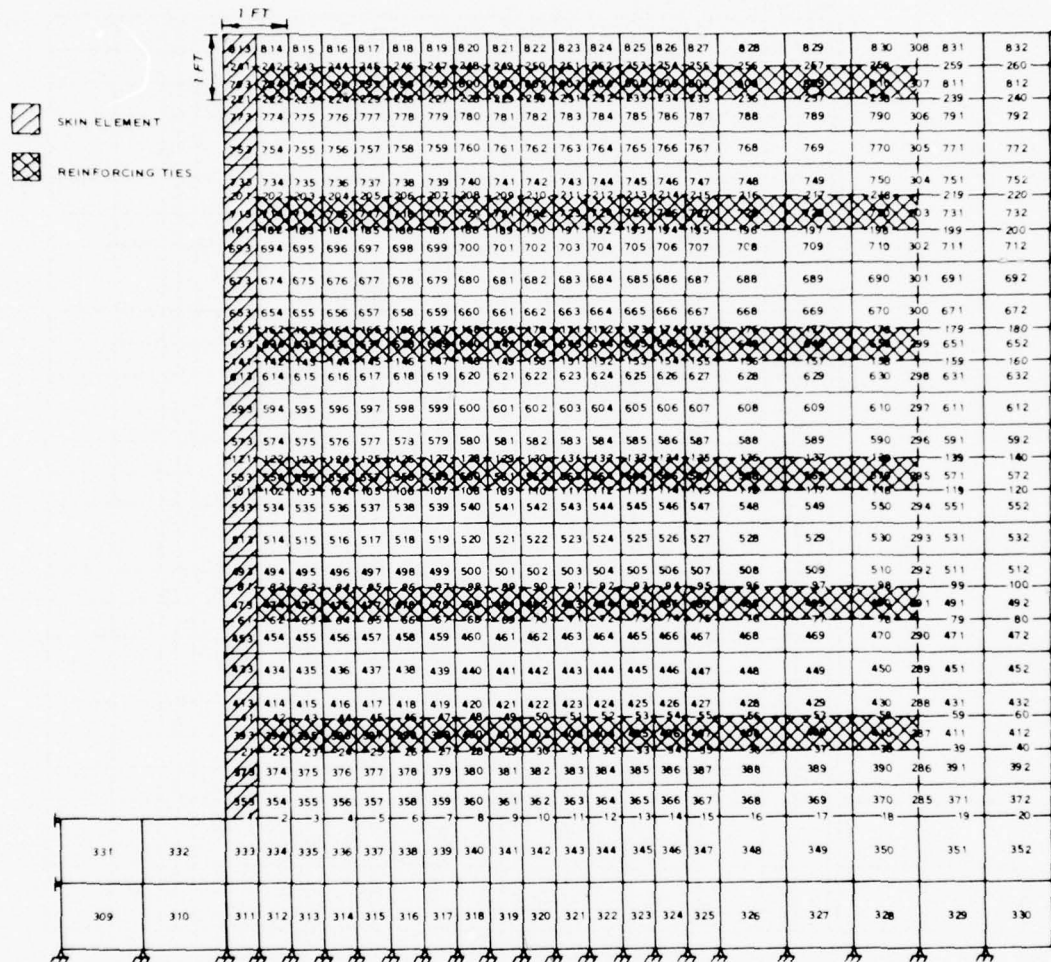


Figure 18. FE mesh I employed in the analysis of the reinforced earth wall

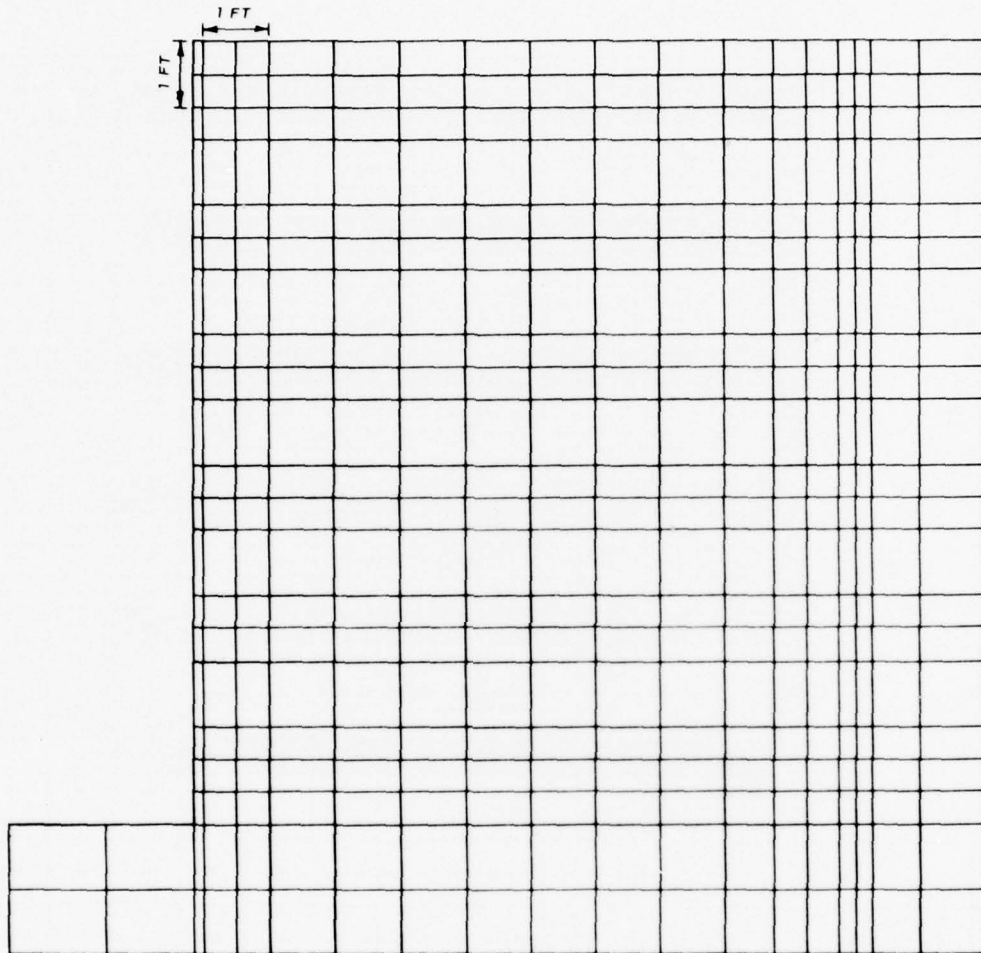


Figure 19. FE mesh II for the reinforced earth wall

where

A_e = equivalent cross-sectional area of the steel strips

E_e = equivalent modulus of the steel strips

L_e = equivalent length of the steel strips

28. Because the stiffness S and the equivalent stiffness S_e should be the same and also because the length L_s and the equivalent length L_e remain the same, thus by equating Equations 3 and 4, the equivalent stiffness E_e can be determined as

$$E_e = \frac{nA_s E_s}{A_e} \quad (5)$$

29. For the prototype reinforced earth wall the cross-sectional area of the reinforcing strip was 0.096 sq in., the modulus of elasticity of the galvanized steel was 31.1×10^6 psi, and the number of strips in each row was 6. The thickness of the equivalent reinforcing strip elements, as shown in mesh I (Figure 18), was 6 in. and as shown in mesh II (Figure 19), 0.024 in. The width of the equivalent plate for both meshes (i.e. length of the reinforced earth wall) was 16 ft. Substituting the appropriate values in Equation 5, the magnitude of E_e can be determined.

$$\text{Mesh I: } E_e = \frac{6 \times 0.096 \times 31.1 \times 10^6}{0.5 \times 16} = 2.24 \times 10^6 \text{ psf}$$

$$\text{Mesh II: } E_e = \frac{6 \times 0.096 \times 31.1 \times 10^6}{0.002 \times 16} = 5.598 \times 10^8 \text{ psf}$$

The unit weight of the equivalent reinforcing strips of mesh I was assumed identical with that of the sand backfill because of the very small cross-sectional area of the actual reinforcing strips. The unit weight of the equivalent reinforcing strips in mesh II was taken as 492 pcf, which is the unit weight of the actual strips; the very small area of these strips should cause little additional contribution to the stresses from gravity using mesh II.

Modeling of skin element

30. The behavior of the skin element, like that of the rest of the reinforced earth mass, was treated as a plane strain problem whose major response is provided by bending. The aluminum panels that represent the skin element, as shown in Figure 1, were replaced by an equivalent beam element of similar deflection response depending on the dimensions of the skin element in the FE meshes, Figures 18 and 19. The equation used to satisfy equal bending deformation response between the prototype and the model was:

$$\frac{E_a I_a}{L_a} = \frac{E_e I_e}{L_e} \quad (6)$$

where

E_a = modulus of elasticity of the aluminum panel

I_a = moment of inertia of the aluminum panel per unit width

L_a = length of the beam (S_z) between any two rows of reinforcing strips (see Figure 1)²

E_e = equivalent modulus of elasticity

I_e = equivalent moment of inertia per unit width

L_e = equivalent length of the beam

31. Since the beam lengths of the skin element and its model are the same (i.e., $L_a = L_e$), the equivalent modulus of elasticity for the skin element can be expressed by:

$$E_e = E_a \frac{I_a}{I_e} \quad (7)$$

From paragraph 16, the modulus of elasticity and the moment of inertia are 10×10^6 psi and 1.368 in.^4 , respectively. The depth of the equivalent beam, as shown in Figure 18 for mesh I, is 6 in.; therefore, the equivalent moment of inertia I_e is equal to 216 in.^4 . Substituting the values of E_a , I_a , and I_e in Equation 7, the magnitude of E_e for mesh I can be obtained as follows:

$$E_e = \frac{10 \times 10^6 \times 1.368}{216} = 6.33 \times 10^4 \text{ psi } (9.13 \times 10^6 \text{ psf})$$

The magnitude of E_e for mesh II (Figure 19) with skin element thickness of 1.6 in. was 3.34×10^6 psi (4.8×10^8 psf).

32. The aluminum panels of the skin element were hinged rather than bonded together into an elastically rigid unit; the actual modulus of the skin element may consequently have been substantially less than that assumed for the FE analyses using meshes I and II.

33. Two iterations were made for computation of stresses during each construction and loading sequence. The first iteration indicated the appropriate modulus (based on input material properties) to use for computation of the stresses during the second iteration.

FE Mesh Design

34. In addition to idealizing the reinforced earth wall as a 2D problem, there are a number of other factors which affect the design of the FE mesh. Some of these factors are:

- a. Design of elements required to obtain a satisfactory result.
- b. Boundary conditions.
- c. Number of construction and loading sequences.
- d. Location of interface elements.

Design of elements

35. It is always desirable to use a minimum number of elements that achieve a satisfactory degree of accuracy so that the computer time and hence computation cost are minimum. However, for a given number of elements, the degree of accuracy in simulating a particular behavior depends upon the correlation between the displacement pattern assumed and the displacement of the actual events. Because of the uncertainties regarding the assumed displacement and the preliminary nature of this study, simple meshes using relatively large numbers of rectangular elements, as shown in Figures 18 and 19, were developed to improve accuracy.

36. The elements in mesh I, Figure 18, were square to minimize distortion of results that might occur if the aspect ratio is different from unity. The elements in mesh II were reduced in total number

compared to mesh I to increase computation efficiency and dimensions were adjusted to closely simulate actual dimensions of the components of the wall.

Boundary conditions

37. The boundaries should be located so that they will have negligible effect on the main structure to be analyzed. In view of the preliminary nature of this analysis, the boundaries were kept at a distance of 2 ft from the reinforced earth mass. No calculation was used to determine the influence of the boundary conditions on the FE results.

38. The left and right vertical boundaries were confined laterally and the bottom horizontal boundary was confined both laterally and vertically. During each construction sequence of the wall, the lateral displacement was set to zero to simulate actual construction in which the lateral displacements of the skin element were restricted.

Construction and loading sequences

39. Twelve buildup increments 1 ft high each were used to construct the wall described by mesh I, while six buildup increments 2 ft high were used to construct the wall described by mesh II. Concentrated loads following construction were placed on each nodal point at the top of the wall mesh to cause surface pressures of 250 psf per increment. Six increments were applied to reach the failure condition of 1500 psf observed with the actual wall.

Location of interface elements

40. The interface elements within the FE meshes are presented in Figures 18 and 19. These interface elements increase flexibility in accounting with the interaction effects between the different components of the wall such as slippage and separation between the different components. Mesh I contains vertical interface elements between the skin element and backfill material and between the back face of the wall and the original in situ earth. Horizontal interface elements are located between the reinforcing strips and backfill material and between the backfill and original ground surface of the wall. Mesh II contains vertical interface elements between the back face of the wall and the

original in situ earth and horizontal interface elements between the reinforcing strips and backfill material.

Examination of the FE Mesh

41. Two FE analyses were performed using mesh I and mesh II in order to determine the influence of the shape of the FE mesh on the results. The results of the FE analyses obtained from both meshes were compared and correlated with field measurements at the end of construction as well as prior to failure. End of construction (EC) refers to completion of construction of the reinforced earth wall; prior to failure (PF) refers to placement of 1500 psf of surcharge load on the top surface of the wall.

Tensile stress distribution in reinforcing strips

42. The tensile stress obtained by the FE method, which is based on a reinforcing plate covering the entire area at a given reinforced elevation of the wall, was converted to tensile stress carried by the reinforcing strips as actually placed in the field by the following expression:

$$\sigma_t = \frac{t_e W_e}{N t W} \sigma_{te} \quad (8)$$

where

σ_t = tensile stress in the reinforcing strip

t_e = equivalent thickness of the reinforcing tie in the FE mesh

W_e = equivalent width of the reinforcing tie in the FE mesh

N = number of reinforcing ties in each reinforced elevation

t = actual thickness of the reinforcing tie

W = actual width of the reinforcing tie

σ_{te} = equivalent tensile stress computed by the FE analysis

The parameters expressed in Equation 8 for mesh I and mesh II are:

<u>Parameter</u>	<u>Mesh I</u>	<u>Mesh II</u>
t	0.024 in.	0.024 in.
W	4.00 in.	4.00 in.
N	6	6
t _e	6.00 in.	0.024 in.
W _e	192.0 in.	192.0 in.

43. Comparisons of tensile stresses obtained from the FE method using mesh I and mesh II and those obtained from actual measurement at the end of construction and prior to failure are shown in Figures 20 and 21, respectively. Figure 20 shows little difference in results between mesh I and mesh II at the end of construction. The tensile stress distribution from the FE analysis assumes a parabolic shape similar to that obtained from actual measurements for the tie at elevation 1 ft above the base of the wall. The locations of the maximum tensile stress as obtained from the FE analysis agreed well with those measured in the field.

44. The tensile stress distribution along the reinforcing ties prior to failure, Figure 21, indicates that the FE results of mesh II are slightly higher than those from mesh I. However, the shapes of the tensile stress distribution curves for mesh II are much closer to actual field data than those obtained for mesh I. These results indicate that the square elements as represented in mesh I reduce the maximum tensile stress as well as the curvature of the tensile stress distribution curve.

Lateral pressure distribution

45. The lateral pressure distributions along a vertical plane 1.25 ft from the skin element as obtained from the FE analyses of mesh I and mesh II are shown in Figure 22. These results indicate that while the lateral pressures at the end of construction are slightly higher for mesh I than for mesh II, the trend reverses itself prior to failure. The results of the FE analyses for both EC and PF cases are approximately similar but somewhat higher than those obtained from the Rankine active earth pressure theory. The PF lateral pressure near the top of

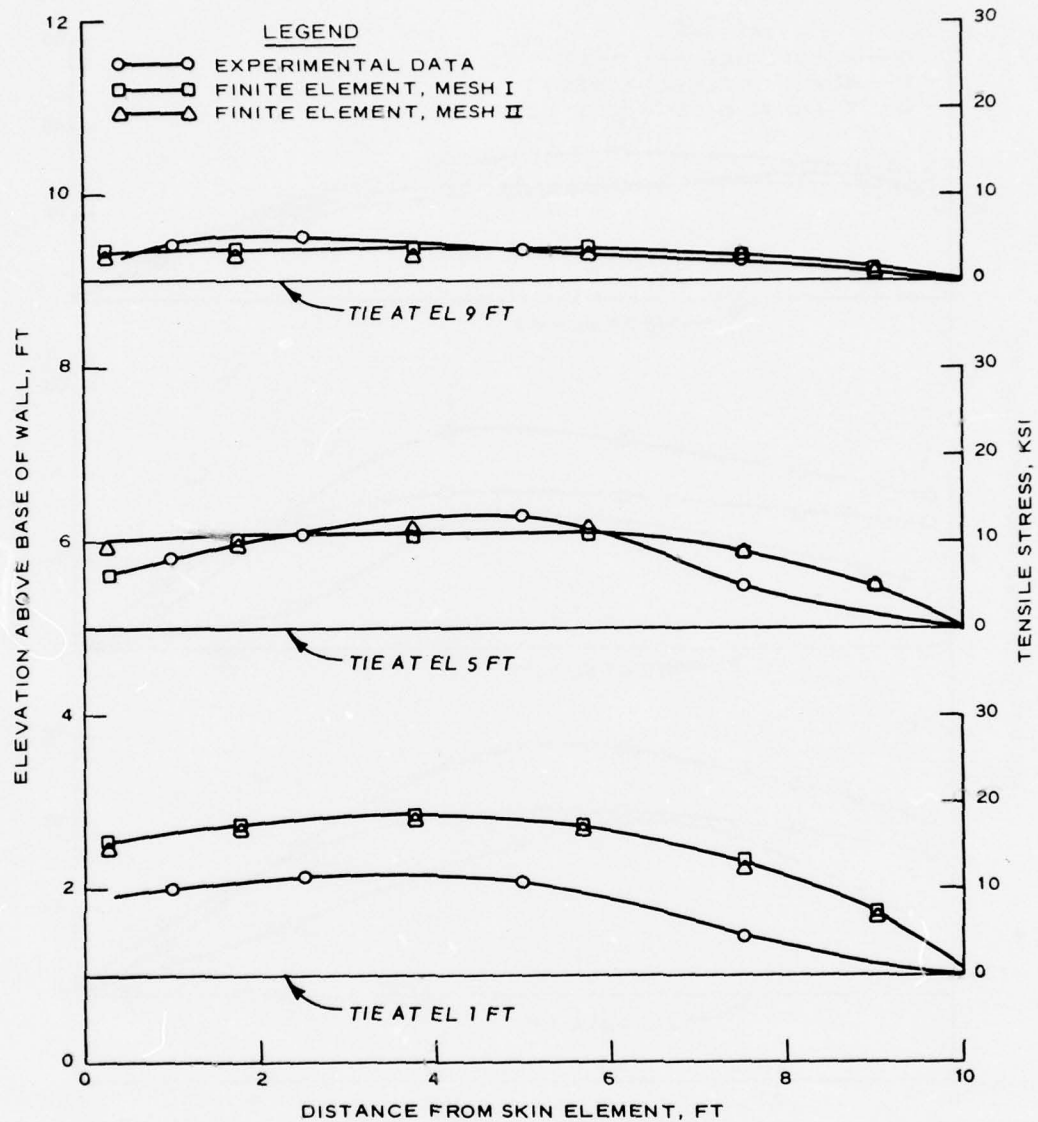


Figure 20. Influence of FE mesh on tensile stress distribution along the instrumented reinforcing strips at end of construction

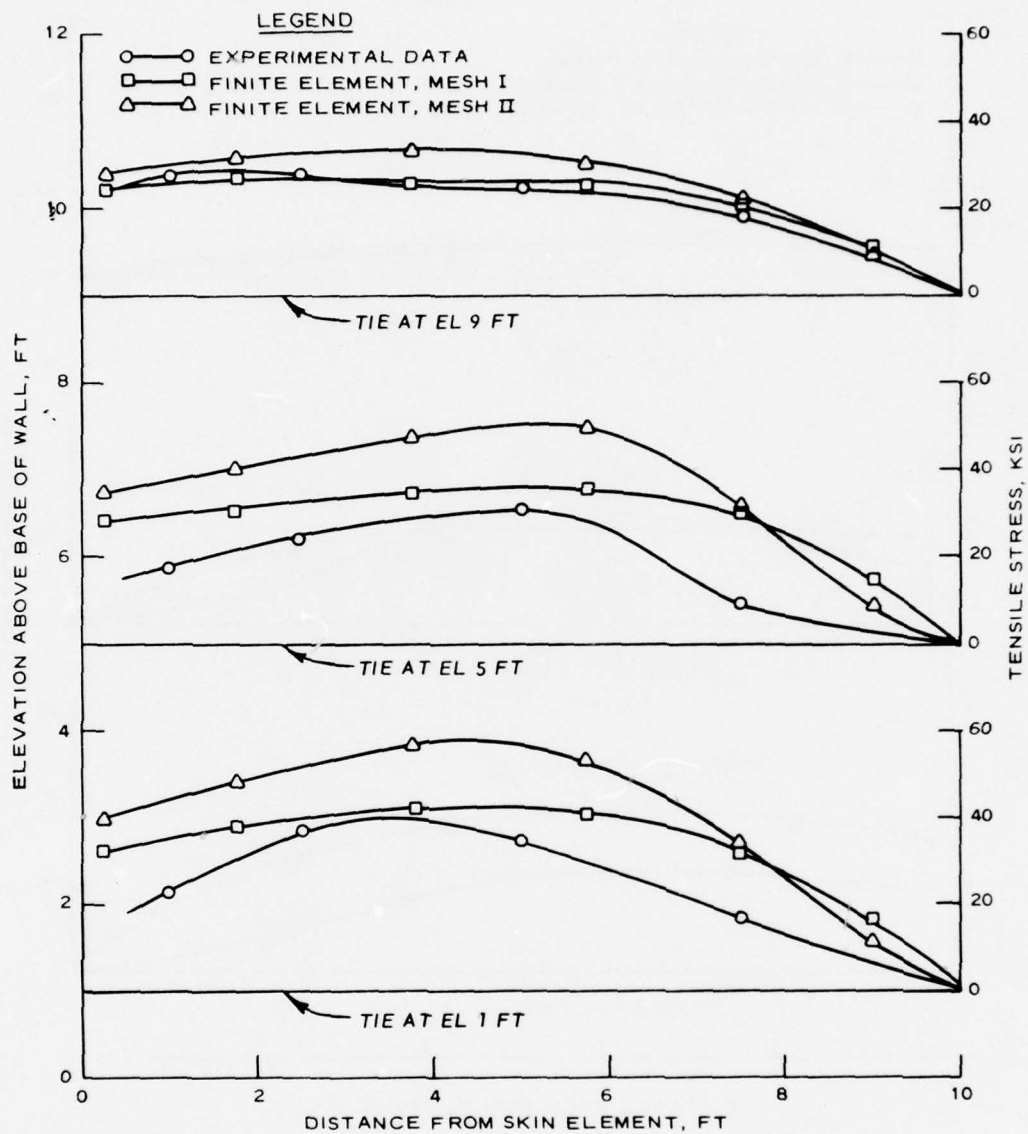
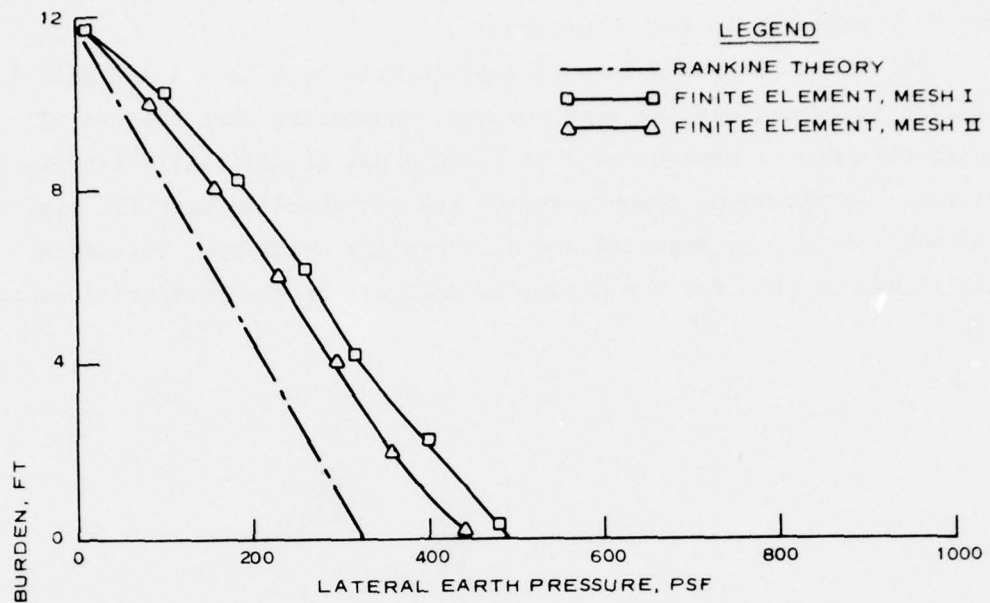
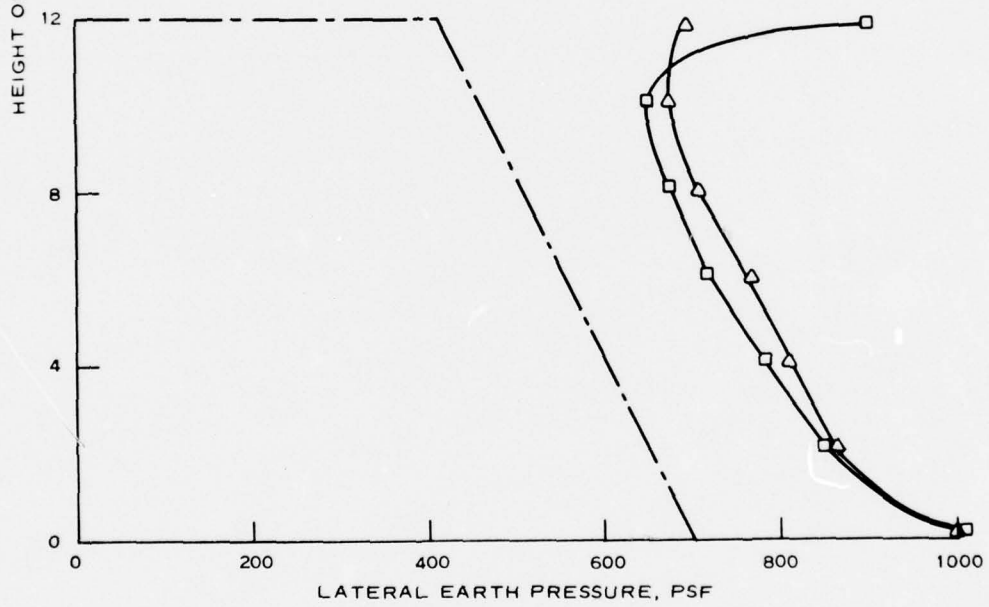


Figure 21. Influence of FE mesh on tensile stress distribution along the instrumented reinforcing strips prior to failure



a. END OF CONSTRUCTION



b. PRIOR TO FAILURE

Figure 22. Influence of FE mesh on lateral pressure acting on vertical plane 1.25 ft from skin element

the wall as obtained from the FE analysis is greatly increased for mesh I, a weakness in the FE program.

46. From the foregoing, it appears that both mesh I and mesh II provided approximately the same results, indicating that the use of square elements of aspect ratio of 1.0 did not significantly improve the results. Furthermore, fewer elements are contained in mesh II, significantly reducing computation and increasing accuracy. Therefore, mesh II was adopted for the actual FE analysis of the reinforced earth wall.

PART IV: FE ANALYSIS OF THE REINFORCED EARTH WALL

47. Reliable FE analysis of the reinforced earth wall requires accurate information on material properties, proper modeling of deformation and failure mechanisms, and proper modeling of the interaction effects between the components of the wall. The previously described models of material behavior (Part II) and idealization of the wall by the computer code (Part III) provide only a rough approximation of the actual field situation. The results of this analysis and comparisons with field observation will consequently be used to help determine more appropriate parameters for material properties of the components of the wall and improved models that may better represent field behavior.

48. An important assumption needed to obtain the FE plane strain solution is that the reinforcing strips cover the entire length of the wall. Such an assumption increases the shear resistance between the reinforcing element and the surrounding sand by a magnification factor m_f , where m_f (see Figure 1) is the ratio of the horizontal cross-sectional area of the wall to the total area of the reinforcing strips at that elevation. Thus,

$$m_f = \frac{L \cdot L'}{N \cdot L \cdot W} = \frac{10 \times 16}{6 \times 10 \times 0.333} = 8 \quad (9)$$

Therefore, the increase in the shear stress at the interface element of mesh II due to the computer code is compensated for by reducing the shear stresses in Equation 2 by m_f . Thus, the constitutive equation for the interface element used in the actual FE analysis is:

$$K_{st} = (1 - \lambda_2)^2 K_i \quad (10a)$$

$$K_i = \frac{K_j}{m_f} \gamma_w \left(\frac{\sigma_n}{P_a} \right)^n \quad (10b)$$

$$\lambda_2 = \frac{R_f \tau}{\frac{C_a}{m_f} + \sigma_n \tan\left(\frac{\delta}{m_f}\right)} \quad (10c)$$

Therefore, the material parameters input in the code are $K_j = 410$ and $\phi = 3$ deg.

49. It must be noted that Equation 10 can only provide a crude simplification of the real behavior between the reinforcing strips and the surrounding soil. More study is needed to provide a better constitutive model to describe the behavior of the interface elements. In Equation 10 the tangent shear stiffness K_{st} is set to a small residual value K_r of 10 psf whenever the shear stress at the interface element exceeds a Mohr-Coulomb strength envelope with cohesion equal to C_a/m_f and an angle of friction equal to δ/m_f .

50. The ribs of the skin element, Figure 8, are extended only along the length of the wall; thus, they contribute very little to the bending resistance of the skin element in the vertical direction. The moment of inertia used in the calculation is that for the aluminum sheet of 0.1-in. thickness rather than that of the integral aluminum panel.

FE Analysis

51. Two FE analyses were performed using mesh II. In the first analysis, case C_1 , the toe of the wall represented by point A of Figure 2 was assumed fixed. In the second FE analysis, case C_2 , point A was assumed free to move in any direction. It must be noted that under field conditions point A is neither fixed nor free and the true answer may be between the two extreme cases. The lateral pressures exerted by the backfill and surcharge loading following construction, lateral movement of the skin element, and the tensile stress and deformation behavior of the reinforcing strips are given below. Comparisons are made with field observations for the EC and PF cases.

Distribution of lateral pressure

52. The distributions of lateral pressure along a vertical plane

1 ft from the wall face determined from the FE analysis for the free- and fixed-end cases are compared with field observations. Figure 23 shows the variation of the lateral pressure as a function of the height of the wall at the end of construction. The differences in results between cases C_1 and C_2 at the end of construction are negligible except at the base of the wall where the fixed end, case C_1 , showed higher lateral pressure than the free end, case C_2 . The results of the FE analysis at the end of construction for C_1 and C_2 cases are somewhat higher than those determined by Rankine theory and those obtained by field measurements.

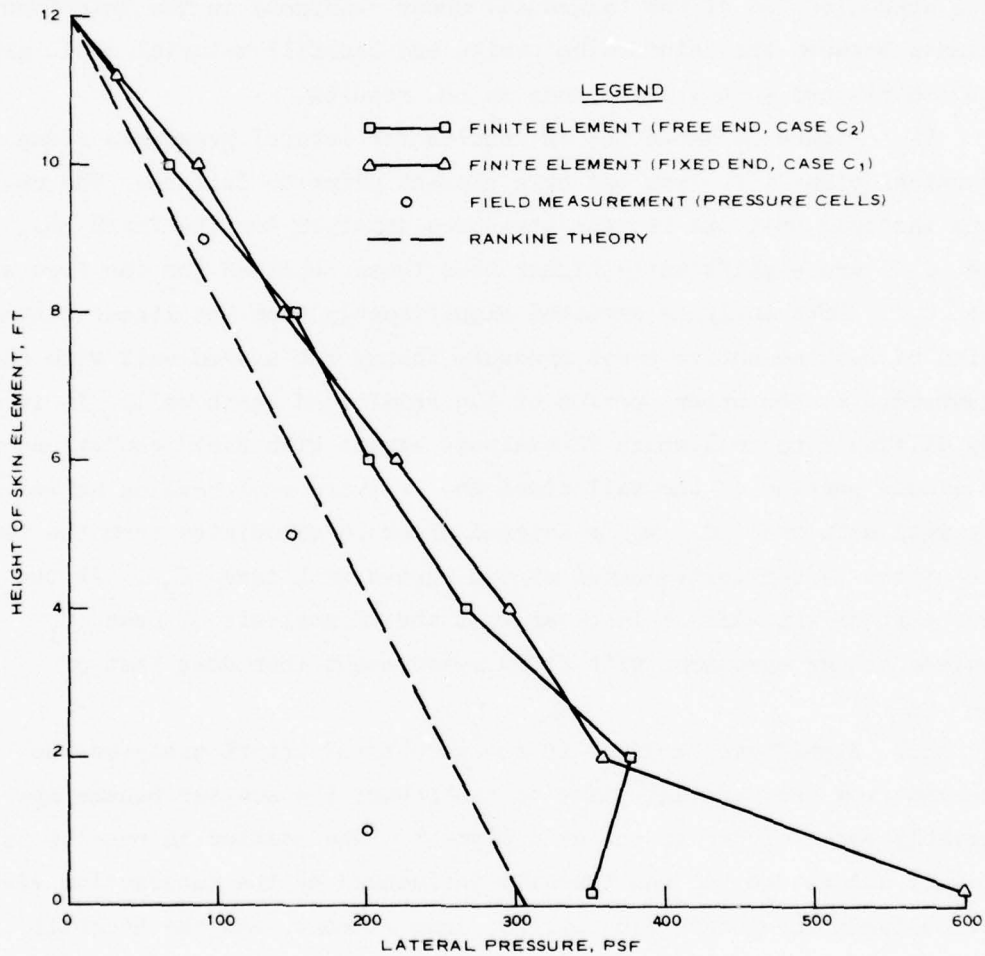


Figure 23. Pressure distribution at vertical plane 1 ft from skin element at end of construction

53. Field measurements for lateral pressures, Figure 23, were obtained directly from readings of earth pressure cells placed along the center line of the wall 1 ft from the skin element, and also from those stresses generated in the instrumented reinforcing strips within a segment of the wall bounded by $S_x S_z$, Figure 1, surrounding the strip. The excessive lateral pressures determined by the FE analysis may be attributed to deficiencies in the computer code and to the poor modeling of the skin element. It must be noted that the panels of the skin element were connected together by horizontal hinged joints, Figure 1, rather than continuous bonded joints as assumed in the FE analyses. The crude approximation of the tangential shear stiffness in the interface elements between the reinforcing strips and backfill material could also have contributed to the difference in the results.

54. Figure 24 shows the FE results for lateral pressures along a vertical plane 1 ft from the skin element prior to failure. The results indicate that the lateral pressures obtained for the fixed end, case C_1 , are significantly higher than those obtained for the free end, case C_2 . Both analyses deviated significantly from the linear distribution of Rankine active earth pressure theory but agreed well with field measurement at the upper portion of the reinforced earth wall. It is very difficult to tell which FE analysis agrees with field conditions at the middle portion of the wall since the pressure cell reading agreed very well with case C_1 while lateral pressure calculated from the tensile stress of the instrumented strips agreed with case C_2 . At the lower part of the wall it is clear that the FE analysis of case C_1 provides better agreement with field measurement than does that of case C_2 .

55. Significant scatter in the results of the FE analyses was observed from one vertical plane to the other; the scatter became appreciably worse closer to the skin element. The scatter in results is not well understood but was probably influenced by the interaction effects between the reinforcing strips, skin element, and the backfill material.

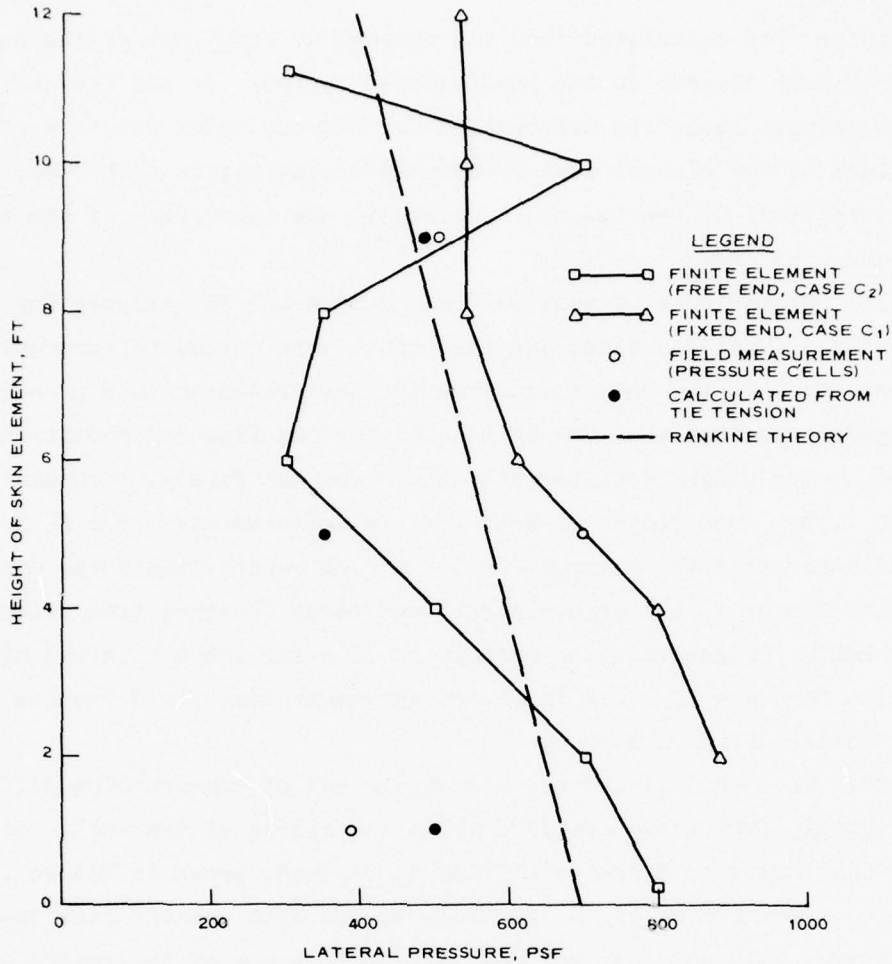


Figure 24. Pressure distribution at vertical plane 1 ft from skin element prior to failure

Distribution of tensile strain in reinforcing strips

56. The reinforcing strips located at elevations of 1, 5, and 9 ft along the center line of the wall were instrumented with full SR-4 bridges on both surfaces at points 1, 2.5, 5, and 7.5 ft from the face of the skin element. The measured strains at the top and bottom of each instrumented point were averaged to eliminate the effect of bending strains; the average strain was considered equal to the tensile strain at that point in the reinforcing strip. Only the strains at the end of construction and prior to failure are presented. For the FE analysis

the strains were calculated from the average deformations of the nodal points of each element in the instrumented strips. It has been noticed that in certain cases the deformation for the two nodal points at the lower face of the element were unbearably excessive; in such case, only the deformations of the two nodal points at the upper face of the element were considered.

57. Comparisons of tensile strains from the FE analyses for the free-end and fixed-end cases and the actual strain gage measurements of the field test at the end of construction are presented in Figure 25. The figure indicates that the FE results for the free-end condition, case C_2 , are slightly higher than those for the fixed-end condition, case C_1 , but much closer to actual field measurements. The FE analysis indicated that the maximum strain in each reinforcing strip occurred at points closer to the skin element than those obtained from actual measurement. In general, the maximum tensile strains at the end of construction for case C_2 are in better agreement with field results than those obtained from case C_1 .

58. The trend of the results at the end of construction differed significantly from those obtained prior to failure of the wall. Strains determined from the FE analysis prior to failure, shown in Figure 26, indicated a maximum strain value close to the skin element that decreased gradually until it vanished at the free end of the reinforcing strips. The results, unlike the end of construction condition, showed higher strains for case C_2 than for case C_1 . For the strips at elevation 5 ft above the base, both C_1 and C_2 cases showed similar values and their maximum values were in good agreement with that obtained from field measurement.

Distribution of tensile stress in reinforcing strips

59. The in situ tensile stress distribution along the reinforcing strips of the reinforced earth wall was calculated from the strain gage readings and the modulus of elasticity of the galvanized steel using modulus of elasticity $E = 31.1 \times 10^6$ psi. Therefore, the variation in the field tensile stress distribution is similar to the variation in

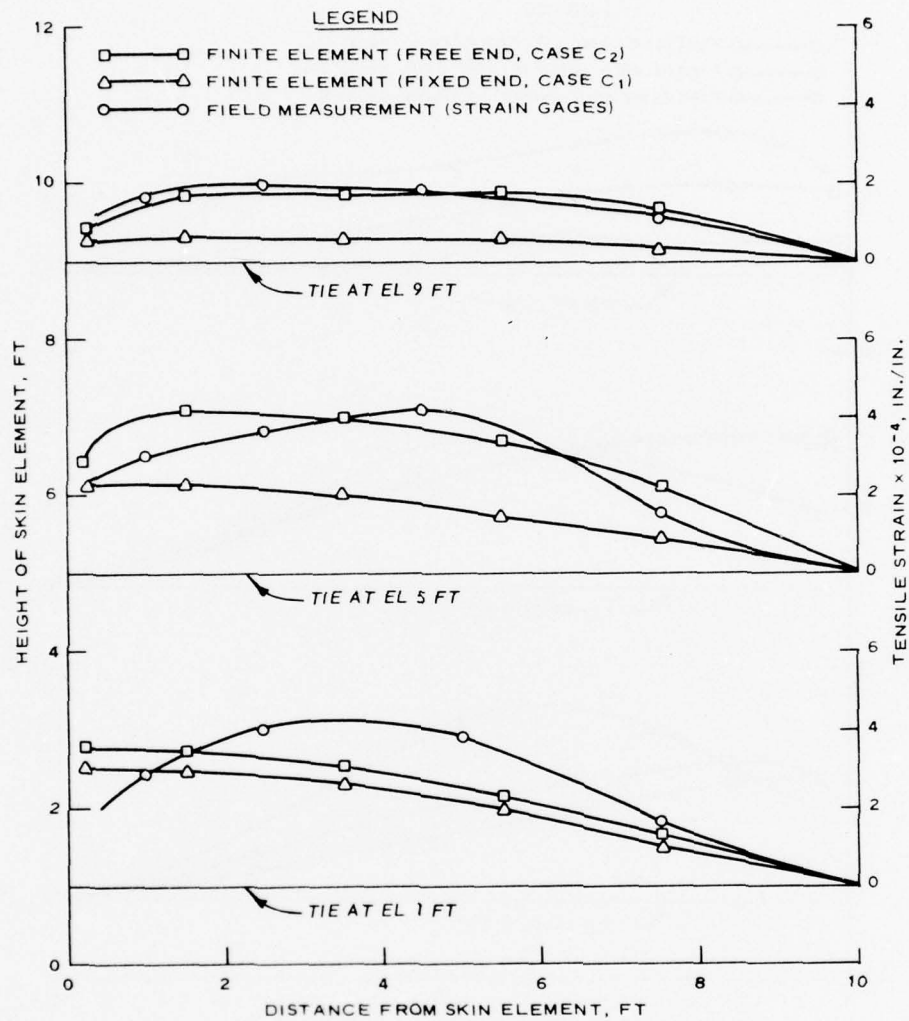


Figure 25. Tensile strain distribution along instrumented ties at end of construction

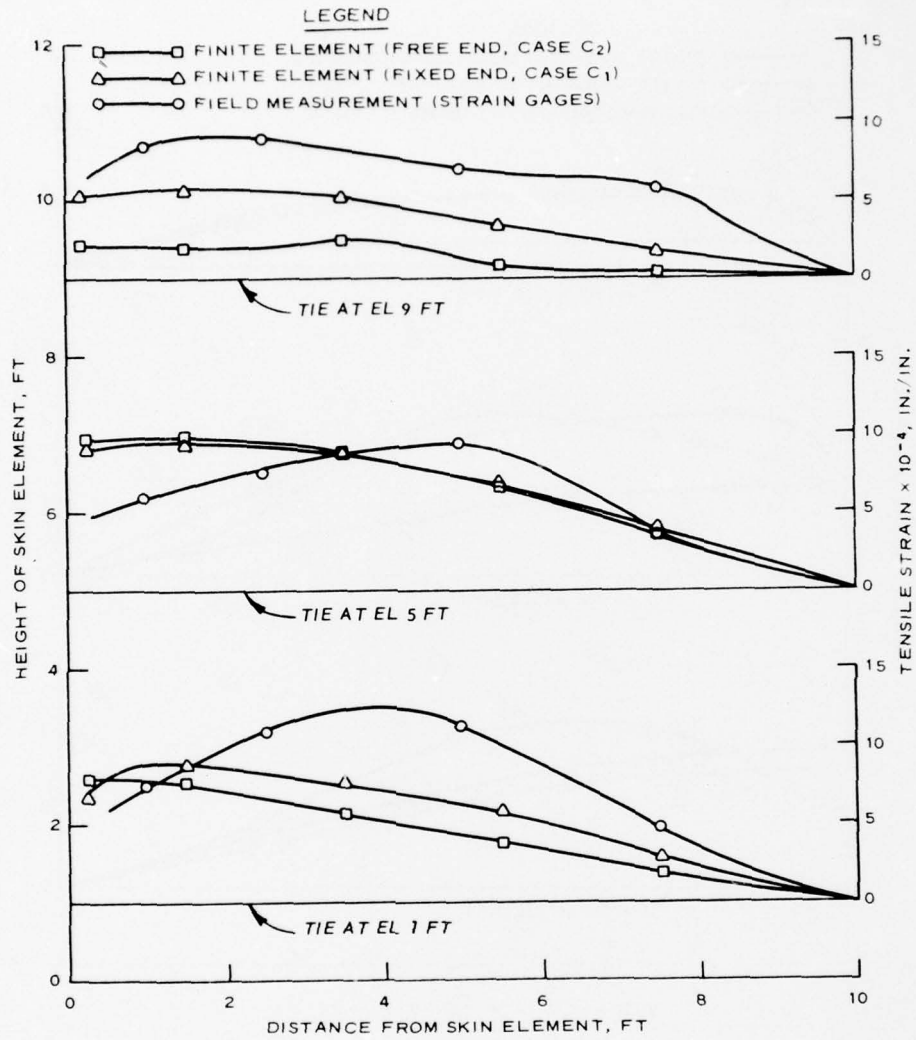


Figure 26. Tensile strain distribution along instrumented ties prior to failure

tensile strain distribution as long as the stresses in the reinforcing strips are within the elastic range. The tensile stress at any point for the FE analysis was obtained from the equivalent tensile stresses using Equation 8. Comparisons of the tensile stress distribution along the instrumented strips at the end of construction between the FE analysis and field test results are presented in Figure 27. The figure shows that the FE results for the free-end case and the fixed-end case are identical, but somewhat different from field measurements. The maximum

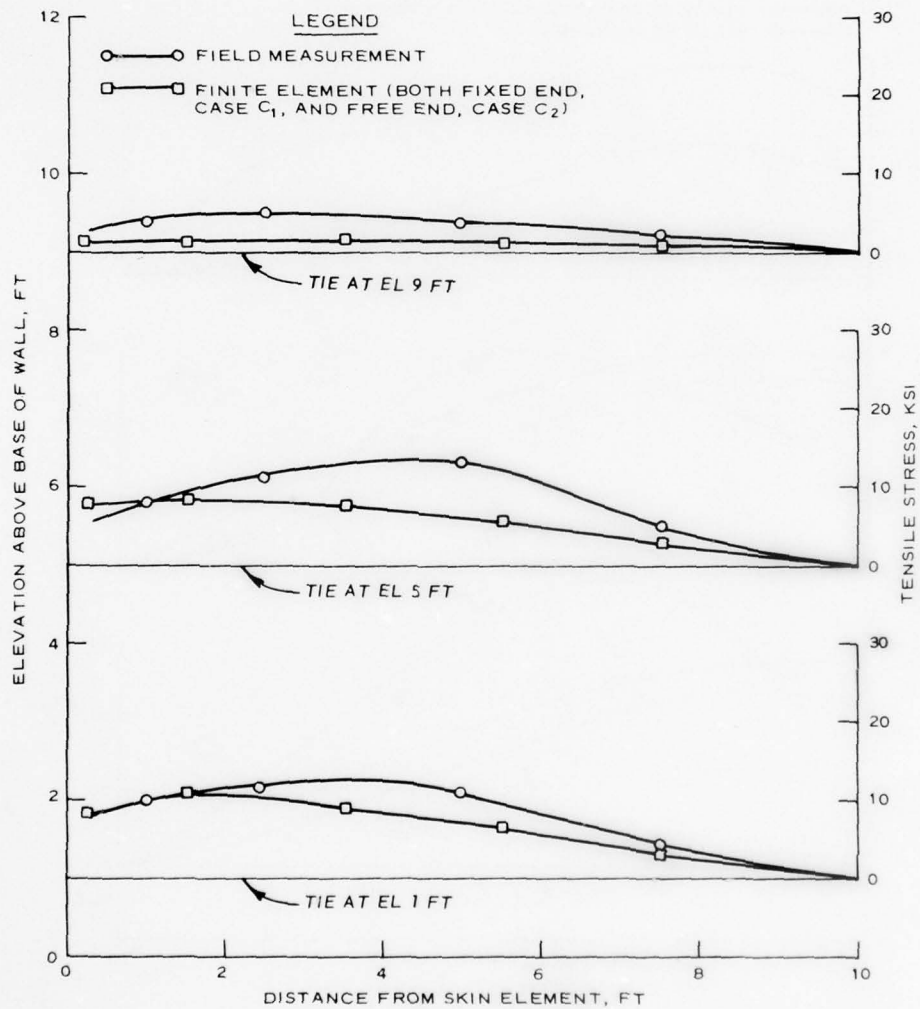


Figure 27. Tensile stress distribution along instrumented ties at end of construction

tensile stress for the FE analysis occurred at a point much closer to the skin element than that observed in the field. Both the FE results and the field data show a gradual decrease in the tensile stress from the maximum until it reached zero at the free end of the reinforcing strip.

60. Comparisons of results between the tensile stress prior to failure for the FE analysis and actual field observations are presented in Figure 28. The figure shows that the tensile stresses obtained from

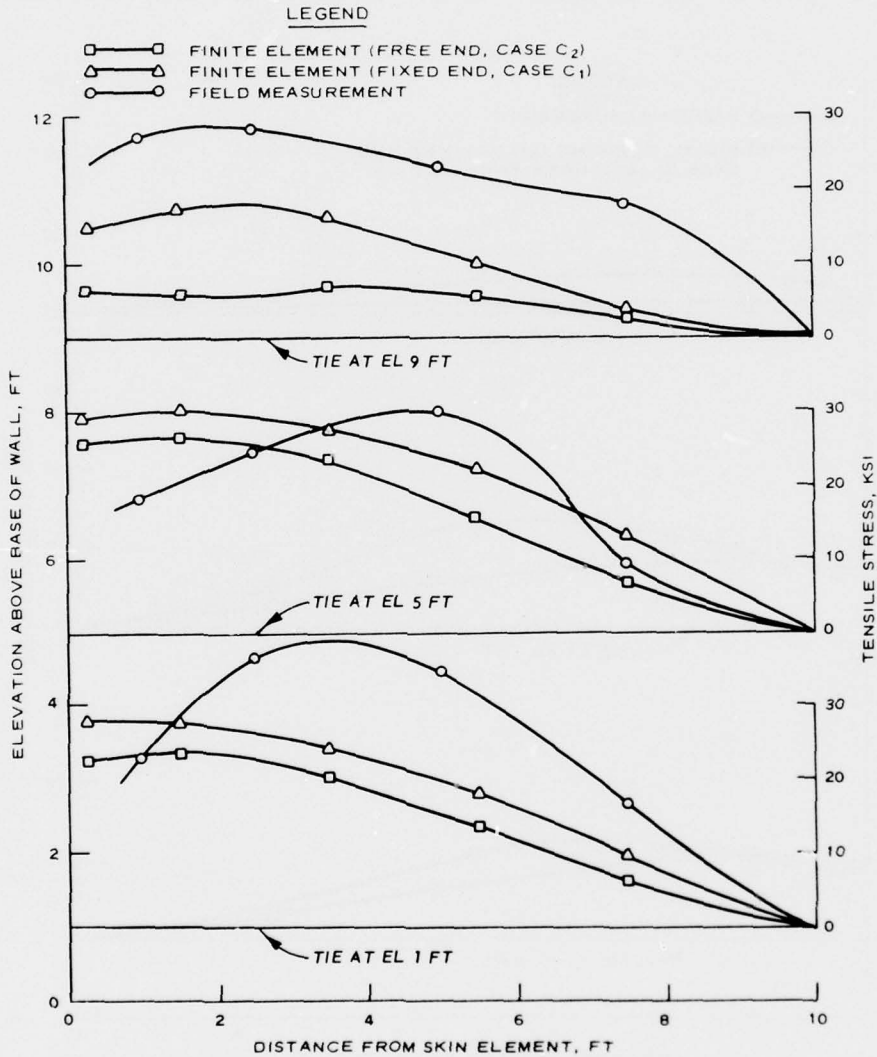


Figure 28. Tensile stress distribution along instrumented ties prior to failure

the FE analysis are generally lower than those obtained from field measurements and the results for the fixed-end condition, case C_1 , are higher than those for the free-end condition, case C_2 . FE analysis results also show that the maximum tensile stresses occurred at a point much closer to the skin element than those obtained from field measurement. Reasons for the differences between the FE results and field observations are not known with certainty; however, deficiencies in the computer code and modeling, difficulty in determining the actual stiffness of the skin element, and lack of precise constitutive equations for describing behavior for the materials are considered major contributing factors.

Lateral movement of skin element

61. The reinforced earth wall was constructed such that each section of aluminum paneling added to form the skin element was held in place to prevent lateral movement while the corresponding layer of backfill was added. Field observations indicated negligible deformations at the end of construction, but the skin element deformations became substantial prior to failure, as shown in Figure 29, with maximum deformation of 3.4 in. at the top of the wall. Comparison between the FE analyses and the field observations, based on the accumulative deformation from one panel to the next, shows good agreement between the field observations and FE results for the fixed-end condition, case C_1 . For the free-end condition, case C_2 , the FE analysis showed excellent agreement with field observations at the lower half of the wall; however, at the upper half of the wall the FE results deviated significantly from actual observations and indicated compression.

Concluding Remarks on the FE Analysis

62. Because of the preliminary nature of this study and the complex interaction between the various components of the reinforced earth wall, it is considered unlikely that total agreement between the FE analyses and field measurements could be obtained. However, it is shown that the boundary conditions of the wall play a significant role in the

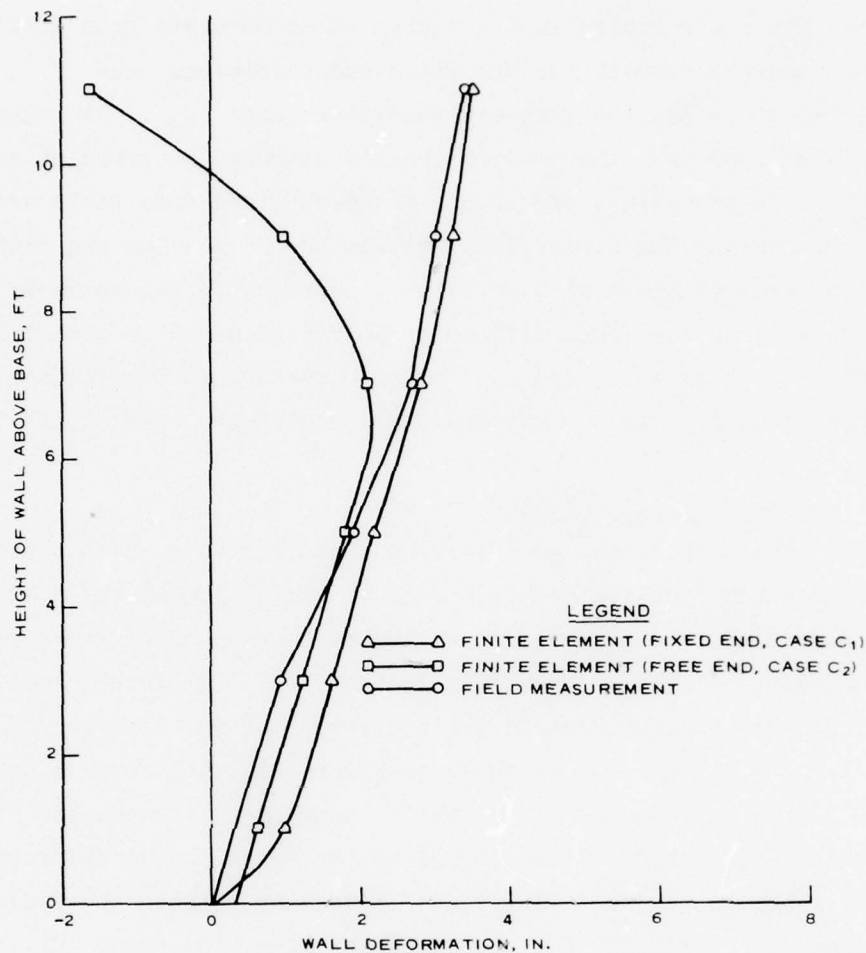


Figure 29. Accumulated lateral skin element deformation prior to failure

FE results. In certain aspects such as the deformation of the skin element, the fixed-end condition showed better agreement with field observations, while in other aspects such as the tensile strain in the reinforcing strips, the free-end condition showed better agreement. Other problems, such as improving the computer code, obtaining better constitutive equations for modelling material properties, and better representation of the skin element stiffness used in the calculation, need further development before a total agreement can be achieved.

PART V: PARAMETRIC STUDY

General Objectives

63. In the previous part of this report it was shown that there are some differences between results of the FE analysis and those obtained from field observation. The differences were attributed to many factors, some of which were discussed previously. Variables which may influence the performance of a reinforced earth wall are also numerous. The influence of the following variables on the tensile stress distribution along the instrumented reinforcing strips was evaluated using the FE analysis: (a) friction between the reinforcing strips and the fill material; (b) end conditions of the skin element; (c) stiffness of the skin element; and (d) length of the reinforcing strips.

Influence of friction between reinforcing strip and fill material

64. Equation 2 represents the constitutive equation which is used to describe the stress-deformation relationship between the galvanized steel and the concrete sand used. Analysis of the test results presented in Figures 12 and 13 indicated that $\delta = 18 \text{ deg}$ and $K_j = 3280$. These parameters were reduced by a magnification factor $m_f = 8$ when used in the FE code to obtain tensile stress distribution for cases C_1 and C_2 , shown in Figures 27 and 28. In order to determine the influence of friction between the reinforcing strips and the fill material, FE runs were performed using the same parameters employed in cases C_1 and C_2 except that δ and K_j were not reduced. The tensile stress distributions for the fixed-end condition, case C_3 , and the free-end condition, case C_4 , are presented in Figures 30 and 31, respectively. Comparison between Figures 30 and 31 for the unreduced interface friction and Figures 27 and 28 for the reduced interface friction indicates that the increase in the interface friction increases the tensile stress in the reinforcing strips; the increase in stress is much higher for the free-end condition, case C_4 , than for the fixed-end condition, case C_3 . Based on this analysis it

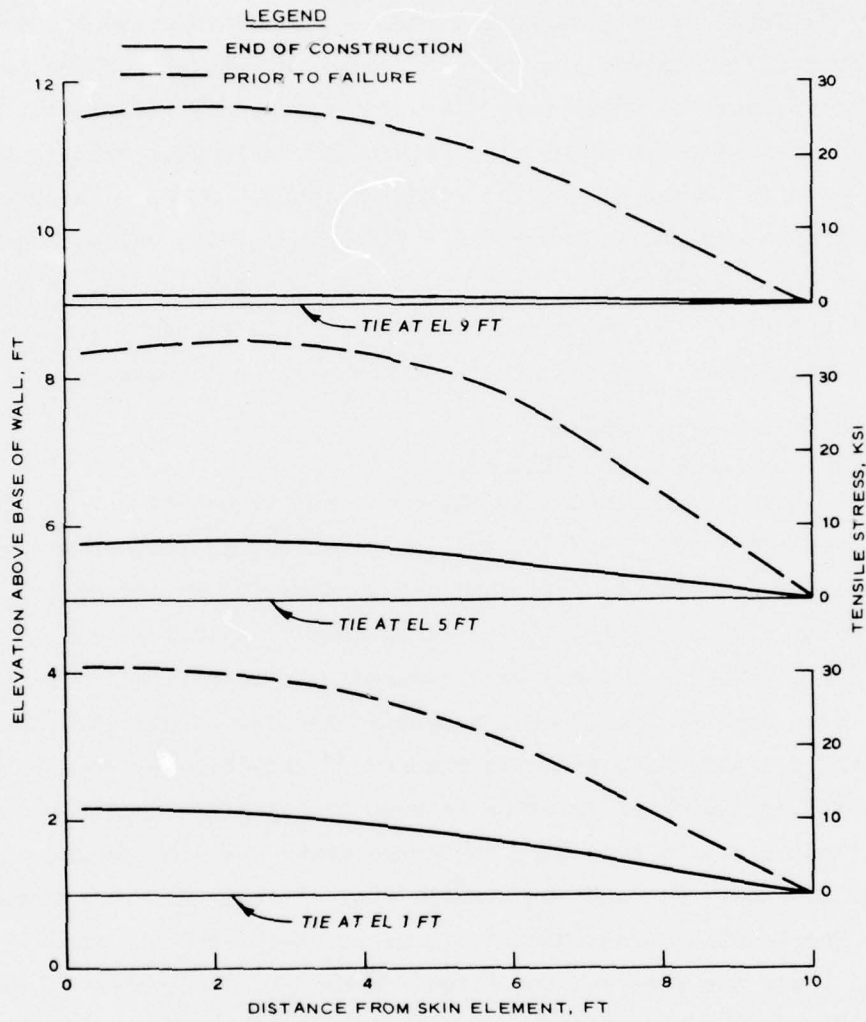


Figure 30. Tensile stress distribution along instrumented reinforcing strips at end of construction and prior to failure for case C_3 (fixed-end condition)

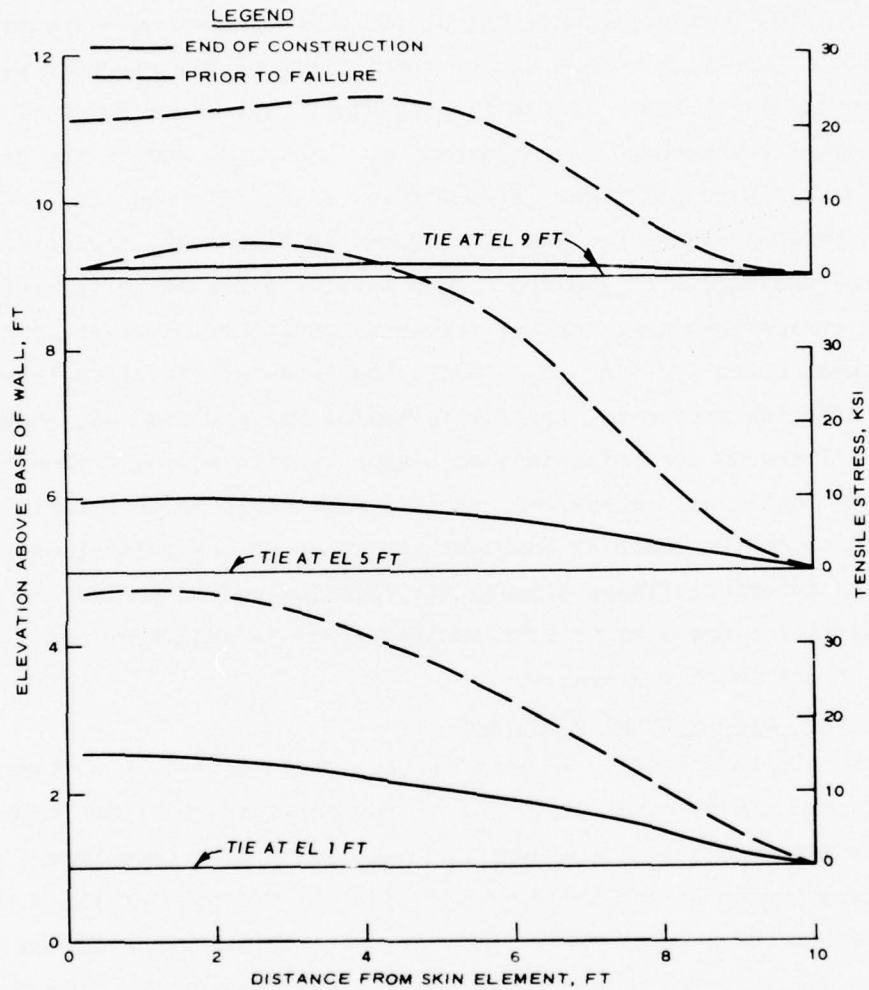


Figure 31. Tensile stress distribution along instrumented reinforcing strips at end of construction and prior to failure for case C_4 (free-end condition)

can be concluded that the increase in the interface friction between the reinforcing strips and the surrounding fill increases the maximum tensile stresses.

Influence of end conditions of skin element

65. Two boundary conditions of the skin element were investigated to determine their influence on the tensile stress distribution within the reinforcing strips. In the first analysis the lower point of the skin element was assumed fixed, cases C_1 and C_3 , and in the second analysis the lower point was assumed free, cases C_2 and C_4 . Comparison between cases C_1 and C_2 , shown in Figure 28, indicates that the fixed-end condition yielded higher tensile stresses in the reinforcing strips than that for the free-end condition. However, comparison between cases C_3 and C_4 , where the interface friction between the reinforcing strips and the fill material was not reduced, shows that the free-end condition induced higher tensile stresses than the fixed-end condition. Therefore, it is not possible to draw definite conclusions on the basis of boundary condition of the skin element alone since the interface stress between the reinforcing strips and the surrounding fill plays a major role in dictating the magnitude and distribution of the tensile stresses.

Influence of skin element stiffness

66. In the previous FE runs the stiffness of the skin element was based on the moment of inertia I_x of the metal sheet at the back of the aluminum panel, on the assumption that the T ribs (see Figure 2), which were placed in the horizontal direction, did not influence the stiffness of the skin element. Knowing that the thickness of the metal sheet is 0.1 in., the moment of inertia I_x per foot of the skin element is 0.0022 in.³ To evaluate the influence of skin element stiffness on the tensile stress along the reinforcing strips, another FE analysis, case C_5 , was conducted. Case C_5 was similar to case C_4 in every respect except that the moment of inertia in case C_5 was 1.368 in.³, which is the moment of inertia per foot of panel as shown in paragraph 16, rather than 0.0022 in.³, which is the I_x for the aluminum

sheet only. The tensile stress distribution along the instrumented strips at the end of construction and prior to failure for case C_5 is shown in Figure 32. Comparison between results for case C_5 and those of case C_4 , shown in Figure 31, indicates that the magnitudes of the maximum tensile stress are not significantly influenced by the stiffness of the skin element. However, maximum tensile stresses for low skin element stiffness, case C_4 , occurred at points much closer

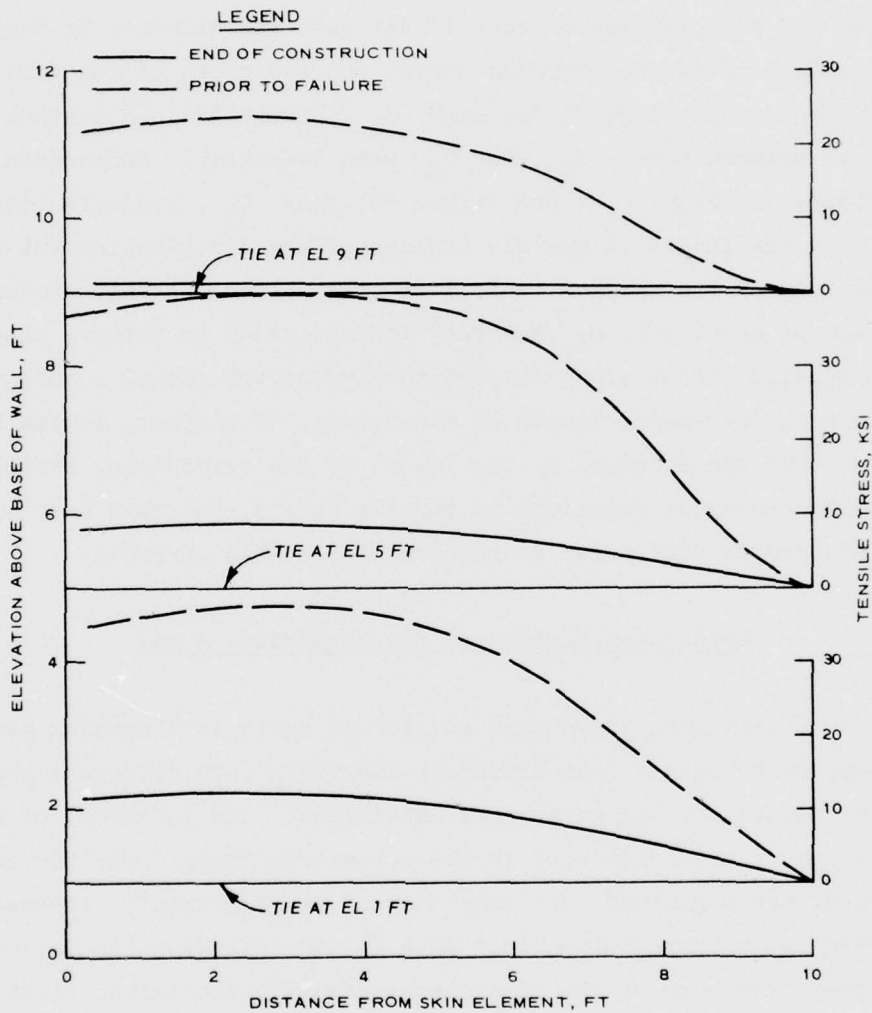


Figure 32. Tensile stress distribution along instrumented reinforcing strips at end of construction and prior to failure for case C_5

to the face of the wall than those for high skin element stiffness, case C_5 . Therefore, it can be concluded that the stiffness of the skin element slightly changes the shape of the tensile stress distribution along the reinforcing strip but not the magnitude of the maximum stress.

Influence of length of reinforcing strips

67. The influence of the length of the reinforcing strips on the magnitude and distribution of tensile stresses was examined by increasing the length of the reinforcing strips and the depth of the wall from 10 ft for case C_3 to 20 ft for case C_6 (Figure 33). All other parameters between cases C_3 and C_6 were identical. Comparison between Figure 33, case C_6 , and Figure 30, case C_3 , indicates that the increase in the length of the tie influenced the distribution but not the magnitude of the maximum tensile stresses along the reinforcing ties at the end of construction. However, for the prior to failure case, maximum tensile stress along the reinforcing strips showed a substantial decrease with increasing length of the strips. Therefore, it can be concluded that the increase in the length of the reinforcing strips tends to decrease the magnitude of tensile stress, and thus less cross-sectional area of strips may be required for design purposes.

Concluding Remarks on the Parametric Study

68. It has been shown that reinforced earth is a complex problem whose complexity arises from different materials with different properties that constitute the reinforced earth mass. The influence of only a few variables was considered in the parametric study. For the cases considered, the magnitudes and locations of maximum tensile stresses are summarized and compared with field data in the following tabulation. It can be seen that none of the FE analyses actually duplicated field conditions. While the magnitude of the tensile stress in case C_3 is closest to the field observation, the location of the maximum stresses in case C_5 correlates most favorably with the actual field data.

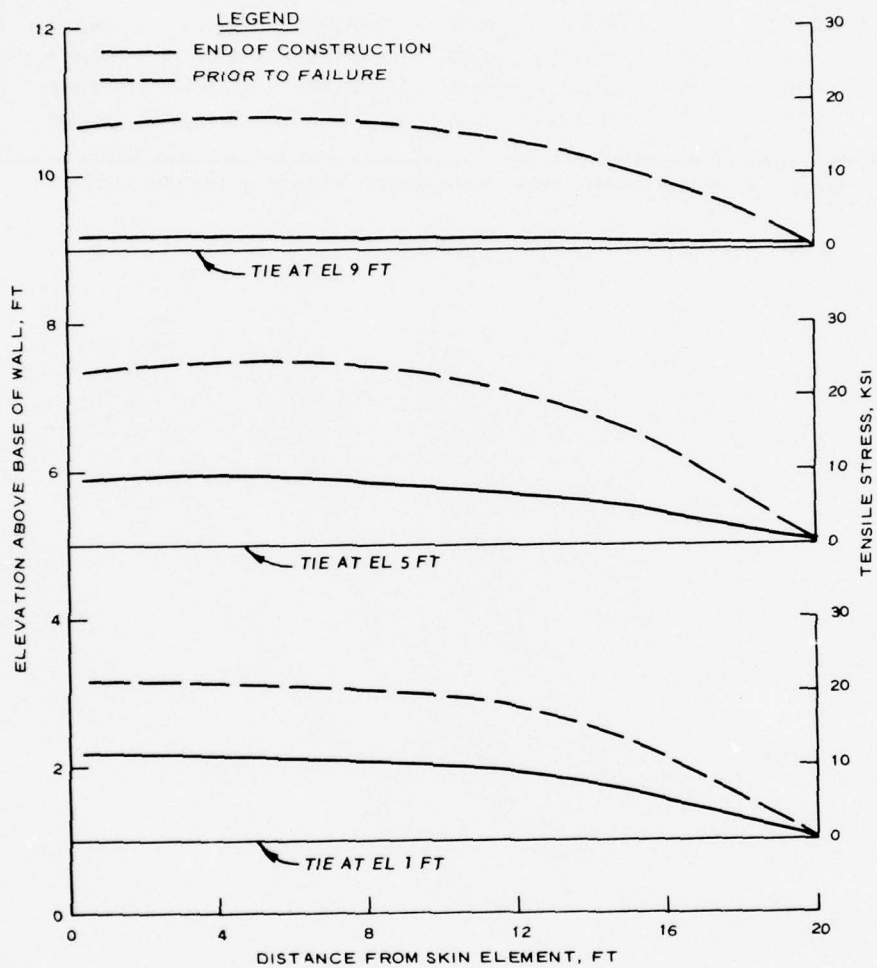


Figure 33. Tensile stress distribution along instrumented reinforcing strips at end of construction and prior to failure for case C_6

	Friction Angle δ , deg	Strip Length L, ft	Tie Elevation Above the Foundation					
			1.0 ft		5.0 ft		9.0 ft	
			Maximum Tensile Stress psi	Location* ft	Maximum Tensile Stress psi	Location* ft	Maximum Tensile Stress psi	Location* ft
Field test	--	10	39,000	2.00	30,000	4.50	29,000	3.50
Case C ₁	3	10	28,700	0.75	29,410	1.50	17,220	2.50
Case C ₂	3	10	25,140	0.75	26,460	1.50	6,770	0.25
Case C ₃	18	10	31,040	0.75	34,980	2.50	26,260	2.50
Case C ₄	18	10	37,020	1.50	44,280	2.50	23,650	4.50
Case C ₅	18	10	37,600	2.50	39,760	3.50	23,670	2.50
Case C ₆	18	20	22,260	1.50	24,510	5.00	17,650	5.00

* The location of the maximum tensile stress was measured relative to the skin element.

PART VI: CONCLUSIONS AND RECOMMENDATIONS

Conclusions

69. An FE study was performed on a reinforced earth wall to investigate the feasibility of using numerical methods in predicting stresses and deformations of the various elements of the wall. The wall used in the FE analyses was 16 ft long, 10 ft deep, and 12 ft high; the earth backfill was reinforced with galvanized steel strips 4 in. wide, 0.025 in. thick, and 10 ft long, spaced at 2- and 2.5-ft intervals in the vertical and horizontal directions, respectively. Based on the results of the FE analyses of this study and results collected from laboratory and field tests, the following conclusions are drawn:

- a. The one-dimensional interface elements vertically inserted between the foundation soil and the back of the reinforced earth wall are necessary to permit separation between the reinforcing strips and foundation soil such that the tensile stresses developed in the reinforcing strips decrease to zero at the back of the wall as observed from field measurements. Interface elements horizontally inserted between the reinforcing strips and backfill of the wall are necessary to model the slippage and friction forces between the reinforcing strips and backfill.
- b. The assumption of using the FE plane strain analysis to solve the 3D problem of a reinforced earth wall by increasing the area of the reinforcing strip, to cover the entire length of the wall, and decreasing the shear resistance between the fill and the reinforcement by the same proportion is a practical and satisfactory assumption.
- c. The FE analyses of both fixed-end and free-end skin elements are necessary to obtain good correlation with field data. It is observed that the FE results of tensile stresses along the reinforcing strips and the lateral deformation of the skin element showed better agreement with field observation for the fixed-end condition than for the free-end condition. However, field measurements of strains along the reinforcing strips agreed better with the FE results of the free-end condition than with those obtained from the fixed-end condition. While lateral pressure cell measurements agreed better with FE results of the fixed-end rather than free-end conditions,

the opposite was observed when comparison was made with lateral earth pressure calculated from tensile stresses in the reinforcing strips.

- d. The magnitude and distribution of tensile stresses along the reinforcing strips increase with increasing interface friction between the strip and surrounding fill material, decrease with increasing reinforcing strip length, and show no significant change with change in skin element stiffness.

Recommendations

70. Based on the findings of this study, it is recommended that the study be expanded as follows:

- a. It is desirable to improve the computer code and make it more accurate and efficient by introducing elements that better simulate actual events. The variable node of bending element is recommended because fewer elements may be needed and oscillation observed in results using the isoparametric elements may be reduced or eliminated.
- b. Better constitutive equations that not only simulate the behavior of each material in the reinforced earth mass but also describe the interaction between different materials should be developed.
- c. More studies are needed to model and improve the behavior of interface elements between the reinforcing strips and surrounding soil.
- d. Hinges between panels that form the skin element need to be considered in the FE code.

REFERENCES

1. Al-Hussaini, M. M. and Perry, E. B., "Effect of Horizontal Reinforcement on Stability of Earth Masses," Technical Report S-76-11, Sep 1976, U. S. Army Engineer Waterways Experiment Station, CE, Vicksburg, Miss.
2. Vidal, H., "Reinforced Earth (A New Material for Public Works)," Annales, de l'Institut Technique du Bâtiment et des Travaux Publics, Vol 19, Nos. 223-224, Series: Materials (30), Jul-Aug 1966, pp 888-938. (Also published as Translation No. 67-12, Dec 1967, U. S. Army Engineer Waterways Experiment Station, CE, Vicksburg, Miss.)
3. Lee, K. L., Adams, B. D., and Vagneron, J. J., "Reinforced Earth Walls," UCLA-ENG-7233, Apr 1972, University of California, Los Angeles, Calif.
4. Clough, G. W. and Duncan, J. M., "Finite Element Analyses of Port Allen and Old River Locks," Contract Report S-69-6, Sep 1969, U. S. Army Engineer Waterways Experiment Station, CE, Vicksburg, Miss.; prepared by University of California under Contract No. DACW39-68-C-0040.
5. Radhakrishnan, N. and Jones, H. W., "User Guide for Program UFRAME" (in preparation), U. S. Army Engineer Waterways Experiment Station, CE, Vicksburg, Miss.
6. Duncan, J. M. and Chang, C. Y., "Analysis of Soil Movement Around a Deep Excavation," Journal, Soil Mechanics and Foundation Division, American Society of Civil Engineers, Vol 96, No. SM5, Sep 1970, pp 1655-1681.
7. Goodman, R. E., Taylor, R. L., and Brekke, T. L., "A Model for the Mechanics of Jointed Rock," Journal, Soil Mechanics and Foundation Division, American Society of Civil Engineers, Vol 94, No. SM3, May 1968, pp 637-659.
8. Kondner, R. L., "Hyperbolic Stress-Strain Response: Cohesive Soils," Journal, Soil Mechanics and Foundation Division, American Society of Civil Engineers, Vol 89, No. SM1, Feb 1963, pp 115-143.
9. Janbu, N., "Soil Compressibility as Determined by Oedometer and Triaxial Tests," Proceedings, European Conference on Soil Mechanics and Foundation Engineering, Weisbaden, Vol 1, 1963, pp 19-25.

APPENDIX A: COMPUTER CODE


```

93 IF(NFILE,EO,1) STOP
94 WRITE(3,2003) IWB(1),I=1,20,NUMP,NUML,NDMMHAT,NUMBOL,NUMJT,NC,NU
95 *MPP,INT,LCORC,GAH,PAT,IRUNC
96 READ(1,1030) NATYP,NCATYP,NB1TYP,NB2TYP
97 WRITE(3,2005) NATYP,NCATYP,NB1TYP,NB2TYP
98 WRITE(3,2030)
99
100
101
102
103
104
105
106
107
108
109
110
111
112
113
114
115
116
117
118
119
120
121
122
123
124
125
126
127
128
129
130
131
132
133
134
135
136
137
138
139
140
141
142
143
144
145
146
147
148
149
150
151
152
153
154
155
156
157
158
159
160
161
162
163
164
165
166
167
168
169
170
171
172
173
174
175
176
177
178
179
180
181
182
183
184
185
186
187
188
189
190
191
192
193
194
195
196
197
198
199
200
201
202
203
204
205
206
207
208
209
210
211
212
213
214
215
216
217
218
219
220
221
222
223
224
225
226
227
228
229
230
231
232
233
234
235
236
237
238
239
240
241
242
243
244
245
246
247
248
249
250
251
252
253
254
255
256
257
258
259
260
261
262
263
264
265
266
267
268
269
270
271
272
273
274
275
276
277
278
279
280
281
282
283
284
285
286
287
288
289
290
291
292
293
294
295
296
297
298
299
300
301
302
303
304
305
306
307
308
309
310
311
312
313
314
315
316
317
318
319
320
321
322
323
324
325
326
327
328
329
330
331
332
333
334
335
336
337
338
339
340
341
342
343
344
345
346
347
348
349
350
351
352
353
354
355
356
357
358
359
360
361
362
363
364
365
366
367
368
369
370
371
372
373
374
375
376
377
378
379
380
381
382
383
384
385
386
387
388
389
390
391
392
393
394
395
396
397
398
399
400
401
402
403
404
405
406
407
408
409
410
411
412
413
414
415
416
417
418
419
420
421
422
423
424
425
426
427
428
429
430
431
432
433
434
435
436
437
438
439
440
441
442
443
444
445
446
447
448
449
450
451
452
453
454
455
456
457
458
459
460
461
462
463
464
465
466
467
468
469
470
471
472
473
474
475
476
477
478
479
480
481
482
483
484
485
486
487
488
489
490
491
492
493
494
495
496
497
498
499
500
501
502
503
504
505
506
507
508
509
510
511
512
513
514
515
516
517
518
519
520
521
522
523
524
525
526
527
528
529
530
531
532
533
534
535
536
537
538
539
540
541
542
543
544
545
546
547
548
549
550
551
552
553
554
555
556
557
558
559
560
561
562
563
564
565
566
567
568
569
570
571
572
573
574
575
576
577
578
579
580
581
582
583
584
585
586
587
588
589
590
591
592
593
594
595
596
597
598
599
600
601
602
603
604
605
606
607
608
609
610
611
612
613
614
615
616
617
618
619
620
621
622
623
624
625
626
627
628
629
630
631
632
633
634
635
636
637
638
639
640
641
642
643
644
645
646
647
648
649
650
651
652
653
654
655
656
657
658
659
660
661
662
663
664
665
666
667
668
669
670
671
672
673
674
675
676
677
678
679
680
681
682
683
684
685
686
687
688
689
690
691
692
693
694
695
696
697
698
699
700
701
702
703
704
705
706
707
708
709
710
711
712
713
714
715
716
717
718
719
720
721
722
723
724
725
726
727
728
729
730
731
732
733
734
735
736
737
738
739
740
741
742
743
744
745
746
747
748
749
750
751
752
753
754
755
756
757
758
759
760
761
762
763
764
765
766
767
768
769
770
771
772
773
774
775
776
777
778
779
780
781
782
783
784
785
786
787
788
789
790
791
792
793
794
795
796
797
798
799
800
801
802
803
804
805
806
807
808
809
810
811
812
813
814
815
816
817
818
819
820
821
822
823
824
825
826
827
828
829
830
831
832
833
834
835
836
837
838
839
840
841
842
843
844
845
846
847
848
849
850
851
852
853
854
855
856
857
858
859
860
861
862
863
864
865
866
867
868
869
870
871
872
873
874
875
876
877
878
879
880
881
882
883
884
885
886
887
888
889
890
891
892
893
894
895
896
897
898
899
900
901
902
903
904
905
906
907
908
909
910
911
912
913
914
915
916
917
918
919
920
921
922
923
924
925
926
927
928
929
930
931
932
933
934
935
936
937
938
939
940
941
942
943
944
945
946
947
948
949
950
951
952
953
954
955
956
957
958
959
960
961
962
963
964
965
966
967
968
969
970
971
972
973
974
975
976
977
978
979
980
981
982
983
984
985
986
987
988
989
990
991
992
993
994
995
996
997
998
999
1000
1001
1002
1003
1004
1005
1006
1007
1008
1009
1010
1011
1012
1013
1014
1015
1016
1017
1018
1019
1020
1021
1022
1023
1024
1025
1026
1027
1028
1029
1030
1031
1032
1033
1034
1035
1036
1037
1038
1039
1040
1041
1042
1043
1044
1045
1046
1047
1048
1049
1050
1051
1052
1053
1054
1055
1056
1057
1058
1059
1060
1061
1062
1063
1064
1065
1066
1067
1068
1069
1070
1071
1072
1073
1074
1075
1076
1077
1078
1079
1080
1081
1082
1083
1084
1085
1086
1087
1088
1089
1090
1091
1092
1093
1094
1095
1096
1097
1098
1099
1100
1101
1102
1103
1104
1105
1106
1107
1108
1109
1110
1111
1112
1113
1114
1115
1116
1117
1118
1119
1120
1121
1122
1123
1124
1125
1126
1127
1128
1129
1130
1131
1132
1133
1134
1135
1136
1137
1138
1139
1140
1141
1142
1143
1144
1145
1146
1147
1148
1149
1150
1151
1152
1153
1154
1155
1156
1157
1158
1159
1160
1161
1162
1163
1164
1165
1166
1167
1168
1169
1170
1171
1172
1173
1174
1175
1176
1177
1178
1179
1180
1181
1182
1183
1184
1185
1186
1187
1188
1189
1190
1191
1192
1193
1194
1195
1196
1197
1198
1199
1200
1201
1202
1203
1204
1205
1206
1207
1208
1209
1210
1211
1212
1213
1214
1215
1216
1217
1218
1219
1220
1221
1222
1223
1224
1225
1226
1227
1228
1229
1230
1231
1232
1233
1234
1235
1236
1237
1238
1239
1240
1241
1242
1243
1244
1245
1246
1247
1248
1249
1250
1251
1252
1253
1254
1255
1256
1257
1258
1259
1260
1261
1262
1263
1264
1265
1266
1267
1268
1269
1270
1271
1272
1273
1274
1275
1276
1277
1278
1279
1280
1281
1282
1283
1284
1285
1286
1287
1288
1289
1290
1291
1292
1293
1294
1295
1296
1297
1298
1299
1300
1301
1302
1303
1304
1305
1306
1307
1308
1309
1310
1311
1312
1313
1314
1315
1316
1317
1318
1319
1320
1321
1322
1323
1324
1325
1326
1327
1328
1329
1330
1331
1332
1333
1334
1335
1336
1337
1338
1339
1340
1341
1342
1343
1344
1345
1346
1347
1348
1349
1350
1351
1352
1353
1354
1355
1356
1357
1358
1359
1360
1361
1362
1363
1364
1365
1366
1367
1368
1369
1370
1371
1372
1373
1374
1375
1376
1377
1378
1379
1380
1381
1382
1383
1384
1385
1386
1387
1388
1389
1390
1391
1392
1393
1394
1395
1396
1397
1398
1399
1400
1401
1402
1403
1404
1405
1406
1407
1408
1409
1410
1411
1412
1413
1414
1415
1416
1417
1418
1419
1420
1421
1422
1423
1424
1425
1426
1427
1428
1429
1430
1431
1432
1433
1434
1435
1436
1437
1438
1439
1440
1441
1442
1443
1444
1445
1446
1447
1448
1449
1450
1451
1452
1453
1454
1455
1456
1457
1458
1459
1460
1461
1462
1463
1464
1465
1466
1467
1468
1469
1470
1471
1472
1473
1474
1475
1476
1477
1478
1479
1480
1481
1482
1483
1484
1485
1486
1487
1488
1489
1490
1491
1492
1493
1494
1495
1496
1497
1498
1499
1500
1501
1502
1503
1504
1505
1506
1507
1508
1509
1510
1511
1512
1513
1514
1515
1516
1517
1518
1519
1520
1521
1522
1523
1524
1525
1526
1527
1528
1529
1530
1531
1532
1533
1534
1535
1536
1537
1538
1539
1540
1541
1542
1543
1544
1545
1546
1547
1548
1549
1550
1551
1552
1553
1554
1555
1556
1557
1558
1559
1560
1561
1562
1563
1564
1565
1566
1567
1568
1569
1570
1571
1572
1573
1574
1575
1576
1577
1578
1579
1580
1581
1582
1583
1584
1585
1586
1587
1588
1589
1590
1591
1592
1593
1594
1595
1596
1597
1598
1599
1600
1601
1602
1603
1604
1605
1606
1607
1608
1609
1610
1611
1612
1613
1614
1615
1616
1617
1618
1619
1620
1621
1622
1623
1624
1625
1626
1627
1628
1629
1630
1631
1632
1633
1634
1635
1636
1637
1638
1639
1640
1641
1642
1643
1644
1645
1646
1647
1648
1649
1650
1651
1652
1653
1654
1655
1656
1657
1658
1659
1660
1661
1662
1663
1664
1665
1666
1667
1668
1669
1670
1671
1672
1673
1674
1675
1676
1677
1678
1679
1680
1681
1682
1683
1684
1685
1686
1687
1688
1689
1690
1691
1692
1693
1694
1695
1696
1697
1698
1699
1700
1701
1702
1703
1704
1705
1706
1707
1708
1709
1710
1711
1712
1713
1714
1715
1716
1717
1718
1719
1720
1721
1722
1723
1724
1725
1726
1727
1728
1729
1730
1731
1732
1733
1734
1735
1736
1737
1738
1739
1740
1741
1742
1743
1744
1745
1746
1747
1748
1749
1750
1751
1752
1753
1754
1755
1756
1757
1758
1759
1760
1761
1762
1763
1764
1765
1766
1767
1768
1769
1770
1771
1772
1773
1774
1775
1776
1777
1778
1779
1780
1781
1782
1783
1784
1785
1786
1787
1788
1789
1790
1791
1792
1793
1794
1795
1796
1797
1798
1799
1800
1801
1802
1803
1804
1805
1806
1807
1808
1809
1810
1811
1812
1813
1814
1815
1816
1817
1818
1819
1820
1821
1822
1823
1824
1825
1826
1827
1828
1829
1830
1831
1832
1833
1834
1835
1836
1837
1838
1839
1840
1841
1842
1843
1844
1845
1846
1847
1848
1849
1850
1851
1852
1853
1854
1855
1856
1857
1858
1859
1860
1861
1862
1863
1864
1865
1866
1867
1868
1869
1870
1871
1872
1873
1874
1875
1876
1877
1878
1879
1880
1881
1882
1883
1884
1885
1886
1887
1888
1889
1890
1891
1892
1893
1894
1895
1896
1897
1898
1899
1900
1901
1902
1903
1904
1905
1906
1907
1908
1909
1910
1911
1912
1913
1914
1915
1916
1917
1918
1919
1920
1921
1922
1923
1924
1925
1926
1927
1928
1929
1930
1931
1932
1933
1934
1935
1936
1937
1938
1939
1940
1941
1942
1943
1944
1945
1946
1947
1948
1949
1950
1951
1952
1953
1954
1955
1956
1957
1958
1959
1960
1961
1962
1963
1964
1965
1966
1967
1968
1969
1970
1971
1972
1973
1974
1975
1976
1977
1978
1979
1980
1981
1982
1983
1984
1985
1986
1987
1988
1989
1990
1991
1992
1993
1994
1995
1996
1997
1998
1999
2000

```

```

105 90 CONTINUE
106 C .....
107 C ..... READ AND PRINT BOUNDARY CONDITIONS .....
108 C .....
109 WRITE(3,2070)
110 READ(1,2080) MB7,NOX,NOXY
111 10 = NOV * 1
112 10 = NOV * NOX
113 10 = 10 * 1
114 10 = NOV * NOX * NOXY
115 IF(NOV .EQ. 0) GO TO 93
116 READ(1,2090) (ZEM1,NE1,NOY)
117 WRITE(4,2075) (IC(N),M1,NOY)
118 IF(NOX .EQ. 0) GO TO 97
119 READ(1,2090) (IC(N),NE1,P1,M)
120 WRITE(3,2080) (IC(N),M1,P1,M)
121 IF(NOX .EQ. 0) GO TO 99
122 READ(1,2090) (IC(N),M1,N1,IO)
123 WRITE(3,2090) (IC(N),M1,N1,IO)
124 C .....
125 C ..... READ AND PRINT OF ELEMENT DATA .....
126 C .....
127 99 N = 0
128 WRITE(3,2100)
129 READ(1,2100) M(L(N)),I(L(N),1)
130 N = N + 1
131 IF(N .EQ. N) GO TO 120
132 I(L(N,1)) = I(L(N),1) + 1
133 I(L(N,2)) = I(L(N),2) + 1
134 I(L(N,3)) = I(L(N),3) + 1
135 I(L(N,4)) = I(L(N),4) + 1
136 I(L(N,5)) = I(L(N),5) + 1
137 WRITE(3,2105) (I(L(N),1),I(L(N),2),I(L(N),3),I(L(N),4),I(L(N),5))
138 IF (M .EQ. N) GO TO 130
139 IF (N .LE. NUMEL) GO TO 110
140 WRITE(3,2107)
141 GO TO 808
142 IF(NUMEL .EQ. 8) GO TO 140
143 GO TO 100
144 140 CONTINUE
145 150 CONTINUE
146 C .....
147 C ..... DETERMINE GARD HIGH .....
148 C .....
149 140
150 DO 250 N=1,NUMEL
151 DO 250 I=1,4
152 DO 250 L=1,4
153 KK=LAB9(I(L(N),1),I(L(N),2))
154 IF(KK=J1240,846,330)
155 JKK
156 MK2=(MK+2)/2

```

```

157 IF (J.LE.MB) GO TO 240
158 WRITE (3,2118) N
159 CONTINUE
160 CONTINUE
161 MBAND=2*J+2
162 IF MBAND.LE.MW / GO TO 300
163 GO TO 600
164 CONTINUE
165 WRITE(3,2120) MBAND
166 NMP = 0
167 NLL = 0
168
169 C * * * * *
170 C * * * * * ESTABLISH INITIAL STRESSES IN SUBROUTINE INITIAL * * * * *
171 C * * * * * CALL INITIAL * * * * *
172 C * * * * *
173 C * * * * * PERFORM INCREMENTAL LOADING * * * * *
174 C * * * * *
175 IRINC .EQ. 01 GO TO 600
176 DO 330 MB = 5,NC
177 WRITE(3,2130) MB
178 READ (1,1030) NUL,NLL,MS,NMP,INT,INF
179 NP(1) = 0
180 DO 305 I = 1,NOMP
181 305 FV(I) = 0.
182
183 C * * * * *
184 C * * * * * READ AND PRINT EXCAVATION DATA * * * * *
185 C * * * * *
186
187 IF NUL .EQ. 01 GO TO 320
188 READ(1,1031) NEL
189 READ(1,1032) (LUL(I),I=1,10),Nal,NEL)
190 WRITE(3,2135)
191 WRITE(3,2140) (LUL(N),I=1,10),NFI,NEL)
192 CALL EXCAV
193 C * * * * *
194 C * * * * * READ AND PRINT BUILD-UP DATA * * * * *
195 C * * * * *
196 310 IF NLL .EQ. 01 GO TO 330
197 READ(1,1050) NLEL,(LEL(N),N = 1,NLEL)
198
199 READ(1,1051) NJ
200 READ(1,1052) NOMP,TMP,INT,N = 1,NOMP)
201 READ(1,1041) NCS,MSB,MTB
202 READ(1,1042) NMPX,ED,OT GO TO 4011
203 FORMAT(215)
204 I=2,I=N,NCR=1
205 READ(1,1042)(C(I),I=1,I,IP2)
206 1042 FORMAT(1619)
207 4001 FORMAT(4X,50NODS FIXED IN X-DIRECTION FOR THIS INCREMENT ONLY)
208 4002 FORMAT(4X,50NODS FIXED IN Y-DIRECTION FOR THIS INCREMENT ONLY)

```

```

209 WRITE(3,4001)
210 WRITE(3,4003) LG((1:3),IP3,IP2)
211 DO 3051 I=1,IP2
212   NNALC(I)
213   3051 FX(INN)=0.0
214 CONTINUE
215 IF(NMPY,NO,0) GO TO 4012
216 IS=IP3+ANNX
217 I=2*IP3-ANNX*(NMPY-1)
218 READ(1,1042) (IC(I),I=IP3,IP4)
219 WRITE(3,4002)
220 FORMATTED(3,2015)
221 WRITE(3,4003) (IC(I),I=IP3,IP4)
222 DO 3052 I=1,IP3,IP4
223   NNALC(I)
224   3052 FY(INN)=0.0
225   4012 CONTINUE
226 WRITE(3,2000)
227 WRITE(3,2001) NLBL,(CEL(M),M=1,NLBL)
228 CALL BU10
229 IF(NJ,LEQ, (NCEL+1)) GO TO 330
230 DO 320 N=1,NLBL
231   M = LEL(N)
232   STG(M)=0.0
233   STFM(M) = 10000000.0
234   320 STFM(M) = 10000000.0
235 C * * * * *
236 C * * * * * GENERATE SEEPAGE LOADING * * * * *
237 C * * * * *
238 330 I=1,NO,0) GO TO 330
239 WRITE(3,2200)
240 CALL SEER
241 C * * * * * READ AND PRINT BOUNDARY PRESSURE LOADING DATA * * * * *
242 C * * * * *
243 350 IF (NMP,LEQ,0) GO TO 360
244 WRITE(3,2200)
245 READ (1,1030) NMP
246 READ (1,1040) (IC(L),J=1,IP3), (L=1,NMP)
247 WRITE(3,2300) (IC(L),J=1,IP3), (L=1,NMP)
248 C * * * * *
249 C * * * * * ACKNOWLEDGE TEMPERATURE LOADING * * * * *
250 C * * * * *
251 360 PRINT (50,0) GO TO 370
252 WRITE(3,2320) HQ
253 C * * * * *
254 C * * * * * ZERO LOADS ON FIXED BOUNDARY POINTS * * * * *
255 C * * * * *
256 370 DO 400 M=1,110
257   M = IC(M)
258   IF(M,GT, NOY) GO TO 390
259   PT(M)=0.0
260   IF(M,LE,NOY) GO TO 400

```

```

261 360 FXIN) = 0,0
262 400 CONTINUE
263 C .....
264 C ..... ACKNOWLEDGE CONCENTRATED FORCE OR DISPLACEMENT LOADING
265 C .....
266 IFTMP = 0, 01 50 TO 470
267 WRITE(3,2340)
268 READ(1,1830) NCL
269 DO 450 I = 1, NCL
270 READ(1,1070) M, X1, Y1, N, X2, Y2
271 FX(M) = FX(M) * X1
272 FY(M) = FY(M) * Y1
273 FXIN) = FXIN) + X2
274 FYIN) = FYIN) + Y2
275 450 WRITE(3,2350) M, X1, Y1, N, X2, Y2
276 470 CONTINUE
277 DO 500 NB = 1, NUNAPP
278 C .....
279 C ..... SET UP STRUCTURE STIFFNESS MATRIX AND LOAD VECTORS
280 C .....
281 C ..... CALL SUBROUTINE
282 C .....
283 C ..... SOLVE SIMULTANEOUS EQUATIONS FOR DISPLACEMENTS
284 C .....
285 C ..... CALL BANSOL
286 C .....
287 C ..... SOLVE FOR ELEMENT STRESSES AT CENTER NODE
288 C .....
289 C ..... CALL STRESS
290 CONTINUE
291 NMPX=0
292 NMPY=0
293 590 CONTINUE
294 600 CONTINUE
295 C .....
296 GO TO 30
297 1000 FORMAT(20A4,10I9,2F10,3,15)
298 1010 FORMAT(8F10,5)
299 1012 FORMAT(19,9,2,7F10,5)
300 1015 FORMAT(5E15,5,15)
301 1020 FORMAT(11I0,6F10,3)
302 1030 FORMAT(8I10)
303 1040 FORMAT(21I0,4F10,4)
304 1050 FORMAT(13I9)
305 1060 FORMAT(32I6,7,5,2,7)
306 1070 FORMAT(21I10,2E10,2)
307 12000 FORMAT(1M,20A4,7,30X, NUMBER OF NODAL POINTS =,15,30X, NUMBER OF
308 ELEMENTS =,15,30X,10A4, NUMBER OF DIFFERENT MATERIALS =,15,30X)
309 21 NUMBER OF DIFFERENT MATERIALS FOR TWO DIMENSIONAL ELEMENTS =,15,
310 330X, NUMBER OF ONE-D ELEMENTS =,15,30X, NUMBER OF LOAD CASES =,15,
311 419,30X, NUMBER OF ITERATIONS PER LOAD CASE =,15,30X, INITIAL STRE
312 555 CODE =,15,30X, MODULUS CALCULATION CODE =,15,30X, UNIT WEIGHT

```



```

1 SUBROUTINE INITIAL
2 IMPLICIT DOUBLE PRECISION (A-H,O-Z)
3 PARAMETER NCL=599
4 PARAMETER NND=761
5 PARAMETER NNS=120
6 PARAMETER NNS2=
7 PARAMETER NNS3=
8 COMMON
9
10 I, NAPP, INITHTYPE, NBY, VOX, ROXY, NCE, NLE, NDB, NDNP, DTB, WCTYP, DBITY
11 2P, N82, YP, NATYP, NBL, NRIP, NLL, NF, NHPF, NUL, M, NG, NQ, NQ, NP, NY, MBAND,
12 3TEMP, NUNBLK, I1, JJ, KK, VOL, UM, SL, XC, YC, RC, RR, PATH, GASH, RKS(20), COJC
13 4TOT, NHT(99), CORP(10), EXP(10), STW(10), STP(10), SBART(20), IEM(10)
14 5UI(20), GOF(20), A0(20), ALPMA(20), PH(20), ONE(20), HCRF(20), HRF(20)
15 6ULCORF(20), FR(20), S(4), P, STR(5), SIG(SEL), NEE(MEL), BMOB(MEL), GUM(
16 7LT, XT, RNDT, TT, RNDT, DTB, NDBZ, TIT, X, RNDT, TIT, RNDT, DTB, NDBZ, TIT, X, RNDT,
18 8), JL(HEL), S, L, L(NEE), S, L(NEE), AP(N4), LBC(MS), JBC(MS), PR(N5), I, I(
19 9, 4), XY(2, 4), I(NB4), A(MB4, MK), IS(10, 10), P(80), C(4, 4), LM(8), BAIS, Z1, A
20 COMMON/DRAIN/NDR(41)/20
21 REAL MED
22 NNPX=0
23 NNPYC=0
24 WRITE(*,*)R0001
25 I1 = 0
26 I1 = 0
27 NG = 1
28 NQ = NUMAPP
29 NTRIP = 1
30 IPIINIT = 59, I1 GO TO 100
31 C . . . . .
32 C . . . . .
33 C . . . . .
34 C . . . . .
35 C . . . . .
36 READ(7, 1000), (S1(I, M), M=1, 4), N31, NUDEL)
37 READ(7, 1020), I(4, 2), M=1, NUMEL)
38 IPI NUMJY , 80, 91 GO TO 170
39 READ(7, 1030), STP(10), STP(10), STP(10), STP(10), STP(10), STP(10), STP(10), STP(10), STP(10), STP(10)
40 GO TO 170
41 C . . . . .
42 C . . . . .
43 C . . . . .
44 C . . . . .
45 C . . . . .
46 DO 130 M = 1, NUDEL
47 SIG(N, M) = 0.0
48 IPI(LINE) = TOTI, NUM86(1) GO TO 140
49 BEIN) = 500000
50 IPI(LIN, B) , EQ) MATWR) BE(N) = 5(NATYP)
51 MATWR = PL(N, 2)
52 GUE = GUI(MTYPE)

```

R0588 01 11-18-76 17.345

```

53 QU(N) = QUI(1700)
54 RMOD(N) = REIN(172.015, * QUE(1,1,2,0UB))
55 GO TO 150
56 140 STFN(N) = 100000000.
57 STFS(N) = 100000000.
58 150 CONTINUE
59 DO 160 N = 170NMP
60 PY(N) = 0.0
61 160 FX(N) = 0.0
62 CALL STRSTP
63 CALL BANSOL
64 CALL STRESS
65
66 170 DO 360 N = 170NMBL
67 RTYPE = IL(N75)
68 IF(INIT .EQ. 0) GO TO 260
69 IF(MTYPE .LE. NUNSO) GO TO 240
70
71
72
73
74 260 SIG(N,1) = ABS(MTYPE)*SIG(N,2)
75 SIG(N,4) = ABS(SIG(N,1) - SIG(N,2))/2.
76
77
78
79
80 DO 250 I=1,4
81 L=IL(N,I)
82
83
84 UNLUU/4, QGANW
85 SIG(N,1)SIG(N,2)SUM
86
87 260 IF(MTYPE .GT. NUNSO) GO TO 340
88
89
90
91
92
93
94
95
96
97
98
99
100
101
102
103

```



```

1 SUBROUTINE EXCAV
2 IMPLICIT DOUBLE PRECISION (A-H,O-Z)
3 PARAMETER M=330
4 PARAMETER MND=761
5 PARAMETER MBR=720
6 PARAMETER M=600
7 PARAMETER NEE=2,NBE=300,N4=20,N5=2
8 COMMON /MED/20,LL,NURMP,NUMEL,NURMAT,NURMSOL,I,PRD,LORUL,INUM,JT
9 I,NURAPP,INIT,NTYPE,NOY,NOX,NOXY,NCE,MLE,NBIE,NONP,PTB,NCYF,IRBITY
10 2P,NB2TP,NATYP,MEL,NTRIP,NLL,NF,NMPF,NUL,M5,MC,MU,NO,NHP,NT,MBAND,
11 3TEMP,NUMRLK,II,JJ,KK,VOL,UM,SL,AC,YC,RDF,RD,PATM,GAMW,ARKS(20),COJ,
12 4201,PHI(20),CORF(20),EXF(20),STFN(20),SYF(20),GAT(20),E(20),G
13 5UL(20),GUF(20),AS(20),ALPHA(20),PHI(20),CONE(20),HCOEF(20),AKP(20)
14 6-ULCOEF(20),FR(20),B(4),PSTR(5),SIG(MEL,4),FER(MEL),BMOD(MEL),GUCHE
15 7L,X(MND),Y(MND),Z(MND),Z1,F(X,MND),FY(MND),FP(MND),DP(MND),TC(30
16 80),LL(MEL,5),LUL(NEE,8),LEL(NBE),NP(N4),IBE(N5),JBC(N5),PR(N5),F(2
17 9,4),XY(2,4),BL(MB4),A(HW,MW),S(10,10),R(10),C(4,4),LM(8),BA(3,2),A
18 IBC(3,4,2),DUC(3,10),SY(3,20)
19 DIMENSION X(9,3),Z(13,3)
20 EQUIVALENCE IS,Z1,(9(10,4),2P)
21 REAL MED
22 C .....
23 III = 0
24 ISTOP = 0
25 S2=SORF(2,1)0.5
26 DO 300 M = 1,MEL
27 NT = COL(M,II)
28 IF (M.EQ.1) GO TO 50
29 MK = LUL(M-1,1)
30 IF (LL(M,5) .LE. NURMSOL) GO TO 90
31 SYF(M,1) = 10.
32 SYFN(M,1) = 10.
33 GO TO 300
34 IL(1,5) = NATYP
35 EG(1) = E(NATYP)
36 BRODINT(E(NATYP))
37 DO 100 I = 1,4
38 IF (LUL(M,1+4) .NE. 0) GO TO 110
39 100 CONTINUE
40 GO TO 300
41 110 CONTINUE
42 III = III + 1
43 DO 25 I = 1,4
44 DO 25 J = 1,3
45 CONTINUE
46 C .....
47 C * * * SET UP CENTER NODE COORDINATE MATRIX SE * * *
48 .....
49 DO 120 NN = 1,4
50 MM = LUL(M,NN)
51 I = LL(M,1)
52 J = LL(M,2)

```


RD498.01 14-18-76 17.350

```

105 240 CONTINUE
106 S(I,I) = SUM
107 142 CONTINUE
108 C
109 S(I,I)=1.
110 C
111 C * * * SOLVE FOR INTERPOLATION COEFFICIENT MATRIX ABC( ) * * *
112 C * * *
113 DO 190 KK = 1,3
114 DO 190 JJ = 1,4
115 ABC(KK,JJ) = 0.
116 DO 190 IJ = 1,7
117 IF(IKK .EQ. 3) R(IJ) = 0.0
118 MM = LUL(M,IJ)
119 ABC(KK,JJ) = ABC(KK,JJ) + S(JJ,I)*R(IJ)*MM * P(IJ)
120 C * * * SOLVE FOR NODAL STRESS MATRIX C( ) * * *
121 C * * *
122 DO 200 KK = 1,4
123 DO 200 KK = 1,4
124 MM = IL(INI,KK)
125 XXX(XMM) = S(I,I)
126 YY = (MM) - S(I,I)
127 IF(DI2) 202, 204, 204
128 DO 200 XX = (DI,XY)*98
129 YY = (YY-DI)*98
130 C * * *
131 IF(IJ) 201, 13 GO TO 220
132 DO 210 I = 1,4
133 IF(IJ) 201, 13 GO TO 220
134 IF(CIL(M,I)) 201, 201, 201 GO TO 290
135 CONTINUE
136 C(JJ,KK) = ABC(JJ,1) * X + ABC(JJ,2) * Y *
137 I * ABC(JJ,3) * X * X +
138 GO TO 250
139 DO 240 K = 1,3
140 C(K,KK) = 0.0
141 CONTINUE
142 CALL EMBFQ(MI)
143 C * * *
144 C * * * ADD EQUIVALENT NODAL FORCES TO CONCENTRATED NODAL FORCES * * *
145 C * * * IF LUL(M,4-8) EQUALS ZERO - NODE NOT LOADED * * *
146 C * * *
147 DO 260 I = 1,4
148 IM = IL(INI,I)
149 IF(CUL(M,I)) 261, 261, 261 GO TO 260
150 FX(IM) = FX(IM) + F(1,I)
151 FY(IM) = FY(IM) + F(2,I)
152 CONTINUE
153 CONTINUE
154 IF(CSTOP .EQ. 1) CALL EXIT
155 RETURN
156 2000 FORMAT(///20Y,'ELEMENT',14,1HAS PRODUCED A SINGULAR INTERPOLATIO

```


1 SUBROUTINE MINV3(D1,D2,D32)
2 IMPLICIT DOUBLE PRECISION (A-H,O-Z)

3
4
5
6
7
8
9
10
11
12
13
14
15
16
17
18
19
20
21
22
23
24
25
26
27
28
29
30
31
32
33
34
35
36
37
38
39
40
41
42
43
44
45
46
47
48
49
50
51
52

THIS SUBROUTINE INVERTS A 3 X 3 MATRIX

DESCRIPTION OF MAJOR VARIABLES

C Z ZP THE MATRIX TO BE INVERTED,

B THE TRANSPOSE OF THE ADJOINT MATRIX,

D1 THE DETERMINANT OF MATRIX Z,

D2 THE DETERMINANT OF MATRIX ZP.

PARAMETER MEL=690

PARAMETER MND=761

PARAMETER MNS=120

PARAMETER MNE=60

PARAMETER NEG=190, N=4, S=NUMBER

COMMON

MEL(20), LL, NUMRP, NUMEL, NUMMAT, NUMSOL, ITRD, LORUL, NUMJUT

1, NUMAPP, INITIATYRE, NOY, NOX, NOXY, ACE, NLEL, NBL16, NONP, ITRB, NCTYP, NBL1TY

20, NBSIZE, MATAT, NBL, NTRIP, NLL, NMF, NHP, NBL, NBS, NCT, NTRAND, NCT, NTRAND

3TEMP, NUMBLK, I1, JU, KK, VOL, UM, SL, XC, YC, RBF, ORD, PATN, GAMM, RKS(20), COJ(

420), PHJ(20), COEFJ(20), EXPJ(20), STFN(20), STFS(320), GAM(20), E(20), G

SUIT(20), SUF(20), SUI(20), ALP, MAT(20), PHT(20), COME(20), MGBE(20), EXP(20)

6, ULCOE(20), PR(20), GZ(4), PSTA(51), SIG(4), FEF, MEL, JMOD(4), S(4)

7L, X(MND), Y(MND), DISP(MND, 2), P(MND), F1(MND), F2(MND), DP(MND), DP(MND), I(30

8), ILM(8), BA(3, 27), ABC(3, 4, 2), DD(3, 10), ST(3, 10)

REAL MSD

DO 20 I=1,3

IA = MOD(I, 3) + 1

IB = MOD(I+1, 3) + 1

DO 10 J=1,3

JAT = MOD(J, 3) + 1

JB = MOD(J+1, 3) + 1

IF(D12) 2, 4, 4

2 B(CJ1) = ZP(IA, JAT) * ZP(I8, JB) - ZP(IA, JB) * ZP(I8, JAT)

GO TO 10

4 B(CJ1) = Z(IA, JAT) * Z(I8, JB) - Z(IA, JB) * Z(I8, JAT)

CONTINUE

CONTINUE

IF(D12) 221-247, 24

22 D=02

RO588 01 11-18-76 17,354

53 GO TO 26
54 24 DDD1
55 26 IPD) 30:100730
56 C
57 30 00 40 144.3
58 00 40 JRIJ
59 Z(1-J)8(1, J)/D
60 40 CONTINUE
61 C
62 100 RETURN
63 END

```

1 SUBROUTINE EONDFO(N1)
2 IMPLICIT DOUBLE PRECISION (A-M,O-Z)
3 PARAMETER M=100
4 PARAMETER MND=761
5 PARAMETER MBR=120
6 PARAMETER M=800
7 PARAMETER NEE=2, NBE=100, N=20, ND=2
8 COMMON HED(20), LL, NUMAP, NUMEL, NUMMAT, NUMSOL, ITRD, CORUL, RUMHJT
9 I, NUMAPP, INIT, HTYPE, NBY, INOX, ROXY, INCE, ILE, CRBIE, NONP, CRTG, INCTYP, INDITY
10 2P, NB2, YP, NATYP, NEL, NTRIP, ALL, NF, NHPF, NUL, MG, NC, HQ, NB, NUP, INT, MBAND,
11 3TEMP, NUMBLK, I1, JJ, KK, VOL, UM, SL, XC, YC, RDP, RD, PATH, GAW, RKS(20), COJ,
12 501(20), PMJ(20), COE(20), EX(20), ST(20), ST(20), ST(20), ST(20), ST(20), ST(20),
13 501(20), 50F(20), AG(20), ALPHAT(20), PHIT(20), COHE(20), HCOEF(20), AXB(20)
14 6, ULCOEF(20), FR(20), S(4), PTR(5), SIG(NE), 4) SEB(MBL), BMOD(MEL), QU(ME
15 6) T, X(MBT), X(MOT), X(MP), X(MD), X(MD), X(MD), X(MD), X(MD), X(MD), X(MD), X(MD),
16 80), IL(MEL), 5), LUL(NEE, 8), LEL(NBE), NP(N4), IBE(M5), JBC(M5), PR(M5), 17(2
17 9, 4), XY(2, 4), R(4B, 4), A(RB, 4M), S(10, 10), P(10), G(4, 4), L(MI), B(A(3, 2)), A
18 1967377878813.1877377777
19 REAL MED
20 C ..
21 C ..
22 C ..
23 C ..
24 C ..
25 C ..
26 C ..
27 C ..
28 C ..
29 C ..
30 C ..
31 C ..
32 C ..
33 C ..
34 C ..
35 C ..
36 C ..
37 C ..
38 C ..
39 C ..
40 C ..
41 C ..
42 C ..
43 C ..
44 C ..
45 C ..

```

```

1 SUBROUTINE BUILD
2 IMPLICIT DOUBLE PRECISION (A-H,O-Z)
3 PARAMETER MLE=800
4 PARAMETER MND=761
5 PARAMETER MB4=120
6 PARAMETER MZ=60
7 PARAMETER NBE=100, N4=20, N3=2
8 COMMON HED(20), ALL, NUMP, NUMEL, NUMMAT, NUMSOL, ITRD, LORUL, BUM, JT
9 I, NDAPP, INI, TRTYPE, NDT, NOXT, NOXTNCE, NLELENB1, NDT, NDT, NDT, NDT, NDT
10 2P, NB2TYP, NATYP, NBL, NTRIP, NLL, NFANPFF, NULSMS, MC, MO, NG, NMP, NTA, MBAND,
11 STEHP, NUMBLK, II, JJ, KK, VOL, UK, SL, AC, YC, RBF, RD, FATH, GASK, RKS(20), COJ(
12 420), PRA(20), COEF(20), EXPJ(20), STFN(20), STVF(20), WARI(20), E(20), JG
13 501(20), GOF(20), AO(20), ALPHA(20), PHI(20), COME(20), MCOEF(20), AMP(20)
14 6 ULCOE(20), P(20), Q(4), PSTB(5), S:GIMEL, 6) TEB(MBL), BMOD(MEL), GUCHE
15 7 UY, Y(PND), Y(PND), DTS(PND), FX(PND), Y(PND), PP(PND), DPF(MD), TC(30
16 80), IL(MEL,5), LUL(NEE,8), LEL(NBE), NP(NA), IBB(M5), JBC(M5), PR(INS), F(2
17 9,4), XY(2), I, B(MB4), AL(MB4), S(10,10), P(80), C(4,4), L(M(8), BA(3,2)), A
18 3803, #27, DDI(3,10), #313, #307
19 REAL MHD
20 C . . . . .
21 LL = 0
22 N1 = NCE * NB1E
23 1001 FORMAT(///12X, 7HELEMENT, 10X, 15HREDUCED MODULUS)
24 1000 FORMAT(5X110, #X7820, #7)
25 WRITE(5,1001)
26 DO 300 L = 1, NLEL
27 MM = LEL(L)
28 DO 90 J = 1, 174
29 SIG(MH, J) = 0.0
30 I = IL(MH, J)
31 J = JL(MH, 2)
32 K = IL(MH, 3)
33 H = IL(MH, 4)
34 YAVG = (Y(I) * Y(J) + Y(K) * Y(H)) / 4.
35 IF (IL(MH, 5) .LE. NUMSOL) GO TO 180
36 C . . . . . ESTABLISH STRESSES AND MATERIAL PARAMETERS . . . . .
37 C . . . . .
38 C . . . . .
39 D1 = X(J) * X(J)
40 DY = Y(J) - Y(I)
41 DL = SORT(DX**2 + DY**2)
42 CSN = D1/DL
43 SNE = DY/DL
44 ANG = 3.1415
45 IFAST(CAN=0) .LT. 0.000001) GO TO 190
46 TANG = SNE/CSN
47 ANG = 2. * ATAN(TANG)
48 190 SS = 6MHD * Y(J) * Y(J) * Y(J) * Y(J)
49 SH = AO * (ABS(I) * J ** 3)
50 SIG(MH, J) = 0.5 * (SS * SR) * 0.5 * (SS * SR) * CBS(ANG)
51 STFS(MH) = 100000000.
52 170 STFS(MH) = 10.

```

```

53 GO TO 308
54 180 M8 = NCTYP
55 IF(L .GT. NCE) M8 = NB2TYP
56 IF(L .GT. N1) M8 = M82TYP
57 I(LM,5) = M8
58 IF(ILMM,2) = 0, NB2TYP, 100, ILMM,3) = 0, NB2TYP, 00 TO 200
59 QU(MH) = QUIZ(NCTYP)
60 BMOD(MH) = E2(NCTYP)/(2.*(1. + QUJ(NCTYP))*.11. + 2.*QUJ(NCTYP)))
61 FE(M) = E2(NCTYP)
62 GO TO 220
63 S(2) = CAM(M)*(.17B-YAV,1)
64 Q(1) = QU(M)*B(2)
65 Q(3) = 0.0
66 Q(4) = 0.0
67 CALL MODCAL(MH)
68 IF(ILMM,5) .EQ. NB2TYP) GO TO 201
69 EE(MH) = EE(MH) * 1.003
70 201 ST(M,2) = Q(2)
71 SIG(M,1) = Q(3)
72 SIG(M,4) = Q(4)
73
74 C . . . GENERATE GRAVITY LOADING FOR BUILD-UP ELEMENTS . . .
75 C . . .
76 280 AREA = 0.0
77 I = IL(MH,1)
78 J = IL(MH,2)
79 K = IL(MH,4)
80 GO TO 260
81 240 I = IL(MH,3)
82 J = IL(MH,4)
83 K = IL(MH,2)
84 ITR = I * J
85 250 AREA = AREA + ITR*(X(I)-X(J))*(Y(I)-Y(J))
86 IF(I .EQ. IL(MH,1)) GO TO 240
87 IF(J .EQ. 260) GO TO 260
88 262 IOT = 0
89 GO TO 266
90 264 IOT = I
91 266 FI = IOT
92 CK = AREA * GAN(MGT/FI)
93 DO 280 I = 1, IOT
94 J = IL(MH,1)
95 280 FY(J) = FY(J) + CK
96 281 FE(J) = FE(J) + CK
97
98 300 CONTINUE
99 RETURN
100 END
    
```


R058B n1 11-18-76 17.35Z

52 VV = 0.
53 DO 157 I = 17 4
54 HH = F(1,1) * HH
55 VV = F(2,1) * VV
56 157 CONTINUE
57 HH = HH/PI
58 VV = VV/PI
59 DO 160 I = 17(1)
60 XY(1,1) = HH
61 160 XY(2,1) = VV
62 180 DO 187 J = 1,107
63 NN = IL(NI, J)
64 FX(NN) = FX(NN) * XV(1, J)
65 FY(NN) = FY(NN) * XV(2, J)
66 187 CONTINUE
67 200 RETURN
68
69 END

```

1 C
2 SUBROUTINE STRSTF
3 IMPLICIT DOUBLE PRECISION (A-H,O-Z)
4 PARAMETER NBL=693
5 PARAMETER NND=761
6 PARAMETER NMB=120
7 PARAMETER NME=2
8 PARAMETER NNE=2,NBE=100,N4=20,N5=2
9 COMMON /STRSTF/ I1,NAPP,INIT,TYPE,NBY,NX,NKY,NCE,LELE,NB1C,NONP,HTB,NCTYP,NB1TY
10 /STRSTF/ I2,NB2,VP,INA,VP,NEL,NAT,RP,ULL,NE,NCE,NLE,NB1C,NONP,HTB,NCTYP,NB1TY
11 /STRSTF/ I3,NB3,VP,INA,VP,NEL,NAT,RP,ULL,NE,NCE,NLE,NB1C,NONP,HTB,NCTYP,NB1TY
12 /STRSTF/ I4,NB4,VP,INA,VP,NEL,NAT,RP,ULL,NE,NCE,NLE,NB1C,NONP,HTB,NCTYP,NB1TY
13 /STRSTF/ I5,NB5,VP,INA,VP,NEL,NAT,RP,ULL,NE,NCE,NLE,NB1C,NONP,HTB,NCTYP,NB1TY
14 /STRSTF/ I6,NB6,VP,INA,VP,NEL,NAT,RP,ULL,NE,NCE,NLE,NB1C,NONP,HTB,NCTYP,NB1TY
15 /STRSTF/ I7,NB7,VP,INA,VP,NEL,NAT,RP,ULL,NE,NCE,NLE,NB1C,NONP,HTB,NCTYP,NB1TY
16 /STRSTF/ I8,NB8,VP,INA,VP,NEL,NAT,RP,ULL,NE,NCE,NLE,NB1C,NONP,HTB,NCTYP,NB1TY
17 /STRSTF/ I9,NB9,VP,INA,VP,NEL,NAT,RP,ULL,NE,NCE,NLE,NB1C,NONP,HTB,NCTYP,NB1TY
18 /STRSTF/ I10,NB10,VP,INA,VP,NEL,NAT,RP,ULL,NE,NCE,NLE,NB1C,NONP,HTB,NCTYP,NB1TY
19 /STRSTF/ I11,NB11,VP,INA,VP,NEL,NAT,RP,ULL,NE,NCE,NLE,NB1C,NONP,HTB,NCTYP,NB1TY
20 /STRSTF/ I12,NB12,VP,INA,VP,NEL,NAT,RP,ULL,NE,NCE,NLE,NB1C,NONP,HTB,NCTYP,NB1TY
21 /STRSTF/ I13,NB13,VP,INA,VP,NEL,NAT,RP,ULL,NE,NCE,NLE,NB1C,NONP,HTB,NCTYP,NB1TY
22 /STRSTF/ I14,NB14,VP,INA,VP,NEL,NAT,RP,ULL,NE,NCE,NLE,NB1C,NONP,HTB,NCTYP,NB1TY
23 /STRSTF/ I15,NB15,VP,INA,VP,NEL,NAT,RP,ULL,NE,NCE,NLE,NB1C,NONP,HTB,NCTYP,NB1TY
24 /STRSTF/ I16,NB16,VP,INA,VP,NEL,NAT,RP,ULL,NE,NCE,NLE,NB1C,NONP,HTB,NCTYP,NB1TY
25 /STRSTF/ I17,NB17,VP,INA,VP,NEL,NAT,RP,ULL,NE,NCE,NLE,NB1C,NONP,HTB,NCTYP,NB1TY
26 /STRSTF/ I18,NB18,VP,INA,VP,NEL,NAT,RP,ULL,NE,NCE,NLE,NB1C,NONP,HTB,NCTYP,NB1TY
27 /STRSTF/ I19,NB19,VP,INA,VP,NEL,NAT,RP,ULL,NE,NCE,NLE,NB1C,NONP,HTB,NCTYP,NB1TY
28 /STRSTF/ I20,NB20,VP,INA,VP,NEL,NAT,RP,ULL,NE,NCE,NLE,NB1C,NONP,HTB,NCTYP,NB1TY
29 /STRSTF/ I21,NB21,VP,INA,VP,NEL,NAT,RP,ULL,NE,NCE,NLE,NB1C,NONP,HTB,NCTYP,NB1TY
30 /STRSTF/ I22,NB22,VP,INA,VP,NEL,NAT,RP,ULL,NE,NCE,NLE,NB1C,NONP,HTB,NCTYP,NB1TY
31 /STRSTF/ I23,NB23,VP,INA,VP,NEL,NAT,RP,ULL,NE,NCE,NLE,NB1C,NONP,HTB,NCTYP,NB1TY
32 /STRSTF/ I24,NB24,VP,INA,VP,NEL,NAT,RP,ULL,NE,NCE,NLE,NB1C,NONP,HTB,NCTYP,NB1TY
33 /STRSTF/ I25,NB25,VP,INA,VP,NEL,NAT,RP,ULL,NE,NCE,NLE,NB1C,NONP,HTB,NCTYP,NB1TY
34 /STRSTF/ I26,NB26,VP,INA,VP,NEL,NAT,RP,ULL,NE,NCE,NLE,NB1C,NONP,HTB,NCTYP,NB1TY
35 /STRSTF/ I27,NB27,VP,INA,VP,NEL,NAT,RP,ULL,NE,NCE,NLE,NB1C,NONP,HTB,NCTYP,NB1TY
36 /STRSTF/ I28,NB28,VP,INA,VP,NEL,NAT,RP,ULL,NE,NCE,NLE,NB1C,NONP,HTB,NCTYP,NB1TY
37 /STRSTF/ I29,NB29,VP,INA,VP,NEL,NAT,RP,ULL,NE,NCE,NLE,NB1C,NONP,HTB,NCTYP,NB1TY
38 /STRSTF/ I30,NB30,VP,INA,VP,NEL,NAT,RP,ULL,NE,NCE,NLE,NB1C,NONP,HTB,NCTYP,NB1TY
39 /STRSTF/ I31,NB31,VP,INA,VP,NEL,NAT,RP,ULL,NE,NCE,NLE,NB1C,NONP,HTB,NCTYP,NB1TY
40 /STRSTF/ I32,NB32,VP,INA,VP,NEL,NAT,RP,ULL,NE,NCE,NLE,NB1C,NONP,HTB,NCTYP,NB1TY
41 /STRSTF/ I33,NB33,VP,INA,VP,NEL,NAT,RP,ULL,NE,NCE,NLE,NB1C,NONP,HTB,NCTYP,NB1TY
42 /STRSTF/ I34,NB34,VP,INA,VP,NEL,NAT,RP,ULL,NE,NCE,NLE,NB1C,NONP,HTB,NCTYP,NB1TY
43 /STRSTF/ I35,NB35,VP,INA,VP,NEL,NAT,RP,ULL,NE,NCE,NLE,NB1C,NONP,HTB,NCTYP,NB1TY
44 /STRSTF/ I36,NB36,VP,INA,VP,NEL,NAT,RP,ULL,NE,NCE,NLE,NB1C,NONP,HTB,NCTYP,NB1TY
45 /STRSTF/ I37,NB37,VP,INA,VP,NEL,NAT,RP,ULL,NE,NCE,NLE,NB1C,NONP,HTB,NCTYP,NB1TY
46 /STRSTF/ I38,NB38,VP,INA,VP,NEL,NAT,RP,ULL,NE,NCE,NLE,NB1C,NONP,HTB,NCTYP,NB1TY
47 /STRSTF/ I39,NB39,VP,INA,VP,NEL,NAT,RP,ULL,NE,NCE,NLE,NB1C,NONP,HTB,NCTYP,NB1TY
48 /STRSTF/ I40,NB40,VP,INA,VP,NEL,NAT,RP,ULL,NE,NCE,NLE,NB1C,NONP,HTB,NCTYP,NB1TY
49 /STRSTF/ I41,NB41,VP,INA,VP,NEL,NAT,RP,ULL,NE,NCE,NLE,NB1C,NONP,HTB,NCTYP,NB1TY
50 /STRSTF/ I42,NB42,VP,INA,VP,NEL,NAT,RP,ULL,NE,NCE,NLE,NB1C,NONP,HTB,NCTYP,NB1TY
51 /STRSTF/ I43,NB43,VP,INA,VP,NEL,NAT,RP,ULL,NE,NCE,NLE,NB1C,NONP,HTB,NCTYP,NB1TY
52 /STRSTF/ I44,NB44,VP,INA,VP,NEL,NAT,RP,ULL,NE,NCE,NLE,NB1C,NONP,HTB,NCTYP,NB1TY

```

```

83 C .....
84 B ..... FORM ELEMENT STIFFNESS MATRIX B(10,10) .....
85 C .....
86 140 MTYPE = IL(N;5) .....
87 IF (MTYPE .LE. NUMSOL) GO TO 150 .....
88 .....
89 CALL JSTIFFM .....
90 DO LOOP INDEX N MAY NOT BE REDEFINED IN CALL OR ABNORMAL FUNCTION .....
91 .....
92 .....
93 .....
94 .....
95 .....
96 .....
97 .....
98 .....
99 .....
100 .....
101 .....
102 .....

```

```

103 J = JBC(L)
104 MR = PR(L)/Z.
105 DV = (V(I) - YC(J))HR
106 DX = (X(I) - X(I))SR
107 LI = 2*1-KSMIFY
108 JJ = ZKSMIFY
109 IF(LI.LE,0) GO TO 150
110 IF(LI.GT,0) GO TO 150
111 B(I) = B(I) + DV
112 B(I) = B(I) + DX
113 450 IF(JJ.LE,0) GO TO 500
114 IF(JJ.GT,0) GO TO 500
115 B(JJ) = B(JJ) + DX
116 B(JJ) = B(JJ) + DX
117 500 CONTINUE
118 C * * * * * MODIFY EQUATIONS FOR BOUNDARY CONDITIONS * * * * *
119 C * * * * *
120 C * * * * *
121 295 IN = NOV * NDX + 1
122 IF(NOV.LE,0) GO TO 295
123 IF(NOV.GT,0) GO TO 295
124 IM2 = IM * NNPY
125 DO 310 MH = 1,IM2
126 H = 16*(MH)
127 IF(MH.GT,NOV) GO TO 200
128 IF(MH.LE,0) GO TO 200
129 U = FV(MH)
130 IF(MH.GT,IM) U = 0.0
131 N = 2*M * KSMIFY
132 GO TO 200
133 U = FV(MH)
134 KK = 1
135 N = 2*M * 1 - KSMIFY
136 IF(MH.LE,NOV) GO TO 310
137 IF(MH.GT,NOV) GO TO 200
138 DO 300 MH = 1,NOV
139 K = M * MH + 1
140 IF(K.LE,0) GO TO 295
141 B(K) = B(K) + A(N,NN)U
142 A(N,NN) = 0.0
143
144 295 K = M * MH + 1
145 IF(MH.LE,NOV) GO TO 300
146 B(K) = B(K) + A(N,NN)U
147 A(N,NN) = 0.0
148
149 300 CONTINUE
150 B(K) = U
151 IF(MH.GT,NOV) GO TO 200
152 CONTINUE
153 C * * * * * WRITE 60X60 BLOCK OF EQUATIONS ON TAPE AND SHIFT UP LOWER BLOCK * * * * *
154

```

```

155 C * * * * *
156 WRITE(S) (B(N),A(N),M) * 1,MBAND),M & S,ND)
157 C * * * * *
158 C * * * * * INITIALIZE FOR NEXT BLOCK OF EQUATIONS *
159 C * * * * *
160 DO 320 M = 1,ND
161 K = N * ND
162 B(K) = 0.0
163
164 DO 320 M = 1,ND
165 A(N,M) = A(N,M)
166
167 C * * * * *
168 C * * * * * CHECK FOR LAST BLOCK *
169 C * * * * *
170 IF (NH .LT. NUMSP) GO TO 105
171 340 CONTINUE
172
173 IF (ISVOP .EQ. 1.7) CALL EXIT
174
175 RETURN
176 2000 FORMAT(1H3, /NEGATIVE AREA ELEMENT # 1,15)
177 3000 FORMAT(1,15)
178 3010 FORMAT(15,F15.5)
179 3020 FORMAT(10E11.4)
180
181 *****
182 EQUALITY OR NON-EQUALITY COMPARISON MAY NOT BE MEANINGFUL IN LOGICAL IF EXPRESSIONS

```

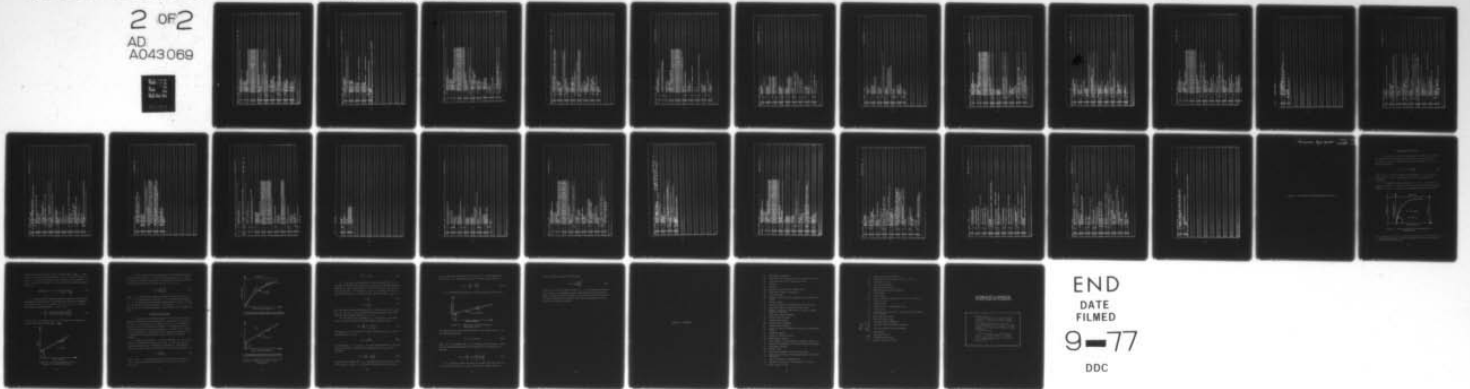
AD-A043 069

ARMY ENGINEER WATERWAYS EXPERIMENT STATION VICKSBURG MISS F/G 8/13
FINITE ELEMENT ANALYSIS OF A REINFORCED EARTH WALL.(U)
JUL 77 M M AL-HUSSAINI, L D JOHNSON
WES-TR-S-77-6

NL

UNCLASSIFIED

2 OF 2
AD
A043 069



END
DATE
FILMED
9-77
DDC


```

53 160 S(IIN,MM) = CKN=80(11,JJ)
54 IF(DY .GE. 0) RETURN
55 C . . . . .
56 C . . . . . ROTATE STIFFNESS TO GLOBAL COORDINATE (AT)*(K)*(A) #
57 C . . . . .
58 COSIN(1,1) = DX/DL
59 COSIN(1,2) = DY/DL
60 COSIN(2,2) = -DY/DL
61 COSIN(2,1) = DX/DL
62 DO 190 NN = 1,4
63 DO 170 II = 1,8
64 JJ = 2*NN - 1
65 TEMP = S(11,JJ)
66 DO 170 KK = 1,2
67 S(11,JJ) = TEMP * COSIN(1,KK) + COSIN(2,KK)
68 JJ = JJ + 1
69 DO 160 II = 1,8
70 JJ = 2*NN
71 TEMP = S(JJ,11)
72 DO 180 KK = 1,2
73 STIFF(11) = COSIN(1,KK)*TEMP + COSIN(2,KK)*S(2*NN,11)
74 JJ = JJ + 1
75 190 CONTINUE
76 2000 FORMATTED PRINTING FROM JOINT ELEMENTS = 1787
77 RETURN
78 END

```

***** 1470 EQUATION OR NON-EQUILITY COMPARISON HAS NOT BE MEANINGFUL IN CONTEXT OF EXPRESSIONS

```

1 SUBROUTINE QUADIN,121
2 TRUCTI DOUBLE PRECISION (A=H,0=Z)
3
4 PARAMETER M=691
5 PARAMETER MND=761
6 PARAMETER MNSIZU
7
8 PARAMETER M=600
9 PARAMETER NEE=2,NBE=100,M=20,NB=2
10 COMMON /HEI20/ILL,KURMP,NOREL,KURMAT,NURSOL,ITRU,LORD,INUMJT
11 1,NUMAPP,INIT,MTYPE,NOY,NOX,NOY,NCE,NLEL,NB1E,NONP,BTB,NOY,NB1Y
12 2P,NB2TP,NATYP,NBL,NTRIP,NLL,NF,NMPP,NUL,NH,NC,HQ,NO,NMP,NY,MBAND,
13 STMP,NUMBLK,IT,JJ,KK,VOL,UM,SL,AC,VC,REF,20,ATM,GRM,RES(20),COU,
14 420),PHJ(20),GOEJ(20),EXMJ(20),STFN(20),STF(20),SFF(20),SOM(20),AMP(20)
15 501(20),GUF(20),A01(20),ALPHA(20),PHI(20),BOME(20),MGEF(20),AMP(20)
16 6ULCOEF(20),PR(20),S(20),SR(20),SIGTREC,4)ITEE(NEKT,PROD(NEKT),BUTRE
17 7L),X(MND),Y(MND),DISP(MND),Z(MND),F(MND),F(MND),PP(MND),DP(MND),TC(30
18 80),IL(MEL),JLUL(NEE,8),LEL(NBE),NP(N4),188(M5),SJB(C(M5),PR(M5)),F(2
19 9)BY(2),B(2),B(2),X(MND),Y(MND),Z(MND),F(MND),F(MND),PP(MND),DP(MND),TC(30
20 DIMENSION Y(18)
21 REAL MED
22 C
23 C
24 C
25 C
26 C
27 C
28 C
29 C
30 C
31 C
32 C
33 C
34 C
35 C
36 C
37 C
38 C
39 C
40 C
41 C
42 C
43 C
44 C
45 C
46 C
47 C
48 C
49 C
50 C
51 C
52 C

```

```

53 IF(INIT .EQ. 0) GO TO 130
54 .....
55 PERFORM GRAVITY LOADING TO CALCULATE INITIAL VERTICAL STRESSES
56 .....
57 CK = VOL*GAM*(NTYPE)
58 DO 120 I = 1, IJ
59 PIZ(I) = CK/PI
60 CONTINUE
61 TEMP = 0.0
62 .....
63 C ..... REDUCE 10X10 QUAD STIFFNESS TO 8X8 BY STATIC CONDENSATION
64 .....
65 IF(G(1,1) > 140.140)
66 CONTINUE
67 DO 130 K = 1, 2
68 I=I0+K
69 I=I+1
70 DO 130 I = 1, IJ
71 S(I,I) = S(I,I)/9.1875
72 DO 130 J = 1, IJ
73 S(I,J) = S(I,J)
74 .....
75 IF(INIT .EQ. 1) GO TO 300
76 IF(NT .EQ. 0 .OR. NTYPE .NE. NCTYP) GO TO 300
77 ..... APPLY TEMPERATURE LOADING TO STRUCTURE MATERIAL IN NT :EQ. 1
78 .....
79 DYAVG0:
80 DO 162 I=1, IOT
81 J=I+1
82 DYAVG(I,J)=DYAVG
83 CONTINUE
84 DYAVG=DYAVG/FI
85 TEMP = DYAVG*(PKX+TYPE)
86 IF (IZ) 170, 170, 300
87 DO 200 I = 1, I4
88 IT = INT(TEMP)
89 YI(2,I) = Y(I,I)*SEMP
90 YI(2,I) = Y(I,I) * TEMP
91 DO 250 I = 1, I8
92 DO 250 K = 1, 8
93 P(I) = P(I) * S(I,K)*TT(K)
94 CONTINUE
95 RETURN
96 END

```

```

1 SUBROUTINE ISOPAR(N)
2 IMPLICIT DOUBLE PRECISION (A-H,O-Z)
3 C
4 C
5 C
6 C THIS SUBROUTINE COMPUTES THE STIFFNESS MATRIX
7 ACCORDING TO THE FIVE-POINT ISOPARAMETRIC ELEMENT.
8 C
9 C
10 C
11 C
12 C
13 C
14 C
15 C
16 C
17 C
18 C
19 C
20 C
21 C
22 C
23 C
24 C
25 C
26 C
27 C
28 C
29 C
30 C
31 C
32 C
33 C
34 C
35 C
36 C
37 C
38 C
39 C
40 C
41 C
42 C
43 C
44 C
45 C
46 C
47 C
48 C
49 C
50 C
51 C
52 C

```

PARAMETER MND=500
PARAMETER MND=761
PARAMETER MSH=120
PARAMETER MSH=800
PARAMETER NBE=100, NBE=100, NBE=20, NBE=2
COMMON / / ILL, NURMP, NURMEL, NUMMAT, NUMSOL, ITRD, LORUL, NUMJUT
1, NURMPP, INIT, MTYPE, NUT, NOK, NICE, NLE, NBE, NOMP, TDB, NCTYP, NODTY
2, NBE2TYP, NATYP, NEL, NTRIP, ALL, NF, NAPP, NUL, NMB, NC, NG, NHP, INT, MBAND,
3, TEMP, NUMBLK, I1, JJ, KK, VOL, LUM, SL, XC, YC, RDF, RD, PATH, GAHM, RKS(20), COJ
4, I, J, K, L, M, N, O, P, Q, R, S, T, U, V, W, X, Y, Z, AA, AB, AC, AD, AE, AF, AG, AH, AI, AJ, AK, AL, AM, AN, AO, AP, AQ, AR, AS, AT, AU, AV, AW, AX, AY, AZ, BA, BB, BC, BD, BE, BF, BG, BH, BI, BJ, BK, BL, BM, BN, BO, BP, BQ, BR, BS, BT, BU, BV, BW, BX, BY, BZ, CA, CB, CC, CD, CE, CF, CG, CH, CI, CJ, CK, CL, CM, CN, CO, CP, CQ, CR, CS, CT, CU, CV, CW, CX, CY, CZ, DA, DB, DC, DD, DE, DF, DG, DH, DI, DJ, DK, DL, DM, DN, DO, DP, DQ, DR, DS, DT, DU, DV, DW, DX, DY, DZ, EA, EB, EC, ED, EE, EF, EG, EH, EI, EJ, EK, EL, EM, EN, EO, EP, EQ, ER, ES, ET, EU, EV, EW, EX, EY, EZ, FA, FB, FC, FD, FE, FF, FG, FH, FI, FJ, FK, FL, FM, FN, FO, FP, FQ, FR, FS, FT, FU, FV, FW, FX, FY, FZ, GA, GB, GC, GD, GE, GF, GG, GH, GI, GJ, GK, GL, GM, GN, GO, GP, GQ, GR, GS, GT, GU, GV, GW, GX, GY, GZ, HA, HB, HC, HD, HE, HF, HG, HH, HI, HJ, HK, HL, HM, HN, HO, HP, HQ, HR, HS, HT, HU, HV, HW, HX, HY, HZ, IA, IB, IC, ID, IE, IF, IG, IH, II, IJ, IK, IL, IM, IN, IO, IP, IQ, IR, IS, IT, IU, IV, IW, IX, IY, IZ, JA, JB, JC, JD, JE, JF, JG, JH, JI, JJ, JK, JL, JM, JN, JO, JP, JQ, JR, JS, JT, JU, JV, JW, JX, JY, JZ, KA, KB, KC, KD, KE, KF, KG, KH, KI, KJ, KK, KL, KM, KN, KO, KP, KQ, KR, KS, KT, KU, KV, KW, KX, KY, KZ, LA, LB, LC, LD, LE, LF, LG, LH, LI, LJ, LK, LL, LM, LN, LO, LP, LQ, LR, LS, LT, LU, LV, LW, LX, LY, LZ, MA, MB, MC, MD, ME, MF, MG, MH, MI, MJ, MK, ML, MM, MN, MO, MP, MQ, MR, MS, MT, MU, MV, MW, MX, MY, MZ, NA, NB, NC, ND, NE, NF, NG, NH, NI, NJ, NK, NL, NM, NN, NO, NP, NQ, NR, NS, NT, NU, NV, NW, NX, NY, NZ, OA, OB, OC, OD, OE, OF, OG, OH, OI, OJ, OK, OL, OM, ON, OO, OP, OQ, OR, OS, OT, OU, OV, OW, OX, OY, OZ, PA, PB, PC, PD, PE, PF, PG, PH, PI, PJ, PK, PL, PM, PN, PO, PP, PQ, PR, PS, PT, PU, PV, PW, PX, PY, PZ, QA, QB, QC, QD, QE, QF, QG, QH, QI, QJ, QK, QL, QM, QN, QO, QP, QQ, QR, QS, QT, QU, QV, QW, QX, QY, QZ, RA, RB, RC, RD, RE, RF, RG, RH, RI, RJ, RK, RL, RM, RN, RO, RP, RQ, RR, RS, RT, RU, RV, RW, RX, RY, RZ, SA, SB, SC, SD, SE, SF, SG, SH, SI, SJ, SK, SL, SM, SN, SO, SP, SQ, SR, SS, ST, SU, SV, SW, SX, SY, SZ, TA, TB, TC, TD, TE, TF, TG, TH, TI, TJ, TK, TL, TM, TN, TO, TP, TQ, TR, TS, TT, TU, TV, TW, TX, TY, TZ, UA, UB, UC, UD, UE, UF, UG, UH, UI, UJ, UK, UL, UM, UN, UO, UP, UQ, UR, US, UT, UV, UW, UX, UY, UZ, VA, VB, VC, VD, VE, VF, VG, VH, VI, VJ, VK, VL, VM, VN, VO, VP, VQ, VR, VS, VT, VU, VV, VW, VX, VY, VZ, WA, WB, WC, WD, WE, WF, WG, WH, WI, WJ, WK, WL, WM, WN, WO, WP, WQ, WR, WS, WT, WU, WV, WW, WX, WY, WZ, XA, XB, XC, XD, XE, XF, XG, XH, XI, XJ, XK, XL, XM, XN, XO, XP, XQ, XR, XS, XT, XU, XV, XW, XX, XY, XZ, YA, YB, YC, YD, YE, YF, YG, YH, YI, YJ, YK, YL, YM, YN, YO, YP, YQ, YR, YS, YT, YU, YV, YW, YX, YY, YZ, ZA, ZB, ZC, ZD, ZE, ZF, ZG, ZH, ZI, ZJ, ZK, ZL, ZM, ZN, ZO, ZP, ZQ, ZR, ZS, ZT, ZU, ZV, ZW, ZX, ZY, ZZ

REAL MED
DEFINE CONSTANTS OF INTEGRATION
WF(1)=1.
WF(2)=1.
PI(1)=3.1415927
PI(2)=PI(1)
ESTABLISH THE THICKNESS OF THE MATERIAL.
TH=1.
VOL = 0.
INITIALIZE THE STIFFNESS MATRIX AND THE FORCE VECTOR.
DO 100 I=1,10
PI(I)=0.
DO 100 J=1,1
S(I,J)=0.
CONTINUE
PERFORM THE NUMERICAL INTEGRATION.
DO 1000 NT=1,2
TTYP(NT)

ROSB8 A1 11-18-76 17.348

```

83 DO 1000 NS=1,2
84 SSS=PY(NS)
85
86 C COMPUTE THE P PRIME MATRIX,
87 C
88 DO 200 I=1,4
89 SI=1e1e1e9e8
90 YI=1e1e1e9e8
91 PP(1,1)=YI*YI*SI,1e5*PP(1,2)
92 PP(2,1)=SSS*SI,1e1e1e0,1e25
93 CONTINUE
94 PP(1,2)=YI*YI*YI*YI*SI,1e5*SI*2
95 PP(2,2)=SSS*SI*2,1e1e1e2
96 C COMPUTE THE JACOBIAN MATRIX,
97 C
98 DO 300 I=1,2
99 DO 300 J=1,2
100 PJ(I,J)=0
101 CONTINUE
102 C
103 DO 400 I=1,4
104 ND=IL(N,I)
105 XXXX(ND)
106 YVY(ND)
107 YJ(I,1)=PP(2,1)+YVY*PJ(I,1)
108 YJ(I,2)=PP(2,2)+YVY*PJ(I,2)
109 FJ(2,1)=PP(2,1)+XXX*FJ(2,1)
110 FJ(2,2)=PP(2,2)+XXX*FJ(2,2)
111 CONTINUE
112 C
113 C COMPUTE THE VOLUME OF THE ELEMENT,
114 C
115 DET=FF(1,1)*FJ(2,2)-FJ(1,2)*F(2,1)
116 VOL=NF(NS)*NF(NT)*DET*H*VOL
117
118 C IF(DEY) 800, 5000, 800
119 C
120 C COMPUTE THE P MATRIX,
121 C
122 DO 600 J=1,5
123 I=PP(I,J)
124 T2=PP(2,I)
125 PP(1,J)=0
126 PP(2,J)=0
127 DO 600 I=1,2
128 PP(I,J)=FJ(I,1)*YI*FJ(I,2)*T2*PP(I,1)
129 CONTINUE
130 C
131 C COMPUTE THE STIFFNESS MATRIX,
132 C
133 T3=NF(NS)*NF(NT)/DET

```


1	SUBROUTINE BANSO	
2	IMPLICIT DOUBLE PRECISION (A-H,O-Z)	
3	PARAMETER M=500	
4	PARAMETER MND=761	
5	PARAMETER MBK=120	
6	PARAMETER MBS=120	
7	PARAMETER MBS2	
8	PARAMETER MBS2	
9	COMMON MBS(20),LL,NUMP,NUMEL,NUMMAT,NUMSOL,IBRD,LORH,NUMJT	
10	ZONKPP,INTTHTY,PE,NOTING,NOATY,NC,LE,EN,SE,NOR,IB,IBNC,IB,IBNT,IBNTY	
11	ZP,NB2,YP,NATYP,NEL,MRIP,NLL,NFN,NRPF,NULS,MB,MC,MD,MB,NMF,MT,MBAND,	
12	STEP,NUMBLK,II,JJ,KK,VOL,UN,SL,AC,YC,RDF,RD,PATM,GABH,RRS(20),COJ,	
13	ZU,TPR(20),BOE(20),EX(20),STY(20),SYF(20),SYB(20),VARI(20),E(20),	
14	PHI(20),Q(20),R(20),ALPHA(20),PHI(20),GOME(20),MCDEP(20),AMP(20)	
15	PHIDEEP(20),PHI(20),R(20),R(4),R(9),R(16),R(23),R(30),R(37),R(44),	
16	LY,XTMND,Z,YTMND,DISTMND,Z,XTMND,Z,XTMND,Z,TMND,PTMND,DFTRD,DTCT(30)	
17	R(4),LL(MEL,5),L(NEE,8),LEL,(NBE,8),LEL,(NBE),NP(N4),IBB(45),JBC(N5),PR(N5),F(2	
18	9,4),XY(2,4),B(MB4),A(MB),MH),S(10,10),P(20),G(4,4),LK(8),BA(5,2),A	
19	ZOO(20),ZOO(20),ZOO(20),ZOO(20)	
20	REAL MBD	
21	MM=1	
22	NN=MM	
23	NL=NN*1	
24	MM=MM*MM	
25	MM=MM*MM	
26	MM=MM*MM	
27	MM=MM*MM	
28	GO TO 158	
29	C	
30	C REDUCE EQUATIONS BY BLOCKS	
31	C	
32	C	
33	C 1. SMIT BLOCK OF EQUATIONS	
34	C	
35	C 100 NB=NB*1	
36	DO 129 M=1,MM	
37	MM=MM*MM	
38	B(M)=B(M)	
39	B(M)=B(M)	
40	DO 125 K=1,MM	
41	A(N,M)=A(N,M)	
42	129 CONTINUE	
43	C	
44	C 2. READ NEXT BLOCK OF EQUATIONS INTO CBRE	
45	C	
46	IF (NUMBLK=NB) GO TO 150	
47	150 READ (5) (B(N),N=1,MM),NENL,MM	
48	151 IF (MM) GO TO 160	
49	C	
50	C 3. REDUCE BLOCK OF EQUATIONS	
51	C	
52	200 DO 300 N=1,MM	

RD988 01 11-18-76 47,358

```

93 IF (A(N,1)) 225,300,225
94 B(N)=B(N)/A(N,2)
95 DO 275 L62,MM
96 IF (A(N,L)) 230,275,230
97 230 D=A(N,L)/A(N,1)
98 L=LN(L)
99 J=J+1
100 DO 250 K61,MM
101 J=J+1
102 250 A(I,J)=A(I,J)-D*A(N,L)
103 R(I)=B(I)-A(N,L)*B(N)
104 A(N,L)=D
105 275 CONTINUE
106 300 CONTINUE
107 C
108 C 4. WRITE BLOCK OF REDUCED EQUATIONS ON TAPE 2
109 C
110 C
111 275 WRITE (4) (B(N),A(N,1),M2,MM),M2,MM)
112 280
113 GO TO 100
114 C BACK-SUBSTITUTION
115 C
116 300 DO 455 M61,MM
117 M=MM+1
118 DO 455 K62,MM
119 L=K+1
120 425 B(N)=B(N)-A(N,K)*B(L)
121 M=M+1
122 C
123 C
124 C
125 C
126 455 A(N,M)=B(N)
127 M=MM+1
128 IF (M) 475,300,475
129 475 BACKSPACE 4
130 READ (4) (B(N),A(N,1),M2,MM),M2,MM)
131 480 BACKSPACE 4
132 C
133 C
134 C
135 C
136 500 K=0
137 DO 600 M62,MM
138 DO 600 M63,MM
139 M=M+1
140 K=K+1
141 600 B(K)=A(N,M)
142 C
143 C
144 600 FORMATTED
145 3000
146 END

```

RC2988 01 11-18-76 17,355

```

1 SUBROUTINE STRESS
2 IMPLICIT DOUBLE PRECISION (A-H,O-Z)
3 PARAMETER MEL=594
4 PARAMETER MND=761
5 PARAMETER MBH=120
6 PARAMETER MN=60
7 PARAMETER NEE=2
8 PARAMETER NBE=100, N4=20, N9=2
9 COMMON
10 I, NUMAPP, I, MIT, MTYPE, N, NTRIP, NUL, NFN, NKP, NUL, NCH, NCM, NMO, NMP, NPT, NRP, NRD,
11 NTRIP, NUL, NFN, NKP, NUL, NCH, NCM, NMO, NMP, NPT, NRP, NRD,
12 NTRIP, NUL, NFN, NKP, NUL, NCH, NCM, NMO, NMP, NPT, NRP, NRD,
13 NTRIP, NUL, NFN, NKP, NUL, NCH, NCM, NMO, NMP, NPT, NRP, NRD,
14 NTRIP, NUL, NFN, NKP, NUL, NCH, NCM, NMO, NMP, NPT, NRP, NRD,
15 NTRIP, NUL, NFN, NKP, NUL, NCH, NCM, NMO, NMP, NPT, NRP, NRD,
16 NTRIP, NUL, NFN, NKP, NUL, NCH, NCM, NMO, NMP, NPT, NRP, NRD,
17 NTRIP, NUL, NFN, NKP, NUL, NCH, NCM, NMO, NMP, NPT, NRP, NRD,
18 NTRIP, NUL, NFN, NKP, NUL, NCH, NCM, NMO, NMP, NPT, NRP, NRD,
19 COMMON/PUNCH/PUMCK
20 REAL MED
21 C
22 C
23 C
24 C
25 C
26 C
27 C
28 DO 300 N = 1, NDMEL
29 ICHECK=0
30 I=0
31 I1(N,5) = IABS(I1(N,5))
32 I1(N,5) = I1(N,5)
33 IF (MND) GO TO 300
34 DO 173 I = 1, 4
35 O(I) = SIGN(I)
36 LL = 0
37 IF (MEL) GO TO 170
38 C
39 C
40 C
41 C
42 C
43 C
44 C
45 C
46 C
47 C
48 C
49 C
50 C
51 C
52 C
53 C
54 C
55 C
56 C
57 C
58 C
59 C
60 C
61 C
62 C
63 C
64 C
65 C
66 C
67 C
68 C
69 C
70 C
71 C
72 C
73 C
74 C
75 C
76 C
77 C
78 C
79 C
80 C
81 C
82 C
83 C
84 C
85 C
86 C
87 C
88 C
89 C
90 C
91 C
92 C
93 C
94 C
95 C
96 C
97 C
98 C
99 C
100 C
101 C
102 C
103 C
104 C
105 C
106 C
107 C
108 C
109 C
110 C
111 C
112 C
113 C
114 C
115 C
116 C
117 C
118 C
119 C
120 C
121 C
122 C
123 C
124 C
125 C
126 C
127 C
128 C
129 C
130 C
131 C
132 C
133 C
134 C
135 C
136 C
137 C
138 C
139 C
140 C
141 C
142 C
143 C
144 C
145 C
146 C
147 C
148 C
149 C
150 C
151 C
152 C
153 C
154 C
155 C
156 C
157 C
158 C
159 C
160 C
161 C
162 C
163 C
164 C
165 C
166 C
167 C
168 C
169 C
170 C
171 C
172 C
173 C
174 C
175 C
176 C
177 C
178 C
179 C
180 C
181 C
182 C
183 C
184 C
185 C
186 C
187 C
188 C
189 C
190 C
191 C
192 C
193 C
194 C
195 C
196 C
197 C
198 C
199 C
200 C
201 C
202 C
203 C
204 C
205 C
206 C
207 C
208 C
209 C
210 C
211 C
212 C
213 C
214 C
215 C
216 C
217 C
218 C
219 C
220 C
221 C
222 C
223 C
224 C
225 C
226 C
227 C
228 C
229 C
230 C
231 C
232 C
233 C
234 C
235 C
236 C
237 C
238 C
239 C
240 C
241 C
242 C
243 C
244 C
245 C
246 C
247 C
248 C
249 C
250 C
251 C
252 C
253 C
254 C
255 C
256 C
257 C
258 C
259 C
260 C
261 C
262 C
263 C
264 C
265 C
266 C
267 C
268 C
269 C
270 C
271 C
272 C
273 C
274 C
275 C
276 C
277 C
278 C
279 C
280 C
281 C
282 C
283 C
284 C
285 C
286 C
287 C
288 C
289 C
290 C
291 C
292 C
293 C
294 C
295 C
296 C
297 C
298 C
299 C
300 C
301 C
302 C
303 C
304 C
305 C
306 C
307 C
308 C
309 C
310 C
311 C
312 C
313 C
314 C
315 C
316 C
317 C
318 C
319 C
320 C
321 C
322 C
323 C
324 C
325 C
326 C
327 C
328 C
329 C
330 C
331 C
332 C
333 C
334 C
335 C
336 C
337 C
338 C
339 C
340 C
341 C
342 C
343 C
344 C
345 C
346 C
347 C
348 C
349 C
350 C
351 C
352 C
353 C
354 C
355 C
356 C
357 C
358 C
359 C
360 C
361 C
362 C
363 C
364 C
365 C
366 C
367 C
368 C
369 C
370 C
371 C
372 C
373 C
374 C
375 C
376 C
377 C
378 C
379 C
380 C
381 C
382 C
383 C
384 C
385 C
386 C
387 C
388 C
389 C
390 C
391 C
392 C
393 C
394 C
395 C
396 C
397 C
398 C
399 C
400 C
401 C
402 C
403 C
404 C
405 C
406 C
407 C
408 C
409 C
410 C
411 C
412 C
413 C
414 C
415 C
416 C
417 C
418 C
419 C
420 C
421 C
422 C
423 C
424 C
425 C
426 C
427 C
428 C
429 C
430 C
431 C
432 C
433 C
434 C
435 C
436 C
437 C
438 C
439 C
440 C
441 C
442 C
443 C
444 C
445 C
446 C
447 C
448 C
449 C
450 C
451 C
452 C
453 C
454 C
455 C
456 C
457 C
458 C
459 C
460 C
461 C
462 C
463 C
464 C
465 C
466 C
467 C
468 C
469 C
470 C
471 C
472 C
473 C
474 C
475 C
476 C
477 C
478 C
479 C
480 C
481 C
482 C
483 C
484 C
485 C
486 C
487 C
488 C
489 C
490 C
491 C
492 C
493 C
494 C
495 C
496 C
497 C
498 C
499 C
500 C
501 C
502 C
503 C
504 C
505 C
506 C
507 C
508 C
509 C
510 C
511 C
512 C
513 C
514 C
515 C
516 C
517 C
518 C
519 C
520 C
521 C
522 C
523 C
524 C
525 C
526 C
527 C
528 C
529 C
530 C
531 C
532 C
533 C
534 C
535 C
536 C
537 C
538 C
539 C
540 C
541 C
542 C
543 C
544 C
545 C
546 C
547 C
548 C
549 C
550 C
551 C
552 C
553 C
554 C
555 C
556 C
557 C
558 C
559 C
560 C
561 C
562 C
563 C
564 C
565 C
566 C
567 C
568 C
569 C
570 C
571 C
572 C
573 C
574 C
575 C
576 C
577 C
578 C
579 C
580 C
581 C
582 C
583 C
584 C
585 C
586 C
587 C
588 C
589 C
590 C
591 C
592 C
593 C
594 C
595 C
596 C
597 C
598 C
599 C
600 C
601 C
602 C
603 C
604 C
605 C
606 C
607 C
608 C
609 C
610 C
611 C
612 C
613 C
614 C
615 C
616 C
617 C
618 C
619 C
620 C
621 C
622 C
623 C
624 C
625 C
626 C
627 C
628 C
629 C
630 C
631 C
632 C
633 C
634 C
635 C
636 C
637 C
638 C
639 C
640 C
641 C
642 C
643 C
644 C
645 C
646 C
647 C
648 C
649 C
650 C
651 C
652 C
653 C
654 C
655 C
656 C
657 C
658 C
659 C
660 C
661 C
662 C
663 C
664 C
665 C
666 C
667 C
668 C
669 C
670 C
671 C
672 C
673 C
674 C
675 C
676 C
677 C
678 C
679 C
680 C
681 C
682 C
683 C
684 C
685 C
686 C
687 C
688 C
689 C
690 C
691 C
692 C
693 C
694 C
695 C
696 C
697 C
698 C
699 C
700 C
701 C
702 C
703 C
704 C
705 C
706 C
707 C
708 C
709 C
710 C
711 C
712 C
713 C
714 C
715 C
716 C
717 C
718 C
719 C
720 C
721 C
722 C
723 C
724 C
725 C
726 C
727 C
728 C
729 C
730 C
731 C
732 C
733 C
734 C
735 C
736 C
737 C
738 C
739 C
740 C
741 C
742 C
743 C
744 C
745 C
746 C
747 C
748 C
749 C
750 C
751 C
752 C
753 C
754 C
755 C
756 C
757 C
758 C
759 C
760 C
761 C
762 C
763 C
764 C
765 C
766 C
767 C
768 C
769 C
770 C
771 C
772 C
773 C
774 C
775 C
776 C
777 C
778 C
779 C
780 C
781 C
782 C
783 C
784 C
785 C
786 C
787 C
788 C
789 C
790 C
791 C
792 C
793 C
794 C
795 C
796 C
797 C
798 C
799 C
800 C
801 C
802 C
803 C
804 C
805 C
806 C
807 C
808 C
809 C
810 C
811 C
812 C
813 C
814 C
815 C
816 C
817 C
818 C
819 C
820 C
821 C
822 C
823 C
824 C
825 C
826 C
827 C
828 C
829 C
830 C
831 C
832 C
833 C
834 C
835 C
836 C
837 C
838 C
839 C
840 C
841 C
842 C
843 C
844 C
845 C
846 C
847 C
848 C
849 C
850 C
851 C
852 C
853 C
854 C
855 C
856 C
857 C
858 C
859 C
860 C
861 C
862 C
863 C
864 C
865 C
866 C
867 C
868 C
869 C
870 C
871 C
872 C
873 C
874 C
875 C
876 C
877 C
878 C
879 C
880 C
881 C
882 C
883 C
884 C
885 C
886 C
887 C
888 C
889 C
890 C
891 C
892 C
893 C
894 C
895 C
896 C
897 C
898 C
899 C
900 C
901 C
902 C
903 C
904 C
905 C
906 C
907 C
908 C
909 C
910 C
911 C
912 C
913 C
914 C
915 C
916 C
917 C
918 C
919 C
920 C
921 C
922 C
923 C
924 C
925 C
926 C
927 C
928 C
929 C
930 C
931 C
932 C
933 C
934 C
935 C
936 C
937 C
938 C
939 C
940 C
941 C
942 C
943 C
944 C
945 C
946 C
947 C
948 C
949 C
950 C
951 C
952 C
953 C
954 C
955 C
956 C
957 C
958 C
959 C
960 C
961 C
962 C
963 C
964 C
965 C
966 C
967 C
968 C
969 C
970 C
971 C
972 C
973 C
974 C
975 C
976 C
977 C
978 C
979 C
980 C
981 C
982 C
983 C
984 C
985 C
986 C
987 C
988 C
989 C
990 C
991 C
992 C
993 C
994 C
995 C
996 C
997 C
998 C
999 C
1000 C

```

43. PSTR(2) & SIG(4,5)

44 PSTR(5) & SIG(4,1)
45 PRIN = PHINRIGSUTYB
46 CR = (2.0*COE(HM)*COS(PHIR))/L1 - SIN(PUIB)
47 RBF = IPSTR(2) * (L1 * SIN(PHIR))/E. - SIN(PHIR) - S1) * CK
48 PSTR(4) & (ABS(SIGN,2) - SIGN,1)/RBF
49 163 CONTINUE
50 GO TO 185
51 185 CONTINUE
52 170 IF(MM .NE. NATP) GO TO 174

R0588.01 11-18-76 17.358

```

53 GO TO 240
54 CONTINUE
55 IF(INIT.EQ.1.OR.NO.EQ.NUMAPP) GO TO 185
56 LL = 1
57 GO TO 240
58 175 PSTRI(4) = Z-ARD/NDP
59 PSTRI(5) = PSTRI(2)
60 185 CALL QUAD (N1)
***** 1457 DO LOOP INDEX N MAY NOT BE REDEFINED IN CALL OR ABNORMAL FUNCTION
61 C .....
62 C ..... SET UP ELEMENT DISPLACEMENT VECTOR
63 C .....
64 DO 195 I = 1,4
65 I1 = 2*I
66 JJ = 2*I1(N1)
67 P(I1-1) = B(JJ-1)
68 P(I1) = B(JJ)
69 C .....
70 C ..... SOLVE FOR STRESSES
71 C .....
72 IF(SOIL.EQ.1)CALL ISOSTATM
*****M 1457 DO LOOP INDEX N MAY NOT BE REDEFINED IN CALL OR ABNORMAL FUNCTION
73 IF(CHECK.EQ.1)Q(1)=QU(N)Q(2)/(1.0-GUEN)
74 LL = 0
75 CONTINUE
76 IF(INIT.EQ.1) GO TO 270
77 C .....
78 C ..... CALCULATE NEW MODULUS AND POISSON RATIO VALUES
79 C .....
80 C .....
81 CALL MODCAL(N)
*****M 1457 DO LOOP INDEX N MAY NOT BE REDEFINED IN CALL OR ABNORMAL FUNCTION
82 IF(ALL.EQ.1) GO TO 175
83 IF(INIT.EQ.1) GO TO 300
84 IF(ITERD.EQ.0)END,NO,INE,NUMAPP) GO TO 300
85 PRINT*PRINTX
86 IF(ITERD.EQ.1) GO TO 275
87 PRINT*
88 WRITE(3,202)M,N,Q
89 CONTINUE
90 WRITE(3,203) N,XC,YC,( Q(1),1=1,3), (PSTR(1),1=1,3),EE(N),GU(N)
91 185CUN
92 IF(NO,NE,NUMAPP) GO TO 300
93 IF(PUNCH.LT.2) GO TO 270
94 PUNCH=307+ACT*CT*PSTR(1)+PSTR(2)+PSTR(5)
95 DO 280 I = 1,4
96 SIG(N,I) = Q(I)
97 CONTINUE
98 IF(CUN) GO TO 340
99 IF(INIT.EQ.1) GO TO 310
100 IF(ITERD.EQ.0)END,NO,INE,NUMAPP) GO TO 300
101 WRITE(3,204)

```

```

102 DO 320 N = 1,NUMBL
103 IF (L(N),GT,NUMSOL) CALL JSTRES(N)
104 ***** 1457 DO LOOP INDEX N MAY NOT BE REDEFINED IN CALL OR ABNORMAL FUNCTION
105 CONTINUE
106 IF (INCL.EQ,0) GO TO 335
107 DO 350 N = 1,NUMEL
108 .MH = LEL(N)
109 .MC = LELMH(5)
110 SIG(MH,4) = 0.0
111 IF (MG.GT,NUMSOL) GO TO 345
112 IF (MG.NE,CTV) BETA(M) = BETA(M)*.001
113 GO TO 350
114 345 IF (ABS(SYFS(MH))-10000000.) .LT, 1.) GO TO 350
115 STRESS(M) = 10.
116 CONTINUE
117 C . . . . .
118 C . . . . . CALCULATE THE DISPLACEMENTS . . . . .
119 C . . . . .
120 355 CONTINUE
121 PRINT* = 1.0R, NO. LEL, NUMAPP, GO TO 360
122 WRITE(3,2000) %
123 J = 1
124 IF (PUNCH(M,2) .EQ. 700)
125 PUNCH 3050, MED, NUMAPP
126 CONTINUE
127 PRINT* = 0.
128 DO 150 N = 1, NUMAPP
129 FX(N) = 0.
130 FZ(N) = 0.
131 IF (NP(J), NE, N) GO TO 130
132 J = J + 1
133 DISP(N,1) = 0.
134 DISP(N,2) = 0.
135 GO TO 150
136 IF (ABS(STRESS(M)) .LT, 100.) AND, ABS(2*NUSS1) .LT, 100.) GO TO 360
137 DISP(N,1) = 0.0
138 DISP(N,2) = 0.0
139 GO TO 150
140 DISP(N,1) = DISP(N,1) + B(2*N-1)
141 DISP(N,2) = DISP(N,2) + B(2*N)
142 IF (PUNCH(M,2) .EQ. 700)
143 PUNCH 3060, NX(N), Y(N), DISP(N,1), DISP(N,2)
144 701 CONTINUE
145 PRINT* = 1.0R,
146 IF (PRINT,LT,51) GO TO 702
147 PRINT* = 1.0R,
148 WRITE(3,2000) %
149 CONTINUE
150 702 CONTINUE
151 WRITE(3,2010) N, X(N), Y(N), (DISP(N,1)), B(2*N-1), B(2*N), P(N), N
152 CONTINUE
153 IF (NO, NE, NUMAPP, OR, INIT, EQ, 1.0R, MC, NE, NC) GO TO 360

```

```

153 WRITE(2,3010) ((SIG(N,M),M=1,4),N=1,NUMBER)
154 WRITE(2,3020) ((DISP(N,M),M=1,2),PP(N),NBITNUMNP)
155 WRITE(2,3030) ((LIN,3),N=1,NUMBER)
156 WRITE(2,3040) ((STF(N),STFN(N),N=1,NUMJT)
157      3010 FORMAT(6F10.2)
158      3020 FORMAT(9F8.3)
159      3030 FORMAT(19I5)
160      3040 FORMAT(6E12.5)
161      2000 FORMAT(11,30X,DISPLACEMENT RESULTS FOR LOADING CASE NO.,1,19777
162      1 2X,IN,1,4X,1X,16X,1,16X,1,TOTAL UKT,3X,TOTAL U,1,
163      13X,INCRM,0X,2X,INCRM,U,1,1X,POE PRESS,12X,N,P,1)
164      2010 FORMAT(13,2F8.3,13F8.3,19I5)
165      2020 FORMAT(11,20X,EFFECTIVE STRESSES,MODULUS VALUES AND PORE PRESSUR
166      4E11/32X,1FOR CASB,1E,2X,ITERATION,12X,1EL NO.,4X,1X,10X,1
167      2Y,4X,1X-STRESS,1X,1Y-STRESS,1X,1X-STRESS,1X,1MAX-STRESS,1X,1
168      3MIN-STRESS,12X,1ANGLE,1X,1MODULUS,1X,1POIS RATI,1X,1S LEV,1,
169      4 1X,1POR PRES,1)
170      2030 FORMAT(11,2E8.3,10F8.3,10F7.4,1E11,10F7.4,10F8.3,10F8.3)
171      2040 FORMAT(11,10X,1,INTERFACE ELEMENT RESULTS,1,19,1,EL NO,13X,1,1,4X,
172      1 1V,1,2X,INCRM STRESS,13X,1TAN STRESS,13X,1MOH DISP,13X,1TAN DISP,
173      2,3X,1TAN STIFF,13X,1NORM STIFF,13X,1PORE PRESS,77777)
174      3000 FORMAT(15)
175      3050 FORMAT(17A4,1A,12A1,21A)
176      3060 FORMAT(110F4E12.3)
177      3070 FORMAT(4E10.3,30E8.18E0.3)
178      360 CONTINUE
179      RETURN
180      END

```

1 C

2 SUBROUTINE ISOSTR (N)

3 IMPLICIT DOUBLE PRECISION (A-H,U-Z)

4

5 C

6 THIS SUBROUTINE COMPUTES THE STRESS AT THE FIFTH NODE

7 OF THE FIVE-NODE ISOPARAMETRIC ELEMENT.

8

9 C

10 SUBROUTINE ISOSTR (N)

11 IMPLICIT DOUBLE PRECISION (A-H,U-Z)

12

13 C

14 THIS SUBROUTINE COMPUTES THE STRESS AT THE FIFTH NODE

15 OF THE FIVE-NODE ISOPARAMETRIC ELEMENT.

16

17 C

18 PARAMETER M=2, NBE=100, N4=20, N5=2

19 PARAMETER MND=764

20 PARAMETER MBM=120

21 PARAMETER M=850

22 COMMON /HEX(20)/ LL, NUMNP, NUMEL, NUMMAT, NUMSOL, ITRD, LORUL, NUMJT

23 /NUMKPE, /INITM, /ELEMAT, /BOX, /MAY, /NCE, /ELEM, /NBS, /MOM, /M, /ACTYP, /MSTY

24 /MNSTYP, /NATYP, /NCL, /NTRIP, /NLL, /NFP, /NPE, /NLS, /NC, /NO, /NB, /NBS, /NT, /MBAND,

25 /STEMP, /NUMBLK, /I, /JJ, /KK, /VOL, /SUM, /SL, /XC, /YC, /RPF, /RQD, /ATH, /GAB, /RMS(20), /COU, /

26 /SOT, /MST(20), /COEF(20), /EX(20), /STRT(20), /PHI(20), /COME(20), /HCOEF(20), /AXB(20)

27 /ULCOEF(20), /FR(20), /SIG(4), /PSTR(5), /ZINEL, /4)TEE(HELM), /BMOD(HELM), /SU(HE

28 /Y, /X(MND), /Y(MND), /DIS(AMND), /Z(IX(MND)), /FX(MND), /FY(MND), /DP(AMND), /CT(30

29 /4), /X(2,4), /B(MBV), /L(AMND), /L(AMND), /N(4), /BCC(5), /JBC(5), /PRIN(5), /F(12

30 /3), /X(12,4), /B(MBV), /L(AMND), /L(AMND), /N(4), /BCC(5), /JBC(5), /PRIN(5), /F(12

31 /3), /X(12,4), /B(MBV), /L(AMND), /L(AMND), /N(4), /BCC(5), /JBC(5), /PRIN(5), /F(12

32 /3), /X(12,4), /B(MBV), /L(AMND), /L(AMND), /N(4), /BCC(5), /JBC(5), /PRIN(5), /F(12

33 /3), /X(12,4), /B(MBV), /L(AMND), /L(AMND), /N(4), /BCC(5), /JBC(5), /PRIN(5), /F(12

34 /3), /X(12,4), /B(MBV), /L(AMND), /L(AMND), /N(4), /BCC(5), /JBC(5), /PRIN(5), /F(12

35 /3), /X(12,4), /B(MBV), /L(AMND), /L(AMND), /N(4), /BCC(5), /JBC(5), /PRIN(5), /F(12

36 /3), /X(12,4), /B(MBV), /L(AMND), /L(AMND), /N(4), /BCC(5), /JBC(5), /PRIN(5), /F(12

37 /3), /X(12,4), /B(MBV), /L(AMND), /L(AMND), /N(4), /BCC(5), /JBC(5), /PRIN(5), /F(12

38 /3), /X(12,4), /B(MBV), /L(AMND), /L(AMND), /N(4), /BCC(5), /JBC(5), /PRIN(5), /F(12

39 /3), /X(12,4), /B(MBV), /L(AMND), /L(AMND), /N(4), /BCC(5), /JBC(5), /PRIN(5), /F(12

40 /3), /X(12,4), /B(MBV), /L(AMND), /L(AMND), /N(4), /BCC(5), /JBC(5), /PRIN(5), /F(12

41 /3), /X(12,4), /B(MBV), /L(AMND), /L(AMND), /N(4), /BCC(5), /JBC(5), /PRIN(5), /F(12

42 /3), /X(12,4), /B(MBV), /L(AMND), /L(AMND), /N(4), /BCC(5), /JBC(5), /PRIN(5), /F(12

43 /3), /X(12,4), /B(MBV), /L(AMND), /L(AMND), /N(4), /BCC(5), /JBC(5), /PRIN(5), /F(12

44 /3), /X(12,4), /B(MBV), /L(AMND), /L(AMND), /N(4), /BCC(5), /JBC(5), /PRIN(5), /F(12

45 /3), /X(12,4), /B(MBV), /L(AMND), /L(AMND), /N(4), /BCC(5), /JBC(5), /PRIN(5), /F(12

46 /3), /X(12,4), /B(MBV), /L(AMND), /L(AMND), /N(4), /BCC(5), /JBC(5), /PRIN(5), /F(12

47 /3), /X(12,4), /B(MBV), /L(AMND), /L(AMND), /N(4), /BCC(5), /JBC(5), /PRIN(5), /F(12

48 /3), /X(12,4), /B(MBV), /L(AMND), /L(AMND), /N(4), /BCC(5), /JBC(5), /PRIN(5), /F(12

49 /3), /X(12,4), /B(MBV), /L(AMND), /L(AMND), /N(4), /BCC(5), /JBC(5), /PRIN(5), /F(12

50 /3), /X(12,4), /B(MBV), /L(AMND), /L(AMND), /N(4), /BCC(5), /JBC(5), /PRIN(5), /F(12

51 /3), /X(12,4), /B(MBV), /L(AMND), /L(AMND), /N(4), /BCC(5), /JBC(5), /PRIN(5), /F(12

52 /3), /X(12,4), /B(MBV), /L(AMND), /L(AMND), /N(4), /BCC(5), /JBC(5), /PRIN(5), /F(12

53 /3), /X(12,4), /B(MBV), /L(AMND), /L(AMND), /N(4), /BCC(5), /JBC(5), /PRIN(5), /F(12

54 /3), /X(12,4), /B(MBV), /L(AMND), /L(AMND), /N(4), /BCC(5), /JBC(5), /PRIN(5), /F(12

55 /3), /X(12,4), /B(MBV), /L(AMND), /L(AMND), /N(4), /BCC(5), /JBC(5), /PRIN(5), /F(12

56 /3), /X(12,4), /B(MBV), /L(AMND), /L(AMND), /N(4), /BCC(5), /JBC(5), /PRIN(5), /F(12

57 /3), /X(12,4), /B(MBV), /L(AMND), /L(AMND), /N(4), /BCC(5), /JBC(5), /PRIN(5), /F(12

DO 400 J0316

40

41 FJ(1,1)10.
42 300 CONTINUE
43 6
44 DO 400 J0316
45 ND = LC INIT
46 XX(X(ND))
47 YY(Y(ND))
48 FJ(1,1)10(1,1)10(1,1)10(1,1)
49 FJ(1,1)10(1,1)10(1,1)10(1,1)
50 FJ(1,1)10(1,1)10(1,1)10(1,1)
51 FJ(1,1)10(1,1)10(1,1)10(1,1)
52 400 CONTINUE

```

53 C
54 DET=PP(J1,1)*PP(J2,2)-PP(J1,2)*PP(J2,1)
55 C IF(DET) 500, 5000, 500
56 C
57 C COMPUTE THE P MATRIX.
58 C
59 C DO 600 J1,4
60 C   Y1 = PP(J1,J)
61 C   T2 = PP(2,J)
62 C   PP(1,J) = 0.
63 C   PP(2,J) = 0.
64 C   DO 600 I1,2
65 C     PP(I1*J1+I2,1) = PP(I1,2)*T2*PP(I1,J)
66 C   CONTINUE
67 C
68 C COMPUTE THE STRAIN VECTOR.
69 C
70 C ST(1)=0.0
71 C ST(2)=0.0
72 C ST(3)=0.0
73 C ST(4)=TEMP
74 C ST(5)=TEMP
75 C
76 C STORING
77 C DO 800 I1,4
78 C   I1 = I1*2
79 C   ST(I1)=PP(I1,1)*PP(I1,2)
80 C ST(2)=U(1)*PP(2,1)+ST(2)
81 C ST(3) = U(1)*PP(2,1) + U(1)*PP(1,2) + ST(3)
82 C CONTINUE
83 C
84 C COMPUTE THE STRESS VECTOR.
85 C
86 C DO 1000 J=1,3
87 C   STT = ST(J)/DET
88 C STY=STT*Y1
89 C DO 1000 J=1,3
90 C   SIG(I1*J1+I2) = SIG(I1)
91 C CONTINUE
92 C
93 C 5000 RETURN
94 C

```

1	SUBROUTINE JSTRESSIN
2	IMPLICIT DOUBLE PRECISION (A-H,O-Z)
3	PARAMETER M=200
4	PARAMETER MND=761
5	PARAMETER MB=120
6	PARAMETER M=600
7	PARAMETER NEE=2, NBE=100, N4=20, N9=2
8	COMMON
9	1, NUNAPP, INI, HIYPE, NOY, NOX, NOXY, NCE, INLEL, NBI, NDN, NHP, HTB, NCTYP, NBI, NBT
10	2P, NBTYP, NATYP, NGL, NTRIP, NLL, NF, NHPF, NUL, N4S, NC, NG, NQ, NHP, N4T, N4BAND,
11	3TEMP, NUMBLK, I1, J1, K1, VOL, UM, SL, XG, YC, RDP, RD, PATM, GMM, RMS(20), COU,
12	400), PRO(20), CORF(20), EXPJ(20), STFN(20), STFN(20), STFN(20), STFN(20), STFN(20), STFN(20),
13	501(20), 805(20), 140(20), ALPHA(20), PHI(20), POME(20), HCOEF(20), A1(20), A2(20),
14	6, ULCOE(20), FR(20), B(4), P978(8), SIGMEL(4), FER(20), RHOD(20), RHOD(20), RHOD(20),
15	7CT, X(NDI), Y(NDI), DISP(NDI), Z(NDI), X(NDI), Y(NDI), Z(NDI), X(NDI), Y(NDI), Z(NDI), X(NDI),
16	80), IL(20), FL(20), FL(20), FL(20), FL(20), FL(20), FL(20), FL(20), FL(20), FL(20), FL(20),
17	9, 4), XY(2, 4), B(4), A(4), A(4), A(4), A(4), A(4), A(4), A(4), A(4), A(4), A(4), A(4), A(4),
18	100), X(2), Y(2), Z(2), X(2), Y(2), Z(2), X(2), Y(2), Z(2), X(2), Y(2), Z(2), X(2), Y(2), Z(2),
19	REAL MED
20	JTYPE = IL(N75)
21	C ROTATE GLOBAL DISPLACEMENTS TO LOCAL COORDINATE SYSTEM
22	C
23	C
24	I = IL(N75)
25	J = IL(N75)
26	XC = X(I) + X(J)/2.
27	YC = Y(I) + Y(J)/2.
28	DX = X(J) - X(I)
29	DY = Y(J) - Y(I)
30	DL = SQRT(DX**2 + DY**2)
31	CSN = DX/DL
32	SNS = DY/DL
33	DO 100 K = 1, 4
34	L = IL(N, K)
35	P = (2*NK) - B(2*NK-1)*SNE + B(2*NK)*CSN
36	100 PZERR = B(2*NK)*CSN + B(2*NK)*SNE
37	ADN = 0.5*(P(6)*R(2) + P(6)*P(4))
38	RDS = 0.5*(P(7)*R(1) + P(7)*P(3))
39	D(1) = SIG(N, 1)
40	D(2) = SIG(N, 2)
41	IF(NLL .EQ. 0) GO TO 110
42	DO 105 K=1, MLEU
43	IF(LELIK) NG, N) GO TO 105
44	GO TO 120
45	105 CONTINUE
46	C COMPUTE STRESSES IN INTERFACE ELEMENT
47	C
48	C
49	110 AA = 0.5
50	IF(INIY .EQ. 1 .OR. NG .EQ. NUNAPP) IA = 1
51	D(1) = SIG(N, 1) + AA*STF(N)*RDN
52	D(2) = SIG(N, 2) + AA*STF(N)*RDS


```

1 SUBROUTINE MODCAL(N)
2 IMPLICIT DOUBLE PRECISION (A-H,O-Z)
3 PARAMETER MEL=500
4 PARAMETER MND=761
5 PARAMETER MBH=120
6
7 PARAMETER NMS=2,NBS=100,NAS=20,NM=2
8 COMMON HBS(20),ALL,NMNP,NUMEL,NUMAT,NHMSOL,IBRD,LOBU,INUMAT
9
10 17*NB2TYP,NATP,MEL,NTRIP,NLL,NP,NPE,NUL,NL,NG,AC,HO,MO,NUP,NY,MBAND,
11 3*TEMP,NUMBLK,II,JJ,KK,VOL,UM,SL,AC,YC,RBF,SD,PA,M,GARH,RRS(20),COUJ
12
13 4200,PHI(20),BOU(20),QU(20),STP(20),STPN(S2),SYF(33),ZAVK(20),Z(20),Z
14 501(20),COF(20),ALPHA(20),PHI(20),GOME(20),HCOEF(20),AXP(20)
15 6,NLCOEF(20),P(20),G(4),PSTA(5),SIGMEL,6,IVES(MEL),AMOD(MEL),SU(ME
16 7),X(CRD),Y(CRD),Z(CRD),DTP(ND),FX(CRD),FY(CRD),FP(CRD),DP(MD),TC(30
17 8),L(MEL,5),LUL(NEE,8),L(LNBE),NP(N4),IBB(45),SUBC(NS),PR(NS),P(2
18 9,4),XY(2,4),B(MPH),A(MH,MM),S(10,10),R(10),G(4,4),LM(8),BA(S,2),A
19
20 REAL MBO
21 TAN(XI),M(XI),GOS(XI)
22
23 XC=0
24 YC=0
25
26 DO 10 I=1,N
27 L=ILAM(I)
28 XG=XI(XC)
29 YG=YI(YC)
30
31 10 CONTINUE
32
33 XC=XC+0.125
34 YG=YG+0.125
35
36
37
38
39
40
41
42
43
44
45
46
47
48
49
50
51
52

```

R0588 01 11-18-76 17.359

```

93 EE(N) = E(NATYP)
94 SHOD(N) = S(NATYP)
95 SL = 0.0
96 DO 120 I = 1,4
97 120 SIG(N,I) = 0.0
98 GO TO 300
99 CD = (G1) * G21/AB
100 DXY = (G11) * G21/2
101 NO = SQR(10X*2 + G31**2)
102 PSTR(1) = CD * AB
103 PSTR(2) = CD * AB
104 SL = 0.0
105 IF (ABS(DRY) .GT. 0.000001) GO TO 149
106 RAD = 0.0
107 GO TO 150
108 145 RAD = ATAN2(SIG(N,3),DXY)/2.
109 150 PSTR(3) = 57.396/RAD
110 IF (E(N)) .GT. 0.0 THEN LINEAR ELASTIC MATERIAL
111 IF (E(N)) .GT. 0.0 THEN GO TO 270
112 PHIR = PH(LM1) * 0.01745
113 CW = (2 * COS(PI/2) * COS(PHIR)) / (1. - SIN(PHIR))
114 HCF = (1 + CW) * 0.0001
115 IF (HCF .EQ. 1) RETURN
116 IF (NO .NE. 0) THEN
117 160 SL = (PSTR(1) + 2 * RD/DF) / 2.
118 IF (PSTR(1) AND PSTR(2) ARE ZERO, THE PROGRAM WOULD CALCULATE
119 A MODULUS = BEIN) OF ZERO FOR NONLINEAR SOIL ELEMENTS
120 THIS CHECK ALLOWS THE PROGRAM TO FIND THIS AND SUBSTITUTE
121 VALUE OF THE INITIAL SLOPE OF THE MODULUS CURVE.
122 THIS WILL OCCUR IF THERE IS NO GRAVITY STRESSES IN A
123 NONLINEAR SOIL MASS OR IF THE STRESSES IN A NONLINEAR SOIL
124 ELEMENT WERE EXACTLY REVERSED.
125 IF (PSTR(1) .EQ. 0.0 .AND. PSTR(2) .EQ. 0.0 .AND. PSTR(3) .EQ. 0.0)
126 1 GO TO 470
127 GO TO 180
128 160 SL = (PSTR(1) + 2 * RD/DF) / 2.
129 IF (PSTR(1) AND PSTR(2) ARE ZERO, THE PROGRAM WOULD CALCULATE
130 A MODULUS = BEIN) OF ZERO FOR NONLINEAR SOIL ELEMENTS
131 THIS CHECK ALLOWS THE PROGRAM TO FIND THIS AND SUBSTITUTE
132 VALUE OF THE INITIAL SLOPE OF THE MODULUS CURVE.
133 THIS WILL OCCUR IF THERE IS NO GRAVITY STRESSES IN A
134 NONLINEAR SOIL MASS OR IF THE STRESSES IN A NONLINEAR SOIL
135 ELEMENT WERE EXACTLY REVERSED.
136 IF (PSTR(1) .EQ. 0.0 .AND. PSTR(2) .EQ. 0.0 .AND. PSTR(3) .EQ. 0.0)
137 1 GO TO 470
138 GO TO 180
139 170 EE(N) = COEF(MHTOP) * PH / 100.0
140 SHOD(N) = SUP(MH)
141 SHOD(ME) = INY
142 G(4) = RD
143 GO TO 400
144 180 CONTINUE
145 IF INIT = 1, CHECK LORUL FOR LOADING-UNLOADING
146 IF INIT = 0, CHECK SD AGAINST 0.047 FOR LOAD-UNLOAD
147 NOTE = INIT = 0 FOR ANY CASE AFTER INITIALIZATION

```

105	C	IF(INIT,0.1) GO TO 182
106	C	IF(RD,1.5) GO TO 180,190
107	C	IF(LORUL=1) GO TO 190,190
108	C	IF(LORUL=1) GO TO 190,190
109	C	UNLOADING MODULUS CALCULATED
110	C	UNLOADING MODULUS CALCULATED
111	C	189 CH = (PSTR(2) * RSTR(9))/2,
112	C	189 CH = (PSTR(2) * RSTR(9))/2,
113	C	CHECK FOR TENSION FAILURE CH LESS THAN ZERO
114	C	CHECK FOR TENSION FAILURE CH LESS THAN ZERO
115	C	CHECK FOR TENSION FAILURE CH LESS THAN ZERO
116	C	IF(CH .LT. 0.0) GO TO 170
117	C	IF(CH .LT. 0.0) GO TO 170
118	C	CHECK FOR EXPONENT OF ZERO
119	C	CHECK FOR EXPONENT OF ZERO
120	C	IF (AXP(MH),GT,0.01) GO TO 188
121	C	IF (AXP(MH),GT,0.01) GO TO 188
122	C	IF (AXP(MH),GT,0.01) GO TO 188
123	C	IF (AXP(MH),GT,0.01) GO TO 188
124	C	IF (AXP(MH),GT,0.01) GO TO 188
125	C	IF (AXP(MH),GT,0.01) GO TO 188
126	C	IF (AXP(MH),GT,0.01) GO TO 188
127	C	IF (AXP(MH),GT,0.01) GO TO 188
128	C	IF (AXP(MH),GT,0.01) GO TO 188
129	C	IF (AXP(MH),GT,0.01) GO TO 188
130	C	IF (AXP(MH),GT,0.01) GO TO 188
131	C	IF (AXP(MH),GT,0.01) GO TO 188
132	C	IF (AXP(MH),GT,0.01) GO TO 188
133	C	IF (AXP(MH),GT,0.01) GO TO 188
134	C	IF (AXP(MH),GT,0.01) GO TO 188
135	C	IF (AXP(MH),GT,0.01) GO TO 188
136	C	IF (AXP(MH),GT,0.01) GO TO 188
137	C	IF (AXP(MH),GT,0.01) GO TO 188
138	C	IF (AXP(MH),GT,0.01) GO TO 188
139	C	IF (AXP(MH),GT,0.01) GO TO 188
140	C	IF (AXP(MH),GT,0.01) GO TO 188
141	C	IF (AXP(MH),GT,0.01) GO TO 188
142	C	IF (AXP(MH),GT,0.01) GO TO 188
143	C	IF (AXP(MH),GT,0.01) GO TO 188
144	C	IF (AXP(MH),GT,0.01) GO TO 188
145	C	IF (AXP(MH),GT,0.01) GO TO 188
146	C	IF (AXP(MH),GT,0.01) GO TO 188
147	C	IF (AXP(MH),GT,0.01) GO TO 188
148	C	IF (AXP(MH),GT,0.01) GO TO 188
149	C	IF (AXP(MH),GT,0.01) GO TO 188
150	C	IF (AXP(MH),GT,0.01) GO TO 188
151	C	IF (AXP(MH),GT,0.01) GO TO 188
152	C	IF (AXP(MH),GT,0.01) GO TO 188
153	C	IF (AXP(MH),GT,0.01) GO TO 188
154	C	IF (AXP(MH),GT,0.01) GO TO 188
155	C	IF (AXP(MH),GT,0.01) GO TO 188
156	C	IF (AXP(MH),GT,0.01) GO TO 188

```

197 E CHECK FOR YIELD CONDITION SL GREATER THAN 1.0
198 C
199 IF (SL .GT. 1.) GO TO 210
200 EE(N) = (HCOEF(MH)*PATH)/(PSTR(2)*PSTR(5))/(2.*PATH)**EXP(MH)*
201 1.*(1./R(MH)*SL**2)
202 199 CONTINUE
203 GU(N) = GUJ(MH)
204 IF (ABS(GU(N)) .GT. .1) .LT. 0.0001) GU(N) = 0.4999
205 SHOD(N) = 88712.*SL.*GU(N)**1.2.*WU(N)**1
206 GO TO 400
207 C
208 SHEAR FAILURE
209 C
210 EE(N) = 10.
211 GU(N) = WU(MH)
212 SHOD(N) = 88712.*SL.*GU(N)**1.2.*WU(N)**1
213 GO TO 400
214 C
215 LINEAR ELASTIC MATERIAL
216 C
217 EE(N) = E(MH)
218 IF (MH .EQ. NCTYP) GO TO 271
219 IF (MH .EQ. NB2TYR) GO TO 272
220 271 IF (10**4) .GT. ABS(1./E**2) .GT. 10**4) EE(N) = 10.
221 GO TO 273
222 272 IF (10**4) .GT. ABS(1./E**2) .GT. 10**4) EE(N) = 10.
223 273 GO TO 200
224 SL = 0.0
225 C
226 SHOD(N) = 88712.*SL.*GU(N)**1.2.*WU(N)**1
227 BB = EE(N)
228 GO TO 400
229 C
230 CALCULATE STIFFNESSES FOR 1-D ELEMENT
231 C
232 300 IF (ABS(S*F(N)-10000000) .LT. 1.) GO TO 400
233 PHIR = PHIR(MH)*0.01785
234 SHRST = COJ(MH) * ABS(1./E)*TAN(PHIR)
235 STFS(N) = MKS(MH)
236 STFNT(N) = K3(MH)
237 IF (ABS(10**2)) .GT. SHRST .OR. Q(1) .LE. 0.) GO TO 400
238 SD = (1./((ABS(Q(2))*FR(MH)/COJ(MH) * Q(1)*TAN(PHIR))))**2
239 SU = COEF(J(MH))*Q(MH)
240 GO TO 350
241 C
242 380 CONTINUE
243 SU = (COEF(J(MH))*Q(MH))/(Q(1)/PATH)**EXP(J(MH))
244 STFS(N) = 30050
245 STFNT(N) = 100000000.
246 400 CONTINUE
247 RETURN
248 C

```

R0585 01 11-18-76 17.359

209 C SETS EEC(N) AND OMOG(N) WHEN A NONLINEAR SOIL ELEMENT HAS NO
210 B STRESSES. SETS THEM EQUAL TO THE INITIAL SLOPE OF THE
211 C INITIAL MODULUS CURVE.

212
213 C 470 EEC(N)=280000.0

214 OMOG(N)=EEN(N)/28.0473.0*OUM(N)/13.0-2*OUM(N))

215
216 RETURN

217 END

***** 1470 EQUALITY OR NON-EQUALITY COMPARISON MAY NOT BE MEANINGFUL IN LOGICAL IF EXPRESSIONS

Preceding Page BLANK - ^{NOT} FILMED

APPENDIX B: NONLINEAR STRESS-STRAIN BEHAVIOR FOR SOIL

Homogeneous Soil Element

1. A simple and practical expression for describing the nonlinear soil behavior has been suggested by Kondner^{8*} who assumed that the stress-strain curve as obtained from triaxial compression tests is the following hyperbola:

$$(\sigma_1 - \sigma_3) = \frac{\epsilon_1}{a + b\epsilon_1} \quad (B1)$$

where $(\sigma_1 - \sigma_3)$ is the principal stress difference, ϵ_1 is the axial strain, and a and b are parameters that can be determined by experiment.

2. The physical meaning attached to a and b can be seen in Figure B1 in which a is equal to the reciprocal of the initial tangent modulus E_i and b is equal to the asymptotic value of the stress

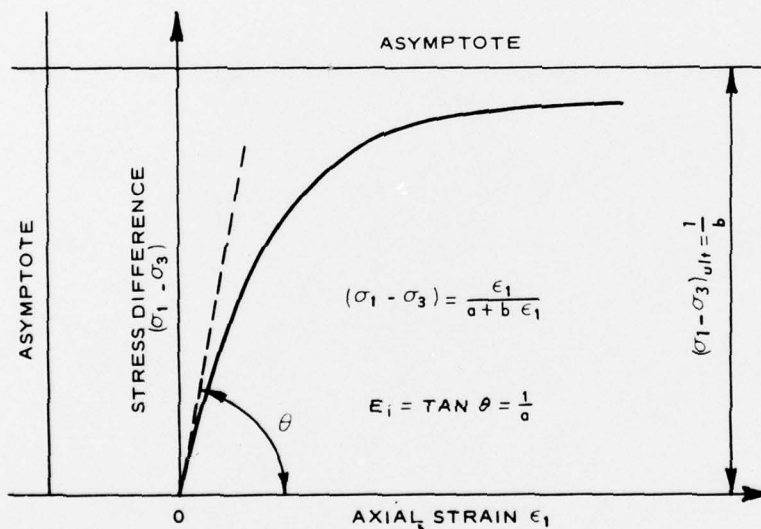


Figure B1. Kondner hyperbola for representation of stress-strain

* Raised numerals refer to similarly numbered items in the References at the end of the main text.

difference called the ultimate stress difference $(\sigma_1 - \sigma_3)_{ult}$. Equation B1 can be simplified by expressing $\epsilon_1/(\sigma_1 - \sigma_3)$ as a linear function of ϵ_1 , which would enable direct evaluation of the parameters a and b as depicted in Figure B2. The linear form of Equation B1 may be written as:

$$\frac{\epsilon_1}{(\sigma_1 - \sigma_3)} = a + b\epsilon_1 = \frac{1}{E_i} + \frac{\epsilon_1}{(\sigma_1 - \sigma_3)_{ult}} \quad (B2)$$

3. Duncan and Chang⁶ expanded Kondner's hyperbolic stress-strain relationship and utilized it for incremental FE analysis by expressing the tangent modulus E_t as a function of $(\sigma_1 - \sigma_3)$, E_i , and the Mohr-Coulomb strength parameters c and ϕ as:

$$E_t = \left[1 - \frac{R_f(1 - \sin \phi)(\sigma_1 - \sigma_3)}{2c \cos \phi + 2\sigma_3 \sin \phi} \right]^2 E_i \quad (B3)$$

in which R_f is the ratio of $(\sigma_1 - \sigma_3)$ at failure to the asymptotic value of the stress difference $(\sigma_1 - \sigma_3)_{ult}$.

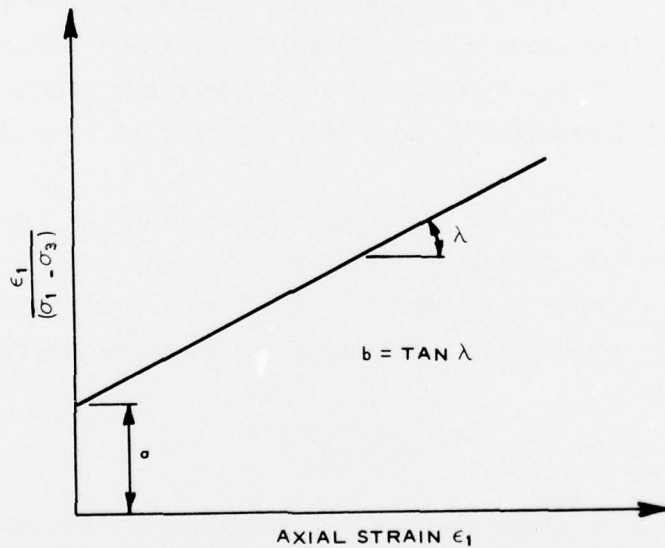


Figure B3. Linear representation of the hyperbolic stress-strain function

4. Another characteristic of many soils is the dependency of the initial tangent modulus E_i upon the confining pressure σ_3 . Janbu⁹ has suggested and Duncan and Chang⁶ have employed the following exponential relation between the confining pressure σ_3 and E_i :

$$E_i = KP_a \left(\frac{\sigma_3}{P_a} \right)^n \quad (B4)$$

where P_a is the atmospheric pressure expressed in the same units as σ_3 , K is a dimensionless number, and n is a dimensionless exponent.

5. The hyperbolic stress-strain relationship as expressed by Equations B3 and B4 is useful and simple. The parameters K , n , c , ϕ , and R_f are all readily determined by conventional triaxial compression tests.

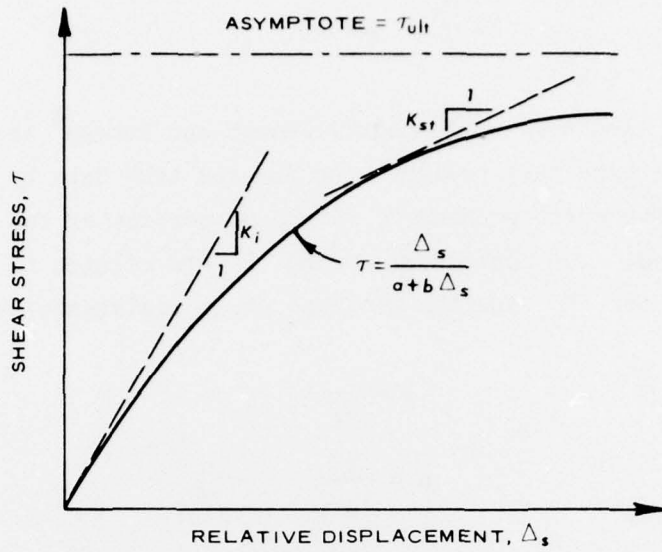
Interface Soil Elements

6. Although the stress-displacement curve from direct shear tests cannot be used directly for determining the stress-strain relationship for soil, it seems likely that a curve for such a test is indicative of the form of the stress-strain relationship. A comprehensive study by Clough and Duncan⁴ has shown a resemblance of the shear stress relative to the displacement to the hyperbolic form suggested by Kondner,⁸ which is appropriate for characterization of the behavior of interface elements.

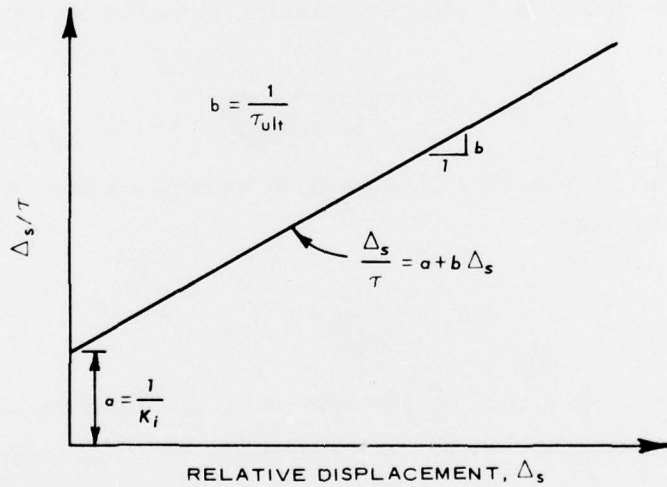
7. Typical shear stress τ versus displacement Δ_s for a direct shear test is presented in Figure B3a, where K_i and K_{st} are the initial and tangent shear stiffnesses, respectively. The hyperbolic form for the shear stress as a function of the relative displacement is:

$$\tau = \frac{\Delta_s}{a + b\Delta_s} \quad (B5)$$

where a and b are parameters that can be obtained from laboratory tests. Equation B5 may be transformed to a linear form as shown in Figure B3b:



a. CONVENTIONAL SHEAR STRESS-DISPLACEMENT



b. TRANSFORMED SHEAR STRESS-DISPLACEMENT

Figure B3. Hyperbolic representation of the variation of shear stress with relative displacement

$$\frac{\Delta_s}{\tau} = a + b\Delta_s \quad (B6)$$

8. It has also been suggested by Clough and Duncan⁴ that it is desirable to determine the straight line for the test data by connecting points on the curve corresponding to 70 and 95 percent of the shear resistance mobilized. The constants a and b are related to the initial shear stiffness K_i and the ultimate shear resistance τ_{ult} as:

$$a = \frac{1}{K_i} \quad (B7)$$

$$b = \frac{1}{\tau_{ult}} \quad (B8)$$

The relationships expressed by Equations B7 and B8 can be used to determine K_i and τ_{ult} from the transformed linear hyperbolic plot shown in Figure B3b by simply evaluating a and b .

9. The tangent shear stiffness K_{st} at any point on the hyperbolic curve may be obtained by differentiating Equation B5 as:

$$K_{st} = \frac{d\tau}{d\Delta_s} = \frac{a}{(a + b\Delta_s)^2} \quad (B9)$$

From Equation B5 it is possible to obtain an expression for Δ_s by rearranging terms to read:

$$\Delta_s = \frac{a\tau}{1 - b\tau} \quad (B10)$$

By substituting a , b , and Δ_s as expressed in Equations B7, B8, and B10, respectively, in Equation B9, an expression for K_{st} can be obtained:

$$K_{st} = K_i \left(1 - \frac{\tau}{\tau_{ult}}\right)^2 \quad (B11)$$

Experiments have shown that τ_{ult} overestimates the actual value of the shear stress at failure τ_f , and the ratio between two shear stresses

R_f does not vary significantly for a given soil. By introducing the failure ratio R_f into Equation B11, the following may be obtained:

$$K_{st} = K_i \left(1 - \frac{R_f \tau}{\tau_f} \right)^2 \quad (B12)$$

10. From Mohr-Coulomb failure criteria, presented in Figure B4,

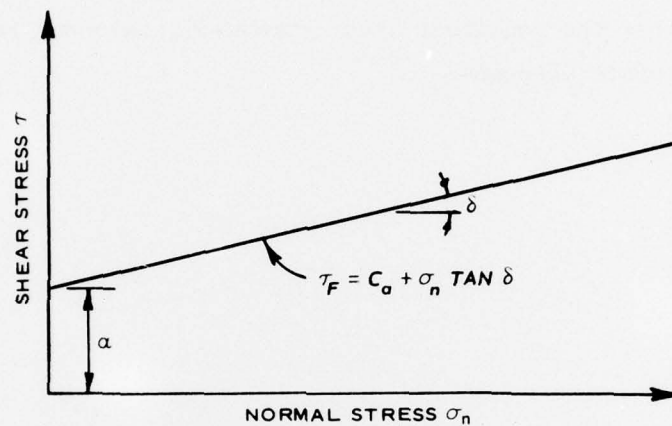


Figure B4. Variation of friction resistance with normal stress

the shear stress at failure may be related to the normal stress σ_n by the following expression:

$$\tau_f = C_a + \sigma_n \tan \delta \quad (B13)$$

where C_a is the adhesion and δ is the angle of skin friction. Therefore, by substituting Equation B13 in Equation B12, the following is obtained:

$$K_{st} = K_i \left(1 - \frac{R_f \tau}{C_a + \sigma_n \tan \delta} \right)^2 \quad (B14)$$

11. Laboratory studies by Clough and Duncan⁴ have shown that the initial shear stiffness K_i may be related to the normal stress σ_n

by the following exponential relationship:

$$K_i = K_j \gamma_w \left(\frac{\sigma_n}{P_a} \right)^m \quad (B15)$$

where γ_w is the unit weight of water, P_a is the atmospheric pressure, and K_j and m are parameters that can be determined from laboratory tests. Equations B14 and B15 define a simplified and practical relationship which describes the nonlinear shear stress-displacement relationship for the interface elements.

APPENDIX C: NOTATION

a,b	Experimental parameters
A_e	Equivalent cross-sectional area of reinforcing strips
A_s	Cross-sectional area of reinforcing strip
c	Cohesion
C_a	Adhesion
E_a	Modulus of elasticity of aluminum panel
E_e	Equivalent modulus of elasticity
E_i	Initial modulus
E_s	Modulus of elasticity of galvanized steel reinforcing strips
E_t	Tangent modulus
I_a	Moment of inertia of aluminum panel per unit width
I_e	Equivalent moment of inertia per unit width
I_x	Moment of inertia of metal sheet at back of aluminum panel per unit width
K	Hyperbolic loading parameter
K_i	Initial shear stiffness
K_j	Dimensionless number
K_r	Residual shear stiffness
K_{st}	Tangent shear stiffness
L_a	Length of beam (S_z) between any two rows of reinforcing strips
L_e	Equivalent length
L_s	Length of reinforcing strip
m_f	Magnification factor
n	Pure number; also total number of strips in each row
N	Number of reinforcing ties in each reinforced elevation
P_a	Atmospheric pressure
R_f	Failure ratio
S	Total axial stiffness of reinforcing strip
S_e	Equivalent stiffness of plate substituting for reinforcing strips
t	Actual thickness of reinforcing tie
t_e	Equivalent thickness of reinforcing tie in FE mesh
w	Water content of soil

W	Actual width of reinforcing tie
W_e	Equivalent width of reinforcing tie in FE mesh
γ_d	Dry density of soil
γ_w	Unit weight of water
δ	Angle of skin friction
Δ	Shear deformation or displacement
Δ_s	Displacement
ϵ_l	Axial strain
λ_1, λ_2	Stress levels; see Equations 1c and 2c, respectively
ν	Poisson's ratio
σ_m	Normal stress
σ_t	Tensile stress in reinforcing strip
σ_y	Yield stress
σ_{te}	Equivalent tensile stress in reinforcing strip computed by FE analysis
σ_1	Major principal stress
σ_3	Minor principal stress
$\sigma_1 - \sigma_3$	Principal stress difference
$(\sigma_1 - \sigma_3)_f$	Principal stress difference at failure
$(\sigma_1 - \sigma_3)_{ult}$	Ultimate principal stress difference
τ	Shear stress
τ_{max}	Peak shear stress
τ_{ult}	Ultimate shear stress
ϕ	Angle of internal friction

In accordance with ER 70-2-3, paragraph 6c(1)(b), dated 15 February 1973, a facsimile catalog card in Library of Congress format is reproduced below.

Al-Hussaini, Mosaid M

Finite element analysis of a reinforced earth wall, by Mosaid M. Al-Hussaini [and] Lawrence D. Johnson. Vicksburg, U. S. Army Engineer Waterways Experiment Station, 1977.

1 v. (various pagings) illus. 27 cm. (U. S. Waterways Experiment Station. Technical report S-77-6) Prepared for Office, Chief of Engineers, U. S. Army, Washington, D. C., under Project 4A161102AT22, Task A2, Work Unit 004.

Includes bibliography.

1. Finite element method. 2. Reinforced earth. 3. Walls. I. Johnson, Lawrence D., joint author. II. U. S. Army. Corps of Engineers. (Series: U. S. Waterways Experiment Station, Vicksburg, Miss. Technical report S-77-6)
TA7.W34 no.S-77-6